8-18-2015

Synthesis and characterization of vanillyl alcohol based thermosetting epoxy resins

Eric Hernandez

SYNTHESIS AND CHARACTERIZATION OF VANILLYL ALCOHOL BASED THERMOSETTING EPOXY RESINS

by
Eric David Hernandez

A Thesis

Submitted to the
Department of Chemical Engineering
College of Engineering
In partial fulfilment of the requirement
For the degree of
Master of Science in Chemical Engineering
at
Rowan University
July 31, 2015

Thesis Chair: Joseph F. Stanzione, III, Ph.D.

Dedication

For mom

Acknowledgements

I would like to offer my sincerest gratitude to Dr. Joseph F. Stanzione, III, who has served as my graduate thesis advisor over the past two years. Dr. Stanzione has been both a knowledgeable and encouraging mentor who has provided me with instrumental guidance and direction throughout the course of this research. I am truly grateful to have had the opportunity to have worked with him. In addition, he has provided me with multiple opportunities to attend conferences and workshops and travel to places I had never before been, including Denver, CO and Washington, DC. He has helped me to network with fellow scientists and engineers and has even afforded me the opportunity to work with some of his colleagues. Dr. Stanzione's keen optimism and support undoubtedly aided me in staying positive when I encountered research roadblocks, and without him this thesis would not have been possible.

I would like to recognize my fellow lab mates and the graduate students who shared an office with me. I would also like to thank Dr. John La Scala and Dr. Joshua Sadler of the Army Research Laboratory for providing me the opportunity to collaborate with them. I would like to acknowledge the late Dr. Richard Wool and Kaleigh Reno of the University of Delaware for the opportunity to collaborate with them as well. In addition, I would like to express gratitude to the Army Research Laboratory for their generous support and funding via Cooperative Agreement W911NF-14-2-0086.

Finally, I would like to thank my family and friends who have been supportive of my goals and career path. Most especially, I would like to thank my mother, Patricia Fabrizio, who has been there for me every step of the way throughout my entire life. She is my inspiration and I am truly indebted to her.

Abstract

Eric D. Hernandez
SYNTHESIS AND CHARACTERIZATION OF VANILLYL ALCOHOL BASED THERMOSETTING EPOXY RESINS
2014-2015
Joseph F. Stanzione, III, Ph. D.
Master of Science in Chemical Engineering

Lignin is a natural and abundant renewable material composed of crosslinked phenylpropenyl units that when strategically depolymerized could potentially yield renewable bio-based aromatic building blocks for applications in high-performance thermosetting epoxy resins. Vanillyl alcohol, a lignin derived aromatic diol, is a potential platform chemical for the production of renewable bisphenols and epoxy thermosets. A new bio-based bisphenol (bisguaiacol) was synthesized via electrophilic aromatic condensation of vanillyl alcohol and guaiacol, from which diglycidyl ether of bisguaiacol (DGEBG) was prepared via epoxidation with epichlorohydrin. The thermomechanical properties of DGEBG blended with a commercial BPA-based epoxy resin and cured with a diamine were investigated via dynamic mechanical analysis (DMA). In addition, two bio-based diepoxy monomers were synthesized from vanillyl alcohol (DGEVA) and gastrodigenin (DGEGD) and characterized via ^{1}H-NMR, ^{13}C-NMR, FTIR, MS, and GPC. Vanillyl alcohol based epoxy resins bear a methoxy group covalently bonded to the aromatic ring *ortho* to the glycidyl ether group. The thermomechanical properties of cured DGEVA and DGEGD thermosets were compared to those of the cured DGEBG and commercially available thermosets to determine the effect of the methoxy moiety. DMA results indicate that the presence of the methoxy lowers the glass transition temperature (T_g), yet increases the storage modulus (E') at 25 °C in cured epoxy-amine systems.

Table of Contents

Table of Contents (Continued)

List of Figures

List of Tables

Chapter 1

Introduction

1.1 Overview and Organization

Recent concerns over social, economic, and environmental sustainability have driven a global initiative toward the development of polymers and composites derived from renewable resources. As a result, polymers derived from biomass feedstocks are becoming considerably attractive as viable and sustainable alternatives to their petrochemical derived counterparts. Thermosetting polymers, including epoxy resins, vinyl ester resins, and unsaturated polyesters, lend themselves to a wide range of industrial and commercial applications including adhesives, coatings, and composites. The versatility of many of these thermosetting polymer resins is indisputably owed to the thermal stability and structural rigidity provided by their incorporated aromatic character. This thesis presents lignin, a highly aromatic biomacromolecule, as a sustainable alternative to fossil fuels for future development and production of thermosetting polymers, specifically epoxy resins. In attempt to contribute to the fields of polymer science, chemical engineering, and green chemistry and engineering, renewable bisphenols and epoxy resins where synthesized from lignin derived compounds and the cured polymer properties of these resins were investigated. Finally, a majority of lignin model compounds, specifically syringyl- and guaiacyl-based compounds, inherently bear a methoxy moiety covalently bonded to their aromatic rings and this work presents a structure-property relationship study of the effect of the methoxy functional group on the cured polymer properties.

Chapter 1 provides an introduction to epoxy resins and a review of the current state of the field of renewable and bio-based epoxy resins. In addition, Chapter 1 provides the

motivation for this study and introduces lignin and its derivatives, in particular vanillin, as renewable feedstocks for the production of synthetic bio-based bisphenols and epoxy resins. Chapter 2 affords a general overview of the various techniques used to characterize the monomers and epoxy pre-polymers used in this study. The experimental methods and procedures employed over the course of this work are detailed in Chapter 3. Chapter 4 presents the results of the study and provides a discussion and comparison of the various polymer properties. Finally, Chapter 5 summarizes the entire study, draws conclusions, and offers recommendations for future work.

1.2 Introduction to Thermosetting Epoxy Resins

Polymers can be divided into two distinct classes known as thermoplastics and thermosets.[1-3] Thermoplastic polymers are characterized by their ability to soften upon heating and to solidify upon cooling. In contrast, thermosetting polymers do not heat soften as they form irreversibly cross-linked three dimensional networks. Once a thermosetting resin is cured (usually through heat and/or UV radiation), it can no longer be thermally processed.[4] Therefore, thermosetting polymers are designed to be molded into their final form prior to curing.[1-3, 5] Unfortunately, the majority of commercial thermosetting polymers are currently synthesized from non-renewable petroleum derived chemicals.

Epoxy resins are a class of thermosetting monomers, pre-polymers, and polymers that bear an epoxide functional group. The epoxide group is a three membered cyclic ether comprising two carbons and one oxygen (IUPAC: oxirane).[2, 5-7] The structure of the epoxide functional group is shown in *Figure 1*.

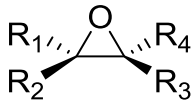

Figure 1. Structure of epoxide functional group.

Epoxy resins dominate the thermosetting polymers market, making up nearly 70 % of all thermosetting polymers.[4] These resins were first invented in Germany by Paul Schlack of IG Farbenindustrie Ag in 1934.[5, 8] In 1938, Swiss chemist Pierre Castan, who had been researching dental materials, discovered that epoxy resins could be reacted with phthalic anhydride to produce hardened plastic resins. Subsequently, the first commercial epoxy resins went in to production in 1947.[8] Epoxy monomers and pre-polymers are generally synthesized from two main precursors, bisphenol A (BPA) and epichlorohydrin. In fact, BPA-based epoxy pre-polymers are found in over 90 % of all thermosetting epoxy resins worldwide, in a market with a global annual production exceeding two million tons as of 2010.[4] Cured epoxy resins display high glass transition temperatures (T_gs) and storage moduli (E's) at room temperature as well as excellent solvent and chemical resistance and superior adhesive properties.[5, 6, 8]

1.3 Bisphenols

Bisphenol A is the U.S. commercial name for 4,4’-isopropylidenediphenol. The commercial name is derived from the reactants that are used to prepare it: two equivalents phenol and one equivalent acetone.[9-11] The overall reaction scheme for the synthesis of BPA is given in *Figure 2*. The mechanism is believed to take place via an acid catalyzed electrophilic aromatic condensation.[10] The electrophilic condensation mechanism for the synthesis of BPA is shown in *Figure 3*. The reaction begins with the protonation of acetone,

followed by the attack on the protonated acetone by the aromatic ring of phenol. Water is expelled producing a tertiary carbocation. Finally, a second phenol attacks the carbocation to form BPA.[10] The synthesis of BPA in the presence of a strong acid favors the *p,p'*-isomer (4,4'-isopropylidenediphenol) due to the location of the electron density. However, some *o,p'*-isomer (2,4'-isopropylidenediphenol) formation is observed as well as other higher molecular weight by-products.[10] The formation of the *o,o'*-isomer (2,2'-isopropylidenediphenol) is typically insignificant. The reaction typically yields 95 % *p,p'*-BPA and 5 % *o,p'*-BPA.[12] To prevent the formation of trimers and oligomers, the reaction is usually carried out in excess phenol that is removed via distillation and subsequently recycled. The desired *p,p'*-BPA is typically obtained through recrystallization and other downstream purification procedures. [9-14]

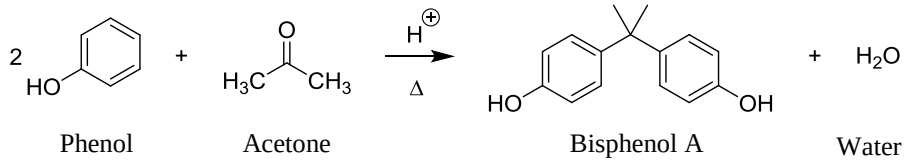

Figure 2. Balanced reaction scheme for the synthesis of BPA.

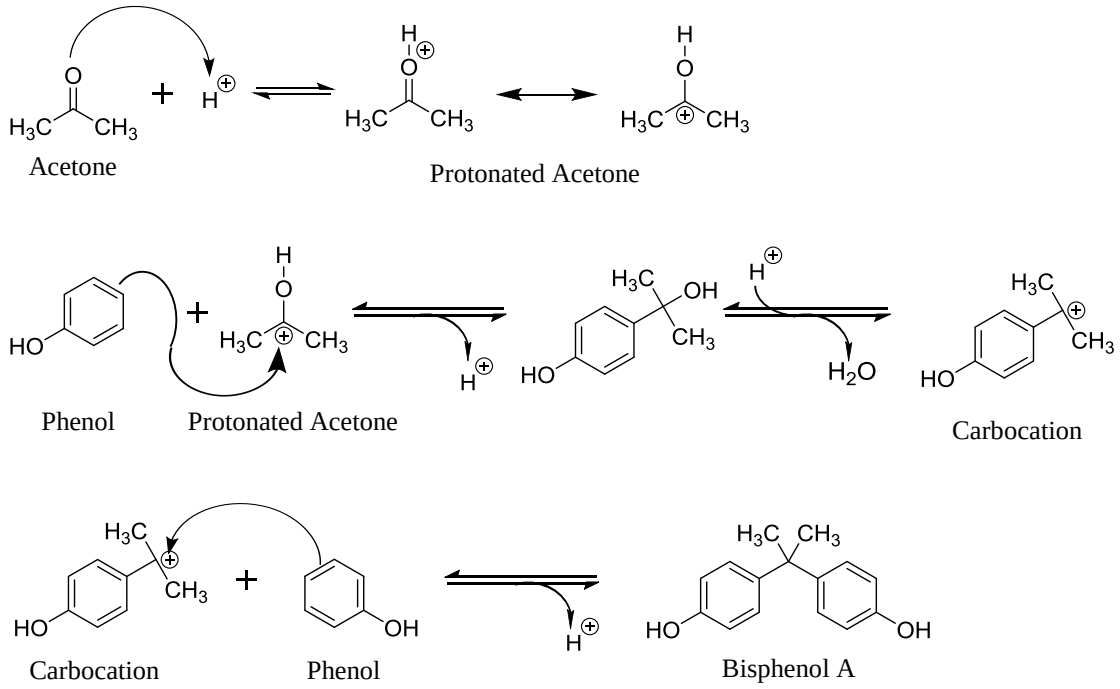

Figure 3. Mechanism for the acid catalyzed condensation of phenol and acetone to form BPA.
Adapted from Neagu.[10]

BPA is an important precursor for the majority of epoxy resins and polycarbonates. Over 1.9 billion pounds of BPA were produced in the US in 2003 of which 1.4 billion pounds were used in the production of polycarbonate resins and 406 million pounds were used in epoxy resins.[15] A smaller quantity of BPA (approximately 100 million pounds) was used in the production of thermal paper for consumer receipts and as a plasticizer in polyvinylchloride (PVC). A 2013 biomonitoring summary by the Center for Disease Control estimates the global annual production of BPA to be about 5-6 billion pounds.[16] BPA is a known human endocrine disruptor that mimics estrogen, specifically estradiol. Endocrine disruptors are chemicals that mimic or block endogenous hormones thereby altering how the endocrine system functions.[17] BPA is believed to mimic estradiol by

binding to estrogen receptors alpha and beta (ER-α and ER-β) as an agonist.[17, 18] Recently, awareness of BPA to act as an endocrine disruptor has raised concerns and debates over its use in consumer products. In their 2003 official report, the European Union stated that while they found no direct human exposure to BPA, BPA-based products that are in direct contact with food represent the greatest potential source of human exposure.[15, 19] Exposure may occur through leaching of residual monomer or through breakdown of BPA-based polymers.[19] For example, BPA-based epoxy resins are often applied as a lining to the interior of metal food and drink containers to prevent corrosion and rust. This particular application has received a great deal of scrutiny since residual BPA may leach from these linings and contaminate the food if the epoxy resins are not fully cured.[18] Exposure of developing fetuses and infants to BPA is of the greatest concern since endocrine disruption at these stages can have the most severe effects.[17] In 2010, Canada became the first country to ban the use of BPA in baby bottles and toys; subsequently in 2011, all European countries followed this initiative and banned the use of BPA in baby bottles as well.[17]

Bisphenol F (BPF), which is the simplest novalac, is occasionally used as an alternative to BPA in epoxy resins. BPF is synthesized via a similar reaction to BPA; however, the BPF synthesis employs the use of formaldehyde in place of acetone. The reaction of phenol with formaldehyde (given in *Figure 4*) typically yields a mixture of several regioisomers as well as low molecular weight novalac oligomers.[20] However, no commercially scalable method exists to separate the regioisomers. Still, the viscosity of BPF-based epoxy resins at room temperature (2.5–4.5 Pa s) is much lower than their BPA-based counterparts

(12 – 14 Pa s).[20, 21] However, a recent study concluded that BPF is an endocrine disruptor analogous to BPA; therefore, BPF is not a safer alternative to BPA.[22]

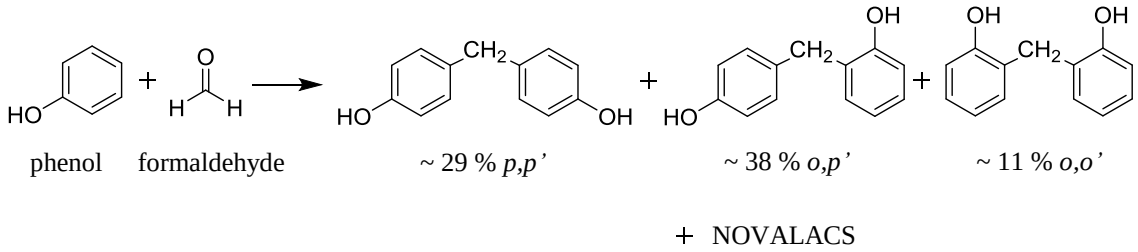

Figure 4. Synthesis of BPF regioisomers and undesired novalacs.

1.4 Epichlorohydrin

The second major precursor in the synthesis of epoxy resins is epichlorohydrin. Historically, epichlorohydrin has been synthesized from propylene via a multistep pathway.[23-25] However, epichlorohydrin can also be synthesized from glycerin through a "simpler" and "greener" two-step process.[23] Today, glycerin is produced as a byproduct of the bio-diesel manufacturing process.[23, 26] The high costs of production of bio-diesel can be offset through development of new manufacturing processes that exploit bio-based glycerin. Furthermore, the manufacture of commodity chemicals from glycerin has recently become commercially viable as a result of its increased availability and declining price.[26] Dow GTE and Solvay Epicerol have developed new processes for the conversion of bio-based glycerin to epichlorohydrin.[23] Both the propylene and glycerin pathways produce a mixture of regioisomers as intermediates, which are 1,3-dichloropropan-2-ol (1,3-DCH) and 2,3-dichloropropan-1-ol (2,3-DCH). The last step in

both of these processes involves reacting 1,3-DCH and 2,3-DCH with NaOH to produce epichlorohydrin and NaCl. Bell et al. report that the glycerin to epichlorohydrin route is much more selective in producing 1,3-DCH.[23] In the conventional propylene process, the mixture of 1,3-DCH to 2,3-DCH produced is a modest 3:1 whereas the bio-based-glycerin process produces a much more efficient 30–50:1. 1,3-DCH can be converted to epichlorohydrin 300 times faster than 2,3-DCH; thus, the increased ratio of 1,3-DCH to 2,3-DCH leads to shorter residence times. A comparison of epichlorohydrin production via the conventional propylene pathway and the renewable glycerin pathway is given in *Figure 5*.

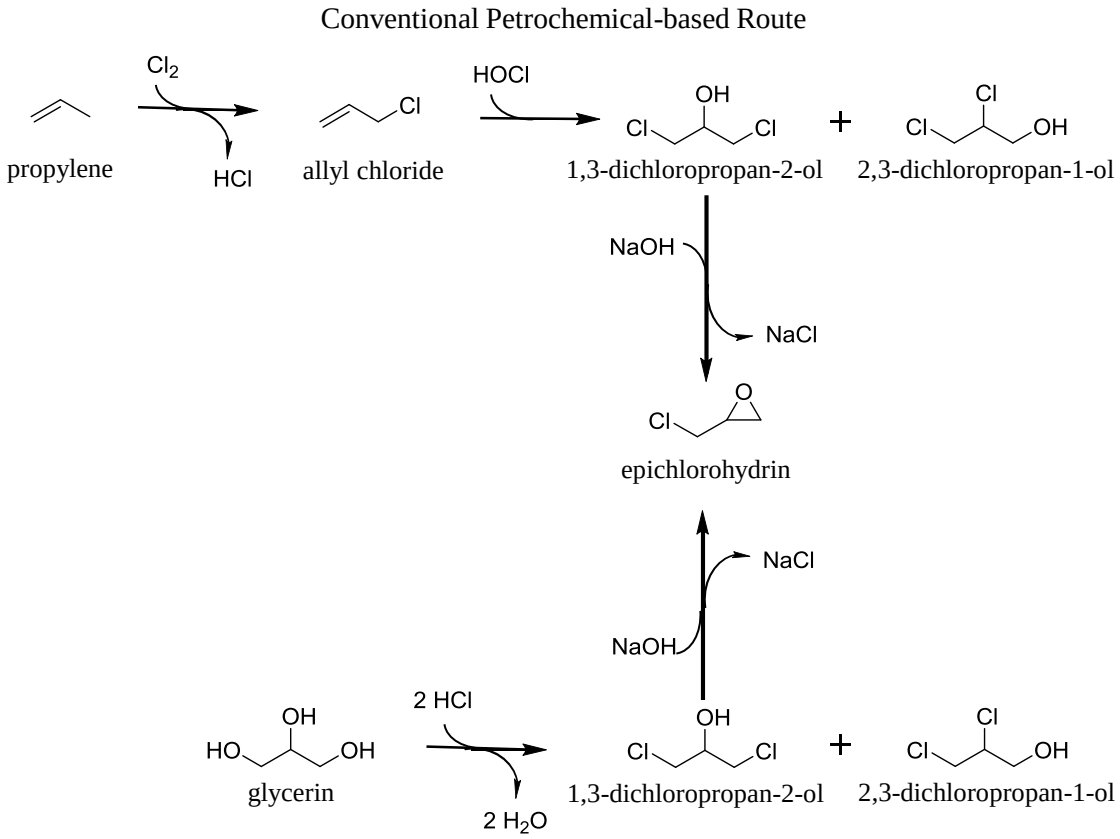

Figure 5. Conventional and renewable pathways for the production of epichlorohydrin.
Adapted from Bell et al.[23]

1.5 Synthesis of Diglycidyl Ethers

Diglycidyl ethers are the most commonly produced liquid epoxy resins. The general structure of a glycidyl ether is shown in *Figure 6*. The glycidyl ether group is an oxiranylmethyl ether derived from an epihalohydrin and an alcohol.

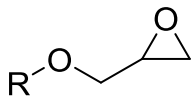

Figure 6. Structure of glycidyl ether.

The reaction of BPA and epichlorohydrin in the presence of NaOH produces diglycidyl ether of bisphenol A (DGEBA) as shown in *Figure 7*.[2-8] The DGEBA product is typically a mixture of oligomers in which *n* can vary from $n = 0$ to $n = 12$.[5] The value of *n* can be controlled through the molar ratio of epichlorohydrin to BPA employed. The stoichiometric ratio is two equivalents of epichlorohydrin for every one equivalent of BPA. However, increasing the amount of epichlorohydrin decreases the formation of higher molecular weight oligomers, effectively lowering the average *n* value. Reactors that employ a large excess of epichlorohydrin can produce pure DGEBA such that $n = 0$. [27] Pure DGEBA is a crystalline solid at room temperature with a melting point of 41–42 ºC. However, standard commercial epoxy resins with *n* values of 0.11 to 0.15 are liquids .[27] The viscosity of DGEBA resins increases as the molecular weight of the resins increases. Typically, resins in which $n > 1$ are amorphous solids. The process of producing a thermoset from epoxy resins involves mixing the resins with a curing agent and transferring the mixture to a mold. This process, known as resin transfer molding (RTM), requires the

uncured resin to be a liquid with a viscosity range between 200-1000 cP so that it may be transferred to the mold without premature curing or the formation of voids.[28] Therefore, liquid epoxy resins are most desirable for RTM; while, higher MW solid epoxy resins lend themselves to surface coating applications such as marine coatings and powder coatings.[29]

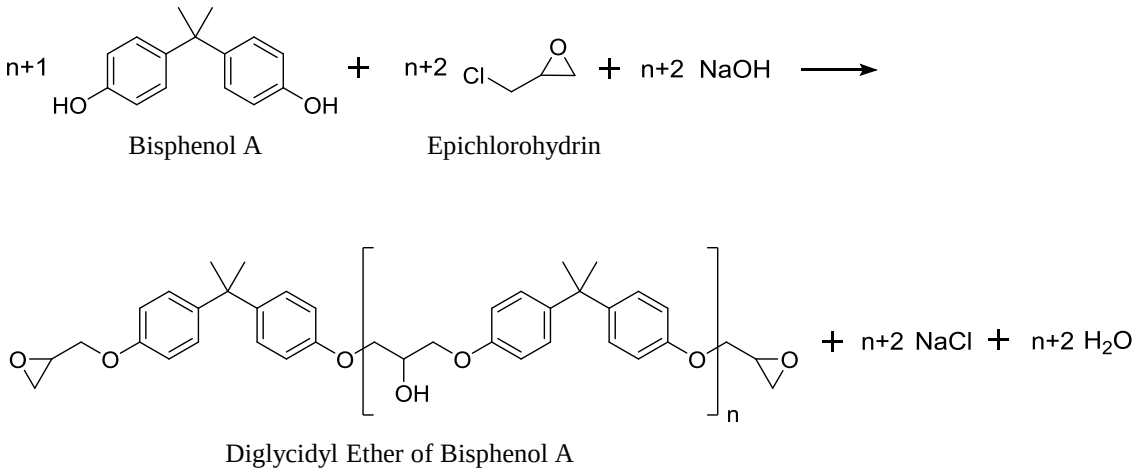

Figure 7. Reaction scheme for the synthesis of DGEBA.

The mechanism for the synthesis of diglycidyl ethers is shown in *Figure 8*. [6, 7, 27] The reaction begins with the formation of a bisphenol anion in the presence of NaOH (I). The bisphenol anion attacks the epoxide group of epichlorohydrin opening the strained ring (II) that subsequently closes back on itself producing a monoglycidyl ether of bisphenol A (MGEBA) and NaCl (III). The reaction proceeds with the addition of a second glycidyl ether group to the other hydroxyl of the MGEBA and the loss of additional NaCl and water via the same mechanism (IV).

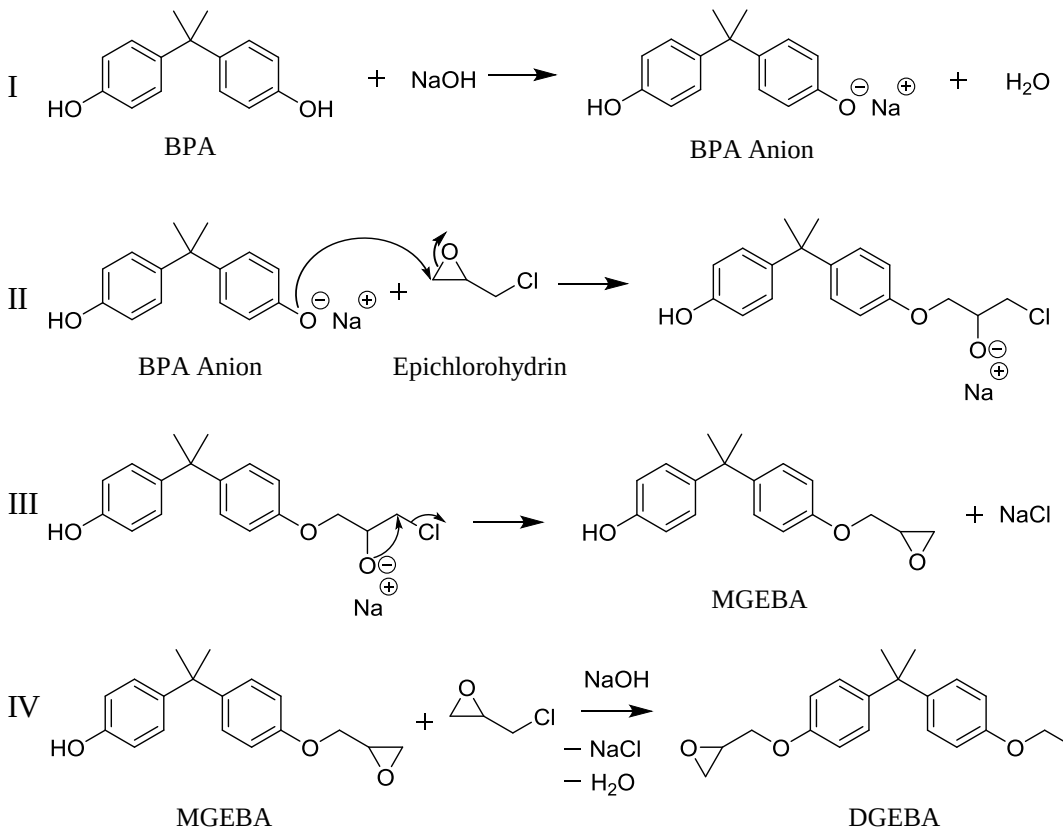

Figure 8. Mechanism for the synthesis of diglycidyl ethers.

There are two industrial processes for the production diglycidyl ethers: the taffy process and the advancement process.[5, 27] The taffy process is generally used to produce low molecular weight liquid epoxy pre-polymers ($n < 1$) as well as low molecular weight solid epoxy pre-polymers, while the advancement process is used to create higher molecular weight oligomers. In the taffy process, BPA is reacted with excess epichlorohydrin in the presence of a 20–50 % solution of $NaOH_{(aq)}$ at approximately 90 °C.[5] The resulting product is an emulsion of epoxy and brine known as the "taffy." The taffy is washed with water and an organic solvent to remove the NaCl. The organic solvent and water are removed via vacuum distillation.[5, 27]

Production of higher molecular weight oligomers leads to higher viscosity resins, making it extremely difficult to remove NaCl via simple washing following the taffy processes.[27] Consequently, the advancement process is generally used to synthesize higher molecular weight oligomers as opposed to the taffy process. In the advancement process, low molecular weight DGEBA resins ($n \cong 0.13$) are reacted with additional BPA in the presence of a catalyst (usually alkyltriphenylphosphonium hydroxides) at higher temperatures and pressures than the taffy process.[5, 27] The reaction scheme is given in *Figure 9*. The majority of oligomers produced by this process have even n values (n = 2, 4, 6, ...) because DGEBA is used as a reactant.[27] It is important to note that NaCl is not produced by the advancement process.

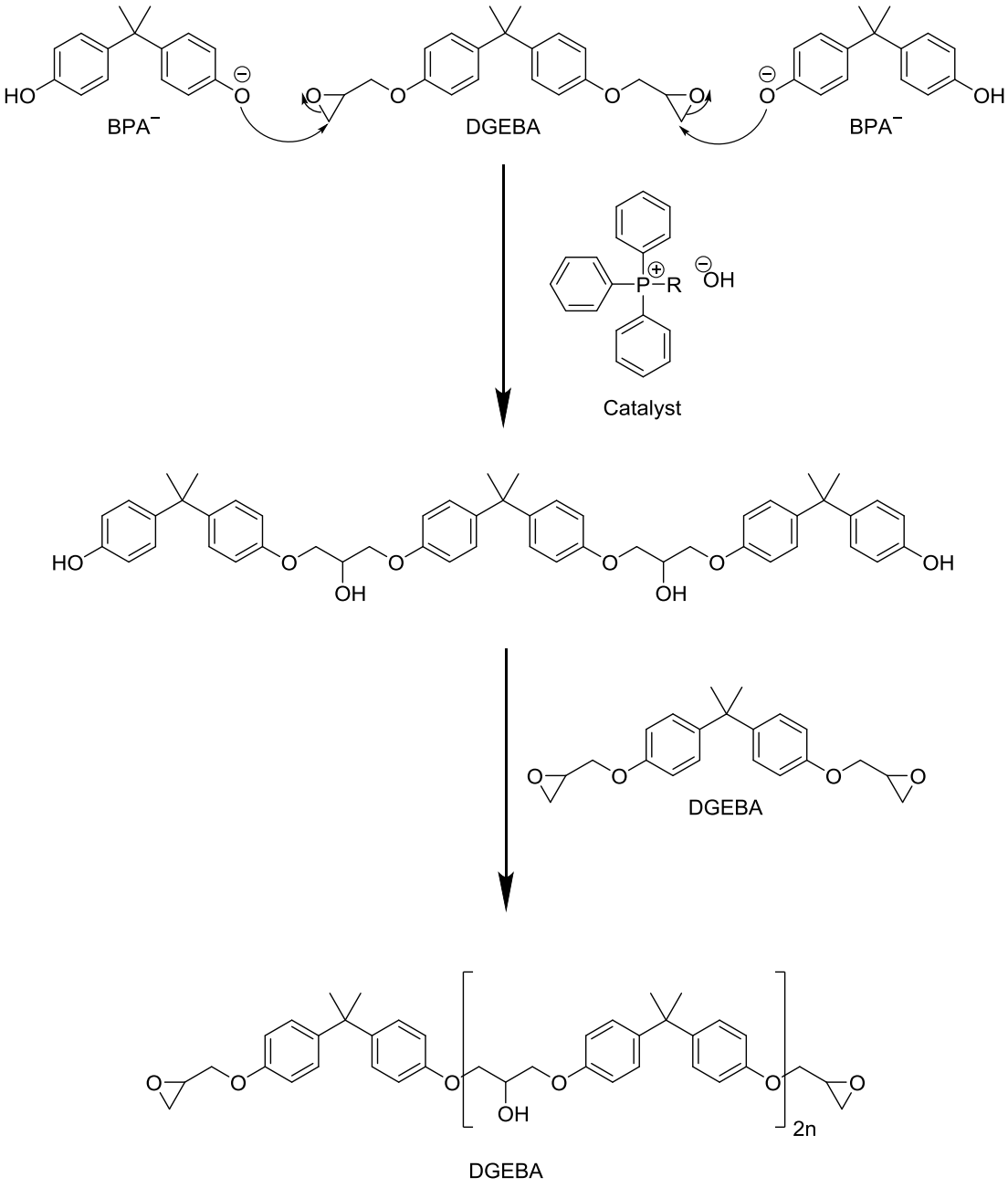

Figure 9. Advancement process for the production of higher molecular weight epoxy resins.

1.6 Epoxy Curing

Epoxy pre-polymers can be cured to produce hardened thermosets via chemical crosslinking with amines or anhydrides.[5, 27] Amines are much more versatile curing agents that react with the terminal epoxide groups whereas anhydrides are typically used to cure higher molecular weight epoxy resins through reaction with free hydroxyls.[5] Both the mechanism and kinetics of epoxy-amine curing systems have been extensively studied for use in industrial applications.[30-32] All epoxy resins used in this work were cured with amine curing agents.

Primary amines have two active hydrogens (functionality, $f_n = 2$) that readily react with terminal epoxide groups at room temperature.[5] Consequently, a secondary amine is formed as the epoxide ring is opened. The secondary amine will then react with a second epoxide ring to form a tertiary amine. However, primary amines are much more reactive than secondary amines, so the second step is rate limiting.[5, 30, 32] The epoxy-amine step growth reaction scheme is given in *Figure 10*.

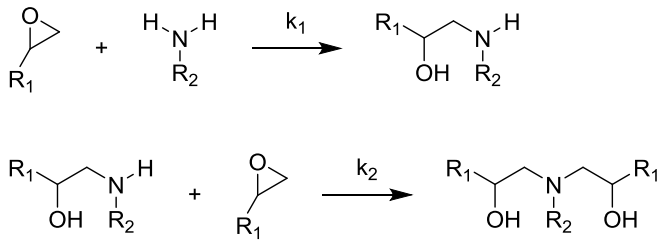

Figure 10. Reaction of epoxy resins with amine curing agents.

When diepoxy pre-polymers ($f_n = 2$) are reacted with diamines ($f_n = 4$) in a stoichiometric ratio the result is a three dimensional macromolecule as gelation occurs.[30]

If the curing temperature is not high enough, vitrification may occur as the mobility of the molecules becomes restricted. When vitrification occurs, the rate of the reaction decreases; therefore, post curing at higher temperatures is usually employed to achieve full conversion.[30] Extent of cure is typically measured via differential scanning calorimetry (DSC) or Fourier transform infrared spectrometry (FTIR).[30, 32]

1.7 Bio-based Epoxy Resins

Renewable bio-based resources can be defined as "*any animal or vegetable species which is exploited without endangering its survival and which is renewed by biological (short term) instead of geochemical (very long term) activities*."[33] The term bio-based should not be confused with bio-degradable, which is an inherent property of the material itself. The current market demand is for bio-based epoxy resins with high performance properties as opposed to epoxy resins with biodegradable properties.[4] A great deal of progress toward the development and engineering of bio-based epoxy resins has been reported in the literature over the last few decades.

Epoxidized vegetable oils are some of the most common commercial examples of bio-based epoxy pre-polymers. Unfortunately, these modified triglycerides have long hydrocarbon chains that lead to a low crosslink density and a high degree of flexibility in the polymer backbone, resulting in poor thermomechanical properties.[34-38] Another noteworthy bio-based epoxy building block recently reported in the literature was isosorbide, a heterocyclic compound derived from glucose.[39-41] Interestingly, cured isosorbide-based epoxies display relatively high T_gs (approximately 73–110 °C when cured with isophorone diamine) that can be attributed to the rigidity provided by the fused heterocyclic rings. However, these resins are plagued by their hydrophilicity.[39, 41]

Recently, Hu et al. reported a cellulose-derived furan-based epoxy resin.[42, 43] In their comparative study, the authors determined that substituting a furan ring in place of the benzene ring in epoxy-amine systems increased both T_g and E' at room temperature. Again, these properties are most likely attributed to the rigidity provided by the heterocyclic furan ring. In addition, the authors hypothesized that additional hydrogen bonding between the oxygen of the furan ring and the hydroxyl groups formed during curing may increase the thermomechanical properties. Still, the additional methylene bridges between the furan ring and both glycidyl ether groups decrease the structural rigidity; resulting in a T_g of only 71 °C. Examples of the aforementioned bio-based epoxy resins are presented in *Figure 11*.

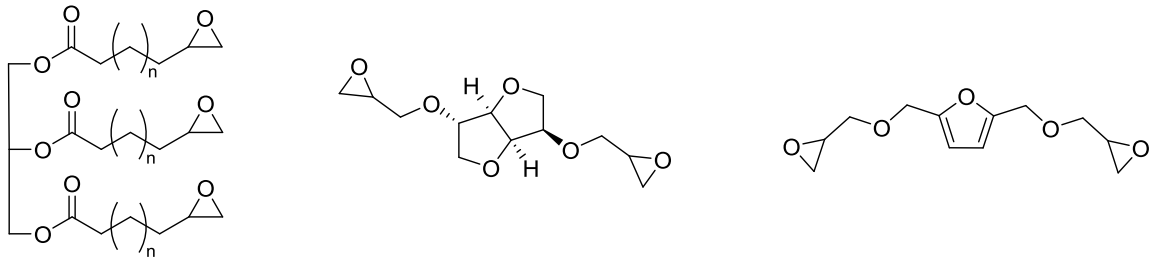

epoxidized triglycerides

diglycidyl ether of isosorbide

diglycidyl ether of bis(hydroxymethyl)furan

Figure 11. Examples of bio-based epoxy resins.

1.8 Lignin

The desirable thermomechanical properties exhibited by BPA-based epoxy resins are undoubtedly owed to the rigidity provided by their aromatic character. Found in the cell walls of vascular plants, lignin is the second most abundant natural resource compromising up to 30 % by weight of lignocellulose; a complex matrix of lignin, cellulose, and

hemicellulose.[44-47] Furthermore, lignin is considered the only readily abundant renewable source of aromatic molecules.[44-46] With estimates of $5–36\times10^8$ tons generated annually on earth, lignin is a highly attractive raw material for the production of renewable polymer building blocks for synthetic bio-based epoxy resins.[33] Extensive research is already ongoing toward the strategic depolymerization of lignin and the isolation of high-value specialty platform chemicals. Several groups have reported pyrolysis of lignin to bio-oils rich in guaiacols and other substituted phenols.[48-50]

Lignin constitutes approximately 25–35 % by weight of gymnosperms (softwoods) and 18–25 % by weight of angiosperms (hardwoods).[33, 45] The structural rigidity and support found in these woody plants is afforded by the complex aromatic structure of lignin. This randomly and highly cross-linked, heterogeneous biomacromolecule is composed of various (methoxy)phenylpropenyl units that are primarily covalently bonded together via β-O-4 linkages.[33, 47] Collectively known as monolignols, there are three main phenolic precursors that plants use to biosynthesize lignin via an enzyme initiated dehydrogenative polymerization. A simplified representation of the polymerization of monolignols to lignin is given in *Figure 12*. The difference between the structures of the building blocks (*p*-coumaryl alcohol, coniferyl alcohol and sinapyl alcohol) is the number of methoxy groups present (see *Figure 13*). The molecular structure of lignin is determined primarily by the ratio of these three precursors that can vary greatly between different plant species. Approximately 95 % by weight of the composition of softwood lignin is generated from coniferyl alcohol with only a small fraction derived from *p*-coumaryl alcohol.[33] Contrastingly, hardwood lignins are derived almost equally from coniferyl alcohol and sinapyl alcohol with no significant contribution to the composition from coumaryl

alcohol.[33] Grass lignin is derived from approximately 70 % coniferyl alcohol, 25 % sinapyl alcohol, and 5 % coumaryl alcohol. The composition of monolignols used to biosynthesize the three different types of lignins mentioned is given in *Figure 14*.

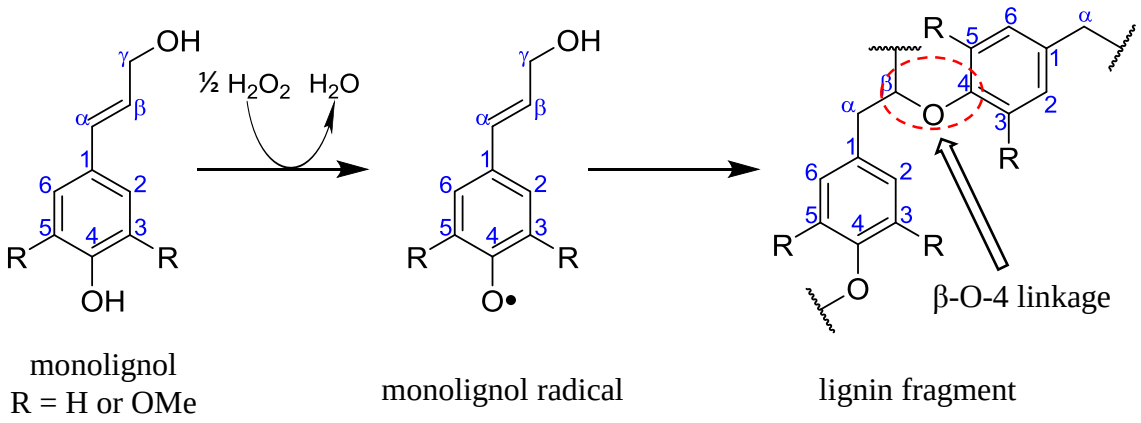

Figure 12. Simplified schematic presenting formation of lignin and β-O-4 linkages from monolignols.

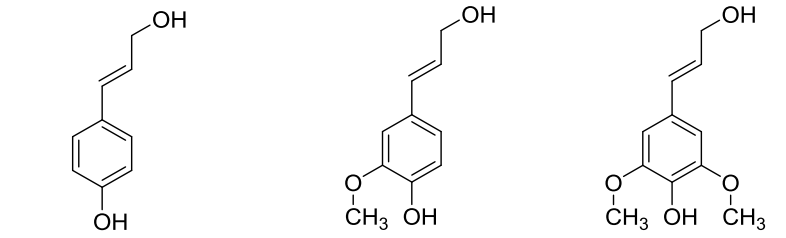

Figure 13. Primary lignin precursors.

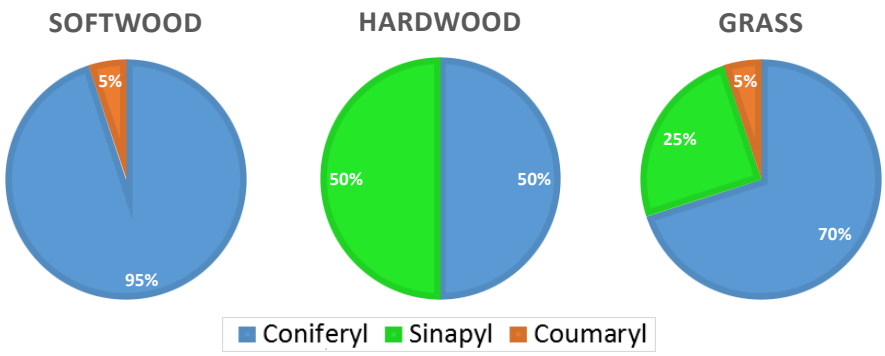

Figure 14. Composition of precursors used in biosynthesis of softwood, hardwood, and grass lignins.

Delignification is the process of separating and isolating lignin from lignocellulosic biomass so that cellulose may be used in paper production processes. The pulp and paper industry is the largest contributor to lignin production, with estimates ranging from 50–70 million tons generated annually as a byproduct of the wood pulping processes.[33] Unfortunately, more than 98 % of the lignin produced by these processes is either burned up in recovery boilers used to produce energy or disposed of in waste streams.[33, 45] Meanwhile, less than 2 % of the lignin produced or about 1 million tons per year is used to manufacture specialty chemicals.[45, 51] This represents an incredible misuse of an abundant renewable source of aromatics that potentially offers high value as a feedstock for the polymer industry.

The two most common industrial chemical processes for wood delignification are the alkaline (Kraft) process and the acid sulfite (Klason) process. Invented by Carl F. Dahl in 1879, the Kraft process is currently responsible for a majority (>95 %) of all lignin generated annually.[33, 44, 45, 51] In general, this process involves treating wood with sodium hydroxide and sodium sulfide (known as the white liquor) at 170 °C to cleave

lignin-cellulose linkages and depolymerize lignin.[33] Cellulose is isolated for papermaking and a waste stream known as the black liquor is generated. The black liquor is an aqueous mixture of lignin, hemicellulose, sugars, and inorganics. Lowering the pH of the black liquor decreases the solubility of the lignin in the aqueous solution, allowing for the separation of the lignin via precipitation.[33] A simplified process diagram of the Kraft process is given in *Figure 15*. In the Kraft process, the black liquors are typically burned to provide additional energy to the pulp and paper plants. In contrast to the Kraft process, the Klason process exposes wood to a sulfite or a bisulfite salt solution at 140–170 °C to isolate the cellulose. This process incorporates sulfonate groups into the lignin structure, cleaving lignin-cellulose bonds that produces a waste stream of lignosulfonates (sulfonated lignin) and hemicellulose sugars. The majority of lignin produced for specialty chemicals and applications is lignosulfonates, and the leading producer of lignosufonates worldwide is Borregaard LignoTech.[33] Other delignification techniques such as Organosolv and steam explosion represent "greener" processes; however, they are still in early or developmental stages and are beyond the scope of this thesis.[45]

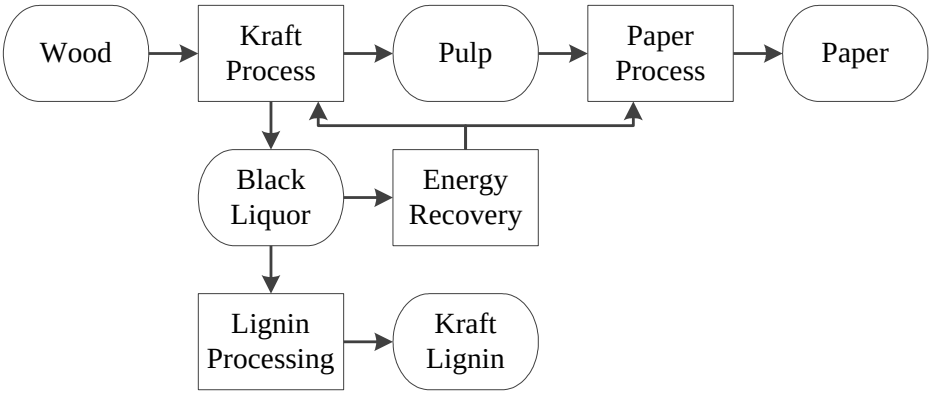

Figure 15. Process flow diagram for production of Kraft lignin.

1.9 Vanillin

Vanillin (4-hydroxy-3-methoxybenzaldehyde) is a single aromatic phenolic aldehyde and the primary constituent of the extract of vanilla beans harvested from *Vanilla* orchid species.[52] In the green beans of *Vanilla* pods where it exists as a vanillin glucoside, vanillin lacks the characteristic flavor and scent of vanilla extract. After harvesting, the beans mature, changing in color from green to brown, and vanillin is produced via enzymatic hydrolysis as shown in *Figure 16*.[52] Vanillin that has been separated from glucose possesses the distinctive aroma and sweet flavor characteristic of vanilla extract.

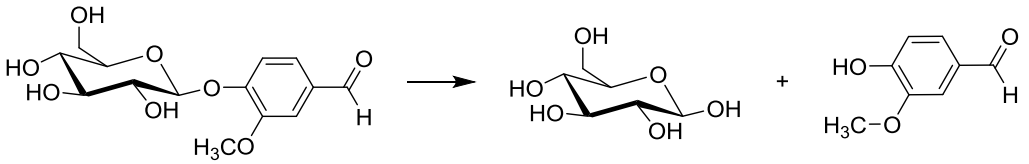

vanillin glucoside glucose vanillin

Figure 16. Enzymatic hydrolysis of vanillin glucoside to glucose and vanillin.

Natural vanilla extracted from the beans of *Vanilla* orchids makes up only a fraction of the total vanilla flavor and fragrance market (< 1%), where it is generally sold as a dilute mixture of several hundred compounds in ethanol.[51] Instead, commercial production of vanillin is dominated by synthetic routes. The leading pathway to synthetic vanillin remains via condensation of petrochemical derived guaiacol with glyoxylic acid to form vanilmandelic acid, which is subsequently converted to vanillin via oxidative decarboxylation.[51] This pathway (see *Figure 17*) currently accounts for approximately 85 % of vanillin production.[51, 53, 54] Interestingly, vanillin can be produced from the

lignosulfonates generated by the sulfite process of the pulp and paper industry. First developed in 1936, this bio-based route involves the degradation and oxidation of the lignin obtained from the pulping process.[47, 52] In the mid-1980s, lignin was the major source of vanillin production and a single pulp and paper mill in Canada supplied approximately 60 % of the world's vanillin[52]; however, as of 2004, lignin to vanillin production only accounts for 15 % of the vanillin market.[53] The decline of vanillin production from lignin can be attributed to the large amounts of environmentally unfriendly waste produced by this process and diminish of the sulfite pulping process in favor of the Kraft process.[53] Borreegaard, a Norwegian company, has developed a method that integrates the production of vanillin into their sulfite pulping process, which includes a recycling of the copper catalyst used for lignosulfonate oxidation.[47]

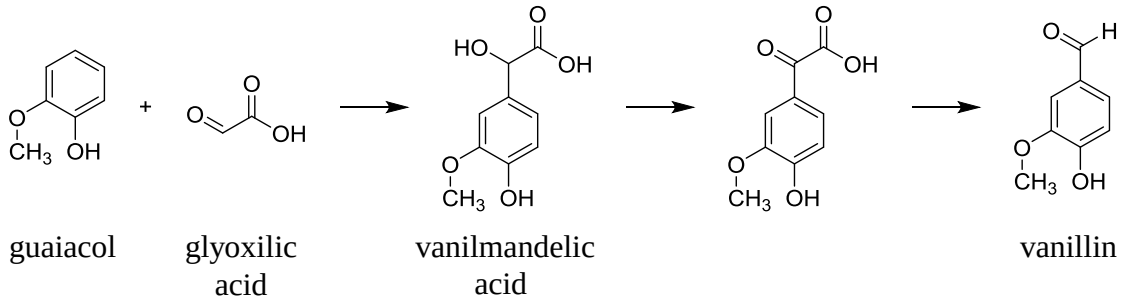

Figure 17. Synthetic pathway to vanillin from guaiacol.

While Borreegaard remains the only commercial manufacturer of lignin derived vanillin, several proposals for processes that integrate the production of vanillin from Kraft lignin have recently been reported in the literature.[51, 54, 55] A simplified flow diagram of the integrated Kraft lignin to vanillin process shown in *Figure 18* was adapted from Borges da

Silva et al.[54] The proposed method begins with the extraction of lignin from a portion of the black liquors via traditional precipitation while the remaining black liquor is sent to recovery boilers. Next, the alkaline lignin is sent to an oxidation bubble reactor.[51, 54, 56] The reaction mixture is then sent to a series of separation processes including membrane processes which separate out higher molecular weight lignins and ion exchange processes which convert sodium vanillate to vanillin.[54] The proposed Kraft lignin to vanillin process represents a shift toward bio-based vanillin once again.

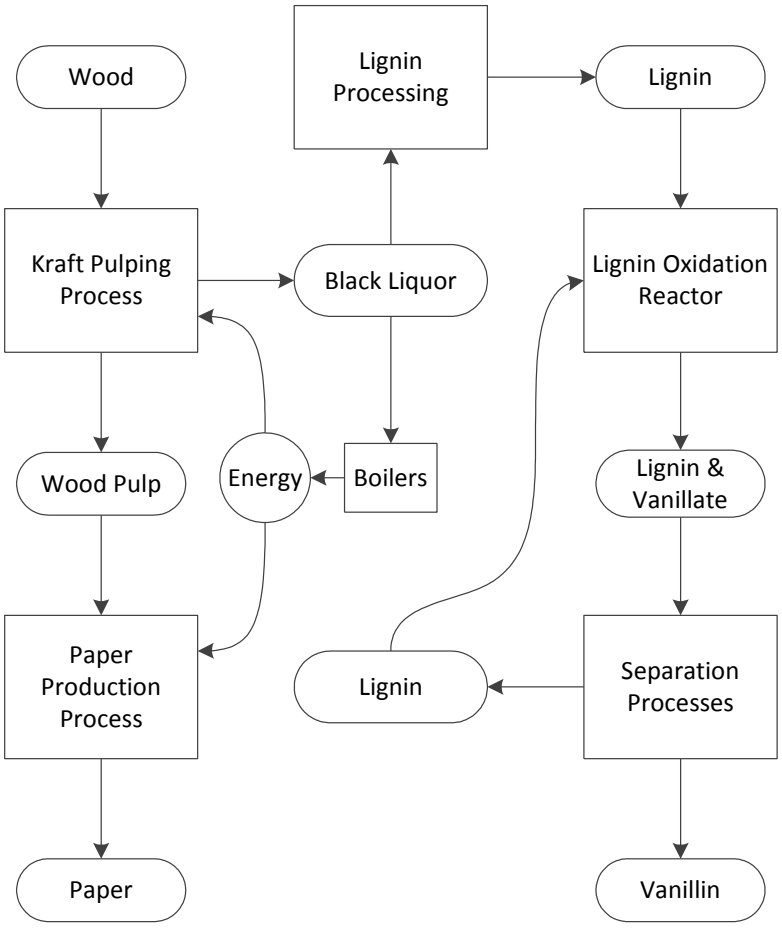

Figure 18. Production of vanillin from Kraft lignin.
Adapted from Borges da Silva et al.[54]

Vanillin is a versatile platform chemical readily oxidized to vanillic acid or reduced to vanillyl alcohol (see *Figure 19*). Vanillin and its redox forms are potential building blocks for the synthesis of epoxy resins and composites. For example, Auof et al. reported the synthesis of a bio-based epoxy resin from vanillic acid via chemo-enzymatic epoxidation with lipase B from *C. antarctica*.[57] Distinct from traditional single step epoxidations with epichlorohydrin, this approach is a two-step process beginning with the allylation of vanillic acid with allyl bromide followed by the epoxidation of the double bond. In a recent review, Koike reports a vanillin-based epoxy synthesized via coupling of two equivalents of vanillin with one equivalent of pentaerythritol, followed by subsequent epoxidation with epichlorohydrin.[58] Interestingly, a diglycidyl ether of vanillyl alcohol (DGEVA) was first reported in 1963; however, it seems that this resin was never commercialized nor studied extensively.[59] More recently, Fache et al. reports the synthesis of epoxy resins from vanillin derivatives.[60, 61] The researchers prepared single aromatic diglycidyl ethers from three different vanillin-based compounds: vanillyl alcohol, vanillic acid, and methoxyhydroquinone. All three of these vanillin-based epoxy resins displayed promising thermomechanical properties when cured with isophorine diamine (T_gs = 97–152 °C). The key difference between these three resins and current commercial BPA-based resins is that vanillin-based resins have a methoxy attached *ortho* to the glycidyl ether of their aromatic rings. However, the authors did not study the direct effect of the methoxy group on cured polymer properties. The various reaction pathways reported in the literature are summarized in *Figure 20*. In this thesis, a new bio-based epoxy resins was synthesized from vanillyl alcohol and the effect of the methoxy moiety on cured polymer properties was investigated via dynamic mechanical analysis (DMA).

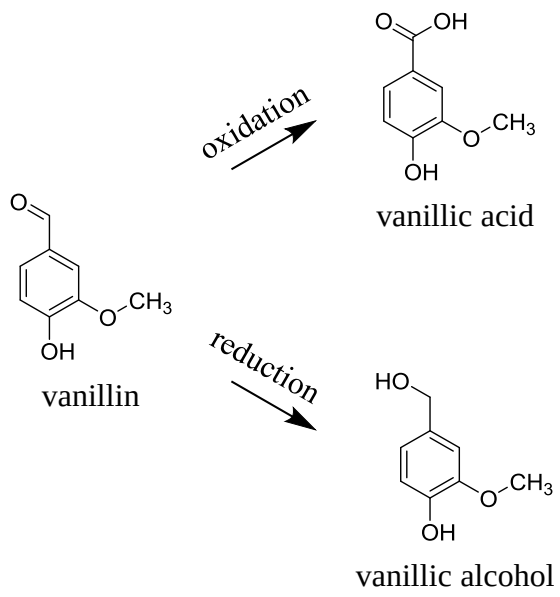

Figure 19. Oxidation and reduction of vanillin.

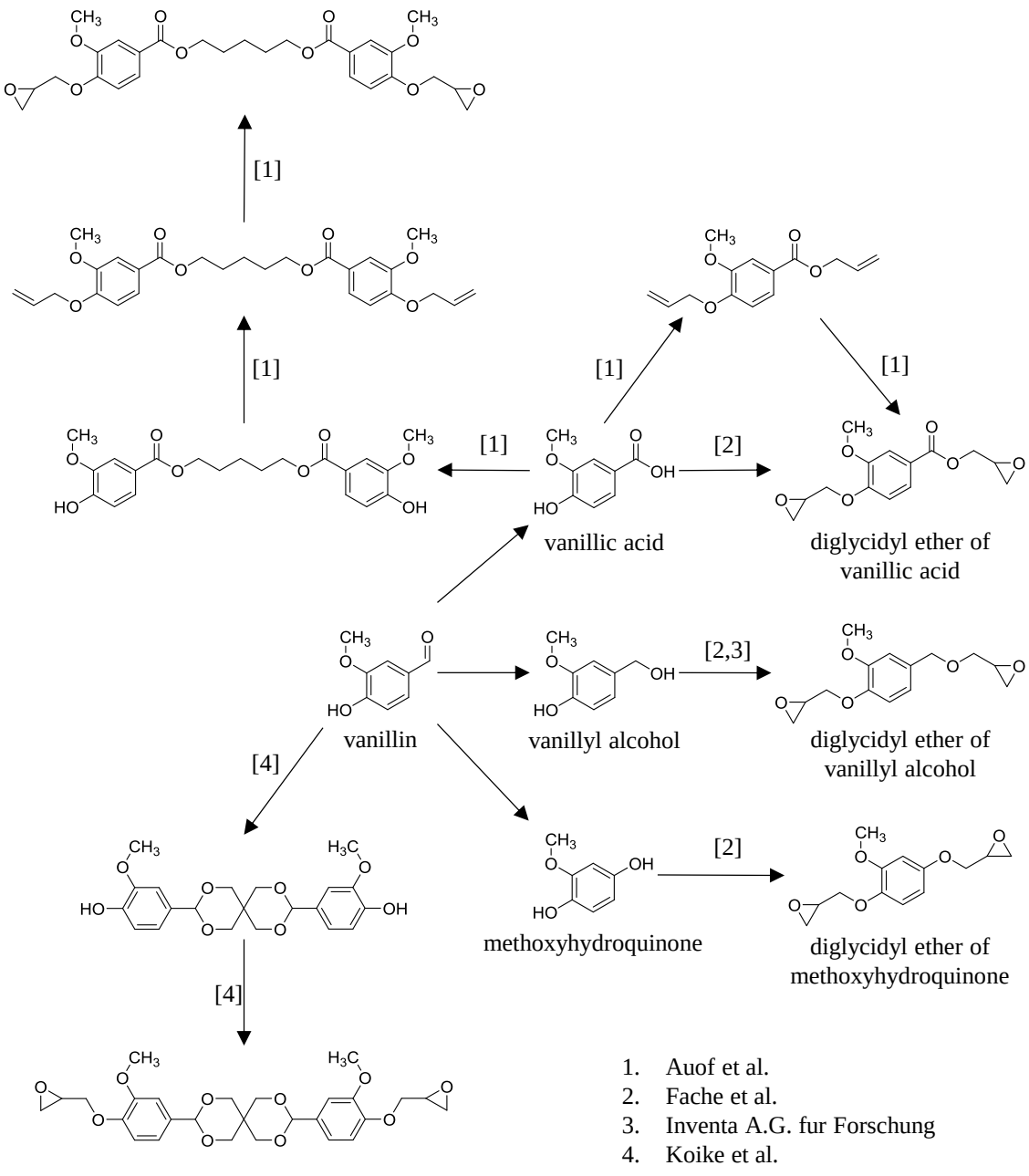

Figure 20. Schematic detailing the various routes to vanillin-based epoxy resins reported in the literature.

Chapter 2

Characterization Methods

2.1 Introduction

This chapter seeks to describe the main techniques that were employed to analyze and characterize molecules and resins that were obtained, purchased, and/or synthesized during the course of this study. The fundamental concepts and theories of each characterization technique are discussed in their respective sections. However, the experimental details and analysis obtained through using these techniques will be discussed in later chapters. The following techniques are discussed in this chapter: Nuclear magnetic resonance spectroscopy (NMR), Fourier transform infrared spectroscopy (FTIR), gel permeation chromatography (GPC), and dynamic mechanical analysis (DMA).

2.2 Nuclear Magnetic Resonance (NMR) Spectroscopy

Nuclear magnetic resonance (NMR) spectroscopy is arguably the most useful and widely used spectroscopy technique. This technique is a powerful tool that can be used to confirm and/or determine the structure of a molecule.[62-65] NMR takes advantage of the change in the magnetic energy of nuclei that occurs when they are placed in the presence of a magnetic field. Following the independent research of Felix Bloch and Edward Purcell in 1945, the first commercial NMR spectrometer was produced by Varian in 1953.[63]

The nuclei of certain elements and their isotopes have a characteristic spin known as nuclear spin (I).[63-65] Nuclei can have zero spin ($I = 0$), integer spins ($I = 0, 1, 2, 3\ldots$), or half integer spins ($I = 1/2, 3/2, 5/2\ldots$).[63] The numerical value of I can be obtained through vector addition of the individual spin quantum numbers of the protons and neutrons such that neutron spins cancel other neutrons spins and proton spins cancel other proton

spins. The spin quantum number (s) has a value of ½.[63, 65] Therefore, nuclei with an even number of protons and an even number of neutrons (having an even mass number), such as ^{12}C, ^{16}O, and ^{32}S, have zero spin. Nuclei having zero spin do not produce NMR spectra. Nuclei with an odd mass number, in which the number of protons (or the number of neutrons) is odd will have half integer spins. Examples of nuclei with half integer spins include ^{1}H, ^{11}B, ^{13}C, ^{19}F, and ^{31}P.[62-64] Finally, nuclei in which both the number of protons and number of neutrons are odd will have integer spins. Examples of nuclei with integer spins include ^{2}H and ^{14}N.

Nuclei having spins of I = ½ are dipolar nuclei. Dipolar nuclei are important for NMR analysis because they act as spherical bodies having a uniform charge distribution.[64] A spinning nucleus generates a magnetic field and the resulting nuclear magnetic moment (μ) is directly proportional to its nuclear spin. This relationship is given by Equation (1):

$$\mu = \gamma I \hbar \tag{1}$$

where $\hbar$ is the reduced Planck's constant ($\hbar = h/2\pi$), h is Planck's constant, and γ is the gyromagnetic ratio.[64] The gyromagnetic ratio is a constant and is characteristic for each specific nucleus.[62-65] When a spinning nucleus is placed in the presence of an external magnetic field (B_0), the nuclear moments orient themselves. However, there are only a certain number of allowable orientations. According to the principles of quantum mechanics, a nucleus with spin I will have $2I + 1$ possible orientations, which are determined by the values of the magnetic quantum number (m_I). m_I may have values of $-I$, $-I + 1$, $-I + 2$, ... I. For example, for nuclei with a spin of I = ½, m_I has values of - ½ and + ½.[63-65]

The energy (E) associated with the interaction of the nucleus with an applied magnetic field ($\boldsymbol{B_0}$) is proportional to the nuclear magnetic moment and the strength of the applied magnetic field. This relationship is given by Equation (2):

$$E = -\gamma m_I \hbar \boldsymbol{B_0}. \tag{2}$$

The change in energy (ΔE) associated with a nuclear magnetic transition is given by Equation (3):

$$\Delta E = \gamma \Delta m_I \hbar \boldsymbol{B_0} = \gamma \hbar \boldsymbol{B_0} \tag{3}$$

where $\Delta m_I = \pm 1$ because only single quantum transitions may occur. The change in electromagnetic radiation is also defined as Equation (4):

$$\Delta E = h\nu \tag{4}$$

where ν is the resonance frequency of the electromagnetic radiation. Therefore, combining Equations (3) and (4) gives Equation (5):

$$h\nu = \gamma \hbar \boldsymbol{B_0}. \tag{5}$$

Equation (5) can be rearranged to the following relationship given by Equation (6):

$$\nu = \frac{\gamma \hbar \boldsymbol{B_0}}{h} = \frac{\gamma \boldsymbol{B_0}}{2\pi} \tag{6}$$

Therefore, Equation (6) states that if a nucleus with a gyromagnetic ratio is placed in a magnetic field of strength $\boldsymbol{B_0}$, that nucleus will exhibit a resonance frequency which causes the nucleus to change its spin orientation. The resonance frequency increases with the increasing strength of the magnetic field.[63-65]

When a nucleus with a spin is placed in the magnetic field it will assume one of its $2I + 1$ orientations with respect to the magnetic field. The orientations have different energies. A nucleus that is aligned with the external magnetic field is of lower energy than

a nucleus that is aligned against the external field.[62-65] These alignments are at a fixed angle with respect to the magnetic field rather than being perfectly parallel or anti-parallel to the external field.[63-65] The nuclei spin at a fixed frequency (Larmor frequency) and specific angle relative to this magnetic field such that the magnetic moment vectors move in a circular path as shown in *Figure 21*.[64, 65] Dipolar nuclei have two possible orientations which are of the same energy when not placed in a magnetic field. However, when in a magnetic field, the lower energy state is the α spin orientation (m_I = + ½) and the higher energy state is in the β spin orientation (m_I = - ½).[62, 64, 65] Increasing the strength of the magnetic field increases the energy difference between these two states. Since the only allowed transitions are $\Delta m_I = \pm 1$, energy can either be absorbed as the nucleus moves from α state to β state or emitted as the nucleus moves from β state to α state.[65]

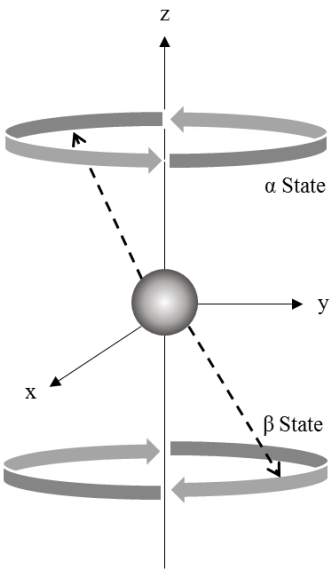

Figure 21. Nuclear spins orientation relative to the magnetic field.

NMR samples are at thermal equilibrium; therefore, the distribution of the nuclei in the two states is determined by the Boltzmann distribution given by Equation (7):

$$\frac{N_\beta}{N_\alpha} = e^{-h\nu/kT} \tag{7}$$

where N_α and N_β represent the number of nuclei with spins in the α and β states, respectively, *T* is absolute temperature, and *k* is Boltzmann's constant.[63-65] This means that when $N_\alpha > N_\beta$ there is a net absorption of energy and an NMR signal is produced, which is proportional to the number of nuclei generating it. If the constant magnetic field was applied to the nuclei with enough power, eventually the number of nuclei in the two states would equalize and no more absorption would occur. This is known as saturation.[63] Relaxation occurs when the nuclei are brought back down from the β state to the α state where the amount of time this takes is called the relaxation time.[65]

The difference in the energies of the two spin states is proportional to the strength of the external magnetic field; so, strong magnets are needed to generate sufficient separation of the spin states such that they fall into the radio frequency region. Most modern NMR spectrometers use magnets that can generate fields of 1 to 20 T that give rise to energy differences of 20 to 900 MHz.[64] In this research, a Varian 400 MHz Fourier Transform NMR Spectrometer was utilized. Fourier transform NMR uses short pulses of strong radio frequency to simultaneously excite all the Larmor frequencies in a sample. Then the spins experience free induction decay (FID) as they return back to equilibrium. The FID produced is a complex time domain signal. A computer uses a Fourier transform mathematical analysis to convert the FID into a frequency domain spectra that can be analyzed.[63-65]

The frequency domain spectra displays nuclei with different chemical shifts (δ) in units of parts per million (ppm). The different chemical shifts of the different nuclei are caused by a phenomenon known as shielding. The electrons of the atoms move in response to the applied external magnetic field, generating an opposing secondary magnetic field (with the exception of electrons in pi orbitals of aromatic nuclei). This secondary magnetic field shields the nuclei from the stronger external magnetic field. Therefore, the strength of the magnetic field needed for the nuclei to achieve resonance at a constant radio frequency is increased. Consequently, those nuclei that experience more shielding will produce resonance signals at lower ppm values and will display upfield while those nuclei that are de-shielded will produce signals downfield at higher ppm values. Since no two magnets produce the same field, a standard is used as a reference. The most widely used reference standard for ^{1}H and ^{13}C NMR is tetramethylsilane (TMS).[64, 65] The chemical shift is therefore given by Equation (8):

$$\delta = \frac{\nu_{\text{reference}} - \nu_{\text{sample}}}{\nu_{\text{reference}}} \times 10^{6} \text{ ppm} \quad (8)$$

where $\nu_{\text{reference}}$ and ν_{sample} are the resonance frequencies of the reference standard and the sample, respectively. This scale is independent of the applied field.[65]

2.3 Fourier Transform Infrared (FTIR) Spectroscopy

Fouier transform infrared (FTIR) spectroscopy is a useful technique used to measure the absorption, transmission, and reflectance of infrared (IR) radiation. This optical technique allows for the detection of molecular bond vibrations and determination of functional groups present.[7, 63] Infrared radiation is a type of electromagnetic radiation with frequencies (ν) less than visible light but greater than microwave radiation and with a wavelength (λ) of approximately 10^{-3} cm.[7] The wavenumber ($\bar{\nu}$), or the number of

wavelengths in a centimeter (cm^{-1}), is the most common unit used for IR spectroscopy because it provides a direct proportionality with the energy and frequency.[63] Infrared spectroscopy encompasses near IR (12800-4000 cm^{-1}), mid IR (4000-200 cm^{-1}), and far IR (200-10 cm^{-1}), but the most commonly used region is mid IR in the range of 4000-670 cm^{-1}.[63]

IR radiation does not contain enough energy to bring about electronic transitions as is the case in ultraviolet (UV) and visible light radiation. When a molecule absorbs IR light, it experiences a change in its dipole moment that causes a vibration or rotation.[63] Generally, IR spectroscopy can be used to discern information about the structure of a molecule based on the various molecular vibrations that are often characteristic and predictable. Stretching vibrations include symmetric and asymmetric stretching while bending vibrations include rocking and scissoring (see *Figure 22*).[7, 63] If a molecule does not experience a net change in dipole moment when it stretches or vibrates then it will not absorb IR. O_2, N_2, and Cl_2 are homonuclear species with zero dipole moments and therefore do not absorb energy when placed in an IR field.[63] These molecules are IR inactive such that they do not produce IR spectra.

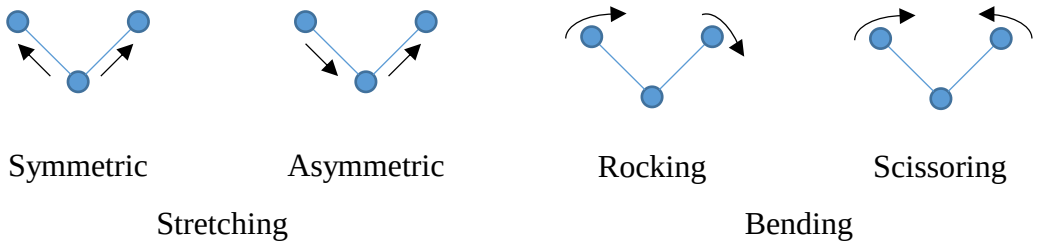

Figure 22. Types of molecular vibrations.

An IR spectrometer is an instrument that directs a beam of IR light through a sample and measures the frequencies of light absorbed by the sample. Early IR spectrometers were dispersive instruments that dispersed IR radiation of all frequencies and measured them each individually. This type of instrument suffered mainly due the fact that it could only measure one frequency at a time requiring strong IR sources and resulting in lengthy scan times.[7] Newer IR spectrometers are Fourier transform (FT) instruments that employ a Michelson interferometer. The interferometer employs a transparent beam splitter with both fixed and moving mirrors that split an incoming single beam and recombine the beam to produce an interferogram. The beam splitter is typically made of a thin film of germanium or silicon on CsI, NaCl, or KBr for mid-IR instruments or a thin film of Fe_2O_3 on CaF_2 for near-IR instruments. These materials allow for 50 % of the light to be reflected and 50 % of the light to be transmitted.[63] All frequencies of light are measured simultaneously and the interferogram, which is a complex time domain signal, is sent to a detector. A computer uses a Fourier Transform algorithm to convert the signal to a frequency domain signal that can be interpreted by the user.[7, 63]

In this thesis, near IR spectroscopy was principally utilized to determine the extent of cure of epoxy-amine resins. Generally, the first overtones of strong vibrations in the mid IR region and combination bands are present in the near IR region.[7] Since there are fewer overlapping bands in the near IR region and the intensity of these bands is lower allowing for utilization of thicker samples, near IR is usually employed to study epoxy resin systems. Epoxy resins characteristically display a band corresponding to the second overtone of the oxirane ring stretching at approximately 4530 cm^{-1}.[30] In addition, several characteristic bands corresponding to stretching of amine hardeners are exhibited in the near IR region,

making the near IR region an invaluable tool for studying epoxy-amine systems. A more in depth explanation of the measurement of extent of cure of epoxy-amine systems using near IR spectroscopy is given in Chapter 4.

2.4 Gel Permeation Chromatography (GPC)

As one of the most valuable analytical tools to the field of polymer science, gel permeation chromatography (GPC) is used to determine the average molecular weight and dispersity of a polymer sample.[2, 63] GPC makes use of the principles of size exclusion chromatography (SEC) to separate polymer distributions based on their size. In this technique, a dilute polymer solution is prepared by dissolving the polymer in a solvent at a concentration typically less than 2 mg/ml followed by filtering the solution to remove any larger particulates.[2] A solvent (most commonly tetrahydrafuran) called the mobile phase is flowed through a small diameter column, packed with highly porous beads, at a rate of 1-2 ml/min. These porous beads, which act as the stationary phase, are usually made of a styrene-divinyl benzene cross-linked gel with a pore size range of $10\text{-}10^7$ Å.[2, 63] The polymer solution is then injected into the column and carried through the column with the mobile phase. As the polymer encounters the porous beads, some of the polymer will leave the mobile phase and enter the stationary phase. Smaller polymers are able to enter the pores of the beads; however, larger polymers are unable to enter these pore so they pass along around the outside of beads. Therefore, the largest polymers will elute first and the smallest polymers that are trapped in the pores will have the highest retention times. The technique is usually monitored by a detector such as a refractive index detector or a UV detector. The signal is sent to a computer that converts the signal into a chromatogram of elution time vs. intensity. This technique is typically not able to separate isomers with

similar molecular sizes.[63] Number average (M_n) and weight average (M_w) molecular weights and dispersities can be determined after developing a calibration curve from standards with known molecular weights (usually polystyrene).[2, 63]

2.5 Dynamic Mechanical Analysis (DMA)

Polymers that exhibit both a tendency to flow (viscous characteristic) and ability to recover (elastic behavior) in response to a mechanical deformation are said to be viscoelastic.[2, 66] Dynamic mechanical analysis (DMA) is a widely used technique for measuring the viscoelastic properties of a polymer as a function of temperature and time. The relationship between stress (σ) and strain (ε) for an ideal elastic solid is given by Hooke's Law shown in Equation (9):

$$\sigma = E\varepsilon \tag{9}$$

where E is the tensile or Young's modulus.[2, 66] On the other hand, the relationship between stress and strain for an ideal viscous liquid is given by Equation (10):

$$\sigma = \eta \frac{\mathrm{d}\varepsilon}{\mathrm{d}t} \tag{10}$$

where η is the viscosity.[2, 66] During dynamical mechanical testing, a sinosiodal strain is applied to the sample of known geometry. This strain is given by equation (11):

$$\varepsilon = \varepsilon^o \sin(\omega t) \tag{11}$$

where ε^o is the amplitude of the applied strain and ω is the angular frequency of oscillation.[2, 66] The resulting stress measured in response to this strain is given by Equation (12):

$$\sigma = \sigma^o \sin(\omega t + \delta) \tag{12}$$

where σ^o is the amplitude of the stress response and δ is the phase angle between the stress and the strain.[2, 66] For an ideal elastic $\delta = 0$.

Viscoelastic materials exhibit a complex modulus (E^*) made up of both an in phase storage modulus (E') and an out of phase loss modulus (E''), which are related through Equation (13), that possesses both real and imaginary components[2, 66]:

$$E^* = E' + iE'' = \sqrt{E'^2 + E''^2} \tag{13}$$

E' is a measure of the potential energy stored due to elasticity and is given in Equation (14):

$$E' = \frac{\sigma^o}{\varepsilon^o} \cos(\delta) \tag{14}$$

whereas the E'' is a measure of the energy lost due to internal motions and is given by Equation (21):

$$E'' = \frac{\sigma^o}{\varepsilon^o} \sin(\delta) \tag{15}$$

The ratio of the loss modulus to the storage modulus is given by Equation (16):

$$\tan \delta = \frac{E''}{E'} \tag{16}$$

A DMA thermograms, as shown in *Figure 23*, is a plot of E', E'', and tan δ vs. temperature at a specific frequency. Polymers at low temperatures are stiff and glassy. Glassy polymers usually have high E' because their long coordinated motions are restricted.[1] As these polymers are heated they begin to soften as they go through their glass-rubber transition.[1, 2, 66] The temperature at which a polymer transitions from glassy to rubbery is known as the glass transition temperature (T_g). The glass transition is a second order phase transition, in contrast to melting, which is a first order transition.[1] As viscoelastic polymers go through their T_g, the E' begins to decrease rapidly as the

polymer approaches its rubbery state. Meanwhile, E'' will increase sharply to a maxima as the polymer transitions from its glassy to rubbery state and long range molecular motions become possible. The temperature corresponding to the peak maxima of the E'' curve or tan δ is often associated with the T_g.[2] The peak of the E'' curve typically corresponds closely to the inflection point of the E' curve.[31] The peak of the E'' curve was used to assign the T_g of the polymers studied in this thesis because the peak of the E'' curve is usually lower than that of the tan δ and thus represents a more conservative estimate of T_g. The rubbery plateau is the region after the T_g in which the E' remains relatively constant with increasing temperature. Thermosetting polymers do not display viscous flow regions as they do not melt.[1]

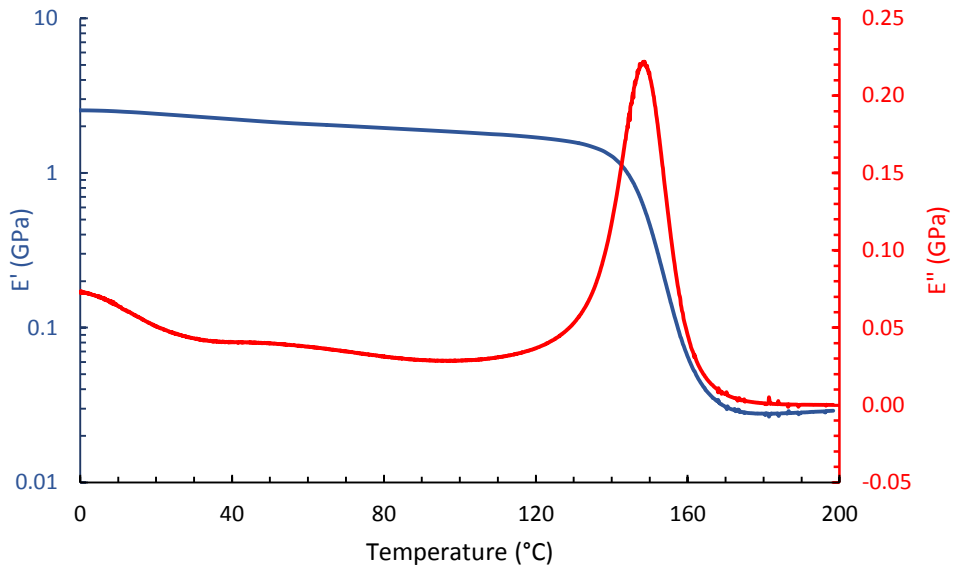

Figure 23. DMA thermogram displaying E' and E'' as a function of temperature.

Chapter 3

Experimental Materials and Methods

3.1 Introduction

This chapter details the experimental materials, methods, and procedures carried out to synthesize and characterize the various monomers and polymers used in this study. The ^{1}H and ^{13}C NMR multiplet assignments, melting points, and high resolution mass spectrometry data of the new monomers and epoxy pre-polymers are given in their respective sections. NMR spectra and mass spectra can be found in Appendix A and Appendix B, respectively.

3.2 Materials

Vanillyl alcohol (4-hydroxy-3-methoxybenzyl alcohol, 99 %), guaiacol (2-methoxyphenol 99+ %), gastrodignenin (4-hydoxybenzyl alcohol, 99 %), bisphenol A (4,4-isopropylidenediphenol, 97 %), tetraethylammonium bromide (TEAB, 99+ %), tetrabutylammonium bromide (TBAB, 99+ %), and chloroform-*d* (99.8 atom % *d*) were purchased from Acros Organics. Dowex® DR-2030 hydrogen form (a styrene-divinylbenzene resin with sulfonic acid functional group), epichlorohydrin (≥ 99 %), and glacial acetic acid (≥ 99 %) were purchased from Sigma Aldrich. Methylene chloride (DCM, 99.9 %), tetrahydrafuran (Optima THF, 99.9 %), hexanes (> 98.5 %), ethyl acetate (> 99.5 %), perchloric acid (60 %), sodium sulfate (anhydrous powder, > 98 %) and a 50 % w/w $NaOH_{(aq)}$ solution were purchased from Fischer Scientific. A 1 % w/v crystal violet in glacial acetic acid solution was purchased from RICCA Chemical Company. Amicure® PACM curing agent (4,4'-methylenebiscyclohexanamine) was obtained from Air Products and Chemicals, Inc. Epon^{TM} Resin 828 (Diglycidyl Ether of Bisphenol A - DGEBA) and

Epon^{TM} 862 (Diglycidyl Ether of Bisphenol F - DGEBF) were obtained from Momentive Specialty Chemicals, Inc. Compressed argon (Ar, 99.999 %) and compressed nitrogen (N_2, 99.998 %) where purchased from Praxair. A polystyrene standard kit (M_n = 492 to 532 Da) was purchased from Waters Corporation. All chemicals were used as received.

3.3 Synthesis of Bisguaiacol

A 500 ml three-neck round-bottom flask equipped with an overhead mechanical mixer, reflux condenser, inlet for dry argon gas, and thermometer was charged with 93.10 g guaiacol (0.75 mol) and 46.25 g vanillyl alcohol (0.30 mol). The mixture was allowed to reflux for 2 hours in a silicone oil bath at 60 °C before 13.94 g (10 wt. %) Dowex DR2030 hydrogen catalyst was slowly added with continuous mixing. The reaction was allowed to continue overnight at 60 °C. The dark amber product was removed from heat and stirring, allowed to cool to room temperature, and then dissolved in approximately 600 ml of methylene chloride. Dowex catalyst was removed via vacuum filtration. The filtrate was washed with 600 ml of deionized water and the organic phase was extracted three times. The organic phase was dried with anhydrous sodium sulfate and concentrated under vacuum. Excess guaiacol was removed via reduced pressure distillation leaving behind a solid bisguaiacol product and some higher molecular weight oligomers with a yield of 70 %. Further purification was achieved on a silica gel column using a hexanes/ethyl acetate gradient. The final product was a mixture of isomers (approximately 82% *p,p'*-, 15% *m,p'*-, 3% *o,p'*-) as shown in *Figure 24*.

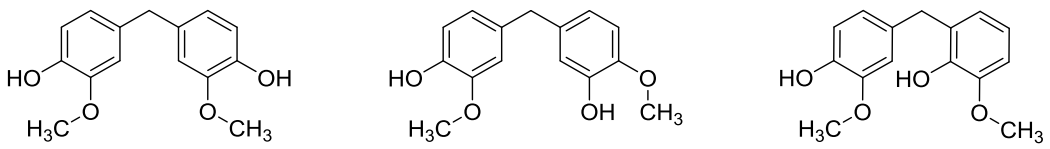

p,p'-bisguaiacol *m,p'*-bisguaiacol *o,p'*-bisguaiacol

Figure 24. Chemical structure of bisguaiacol isomers.

Bisguaiacol was characterized by nuclear magnetic resonance spectroscopy (^{1}H-NMR and ^{13}C-NMR) and time of flight high resolution mass spectrometry (TOF HRMS). The purified *p,p'*-bisguaiacol is a white solid with a melting point of 102-105 °C. The ^{1}H-NMR and ^{13}C-NMR multiplets and the calculated and measured TOF HRMS masses are given below. NMR spectra with peak assignments are available in Appendix A. Mass spectra are available in Appendix B.

^{1}H NMR ($CDCl_3$, 400 MHz) δ ppm 3.83 (6 H, s), 3.85 (2 H, s), 5.51 (1 H, s), 6.65 - 6.71 (4 H, m), 6.85 (2 H, d, *J*=8.19 Hz).

^{13}C NMR ($CDCl_3$, 101 MHz) δ ppm 41.33 (1 C, s), 56.02 (2 C, s), 111.48 (2 C, s), 114.35 (2 C, s), 121.63 (2 C, s), 133.50 (2 C, s), 144.03 (2 C, s), 146.63 (2 C, s).

HRMS (m/z, TOF FD+) ($C_{15}H_{16}O_4$) - Calculated: 260.1049 Da, Found: 260.1068 Da.

3.4 Synthesis of Diglycidyl Ether of Bisguaiacol (DGEBG)

A 250 mL three-neck round-bottom flask equipped with reflux condenser, constant pressure dropping funnel, inlet for dry argon gas, magnetic stir bar, and thermometer was charged with 7.11 g bisguaiacol (27.3 mmol), 25.30 g epichlorohydrin (273 mmol), and 0.90 g tetrabutylammonium bromide (2.79 mmol). The flask was heated to 40 °C for 3

hours with constant stirring. Then, the flask was placed in an ice bath and allowed to cool to approximately 4 °C before 9.60 mL of a 40 % w/w $NaOH_{(aq)}$ solution was added dropwise (30 drops/min) with constant stirring. After the addition of the $NaOH_{(aq)}$ solution, the mixture was removed from the ice bath and left to react overnight at room temperature. The epoxy brine was dissolved in methylene chloride and washed with deionized water. The organic phase was extracted three times, concentrated under reduced pressure, and placed in a vacuum oven overnight. The resulting epoxy was a white solid with a yield of 73 %. Further purification was carried out on a silica gel column using a hexanes/ethyl acetate gradient. The epoxy equivalent weight was determined to be 210 g/eq. ($n \approx 0.15$) before chromatography and 193 g/eq. ($n \approx 0.04$) after chromatography according to ASTM D-1652.[67] The chemical structure is given in *Figure 25*.

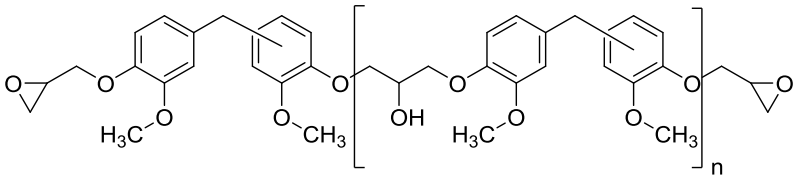

Figure 25. Chemical structure of diglycidyl ether of bisguaiacol.

Diglycidyl ether of bisguaiacol (DGEBG) was characterized by ^{1}H-NMR and ^{13}C-NMR and TOF HRMS. DGEBG is a white solid with a melting point of 112-114 °C. The ^{1}H-NMR and ^{13}C-NMR multiplets and the calculated and measured TOF HRMS masses are given below. NMR spectra with peak assignments are available in Appendix A. Mass spectra are available in Appendix B.

^{1}H NMR ($CDCl_3$, 400 MHz) δ ppm 2.73 (2 H, dd, J=4.88, 2.54 Hz), 2.88 (2 H, dd, J=4.75 Hz), 3.35 - 3.41 (2 H, m), 3.81 (6 H, s), 3.87 (2 H, s), 4.01 (2 H, dd, J=11.51, 5.66 Hz), 4.21 (2 H, dd, J=11.51, 3.71 Hz), 6.65 - 6.72 (4 H, m), 6.85 (2 H, d, J=8.85 Hz). ^{13}C NMR ($CDCl_3$, 101 MHz) δ ppm 41.21 (1 C, s), 45.16 (2 C, s), 50.44 (2 C, s), 56.09 (2 C, s), 70.58 (2 C, s), 112.87 (2 C, s), 114.44 (2 C, s), 121.03 (2 C, s), 135.14 (2 C, s), 146.53 (2 C, s), 149.75 (2 C, s).

HRMS (m/z, TOF FD+) ($C_{21}H_{24}O_6$) - Calculated: 372.1573 Da, Found: 372.1577 Da.

3.5 Synthesis of Diglycidyl Ether of Vanillyl Alcohol (DGEVA)

A 500 mL three-neck round-bottom flask equipped with reflux condenser, overhead mechanical mixer, thermometer, and constant pressure dropping funnel was charged with 30.8 g vanillyl alcohol (0.20 mol), 185.0 g epichlorohydrin (2.0 mol), and 6.45 g tetrabutylammonium bromide (0.02 mol). The flask was heated to 50 °C with constant stirring. Color change was observed from light brown to dark brown after 1 hour. After 3 hours, the mixture appeared to be dark brown and transparent. The flask was removed from the heat, placed in an ice bath, and allowed to cool to approximately 3 °C before 90 ml of a 33 % w/w $NaOH_{(aq)}$ solution was added dropwise (30 drops/min) with constant stirring. The mixture was left to react for another 16 hours overnight with the ice bath melting. The epoxy brine mixture was dissolved in methylene chloride and washed with deionized water. The organic phase was extracted three times, dried with anhydrous sodium sulfate, concentrated under reduced pressure, and placed in a vacuum oven overnight. The resulting pale amber liquid is a mixture of 85 % di-epoxidized vanillyl alcohol and 15 % mono-epoxidized vanillyl alcohol with a total yield of 92 %. Further purification was carried out

on a silica gel column using a hexanes/ethyl acetate gradient to obtain pure DGEVA. The epoxy equivalent weight was determined to be 133 g/eq. ($n \approx 0$) according to ASTM D-1652.[67] The chemical structure of diglycidyl ether of vanillyl alcohol is given in *Figure 26*.

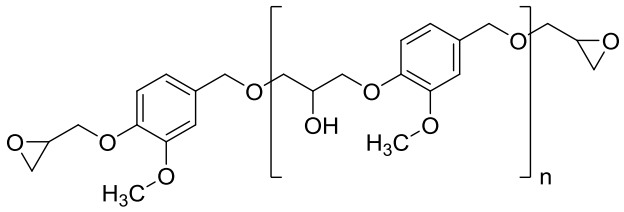

Figure 26. Chemical structure of diglycidyl ether of vanillyl alcohol.

Diglycidyl ether of vanillyl alcohol (DGEVA) was characterized by ^{1}H-NMR, ^{13}C-NMR and TOF HRMS. DGEVA is a white solid with a melting point of 54-55 °C. The ^{1}H-NMR and ^{13}C-NMR multiplets and the calculated and measured TOF HRMS masses are given below. NMR spectra with peak assignments are available in Appendix A. Mass spectra are available in Appendix B.

^{1}H NMR ($CDCl_3$, 400 MHz) δ ppm 2.61 (1 H, dd, J=4.98, 2.64 Hz), 2.74 (1 H, dd, J=4.98, 2.64 Hz), 2.80 (1 H, dd, J=4.98, 4.10 Hz), 2.89 (1 H, dd, J=4.98, 4.10 Hz), 3.15 - 3.21 (1 H, m), 3.36 - 3.40 (1 H, m), 3.40 (1 H, dd, J=11.50, 6.00 Hz), 3.76 (1 H, dd, J=11.43, 2.93 Hz), 3.88 (3 H, s), 4.03 (1 H, dd, J=11.29, 5.42 Hz), 4.23 (1 H, dd, J=11.43, 3.52 Hz), 4.52 (2 H, q, J=11.67 Hz), 6.82 - 6.87 (1 H, m), 6.88 - 6.91 (1 H, m), 6.92 (1 H, d, J=1.76 Hz).

^{13}C NMR ($CDCl_3$, 101 MHz,) δ ppm 44.43 (1 C, s), 45.09 (1 C, s), 50.34 (1 C, s), 51.02 (1 C, s), 56.07 (1 C, s), 70.47 (1 C, s), 70.85 (1 C, s), 73.29 (1 C, s), 111.78 (1 C, s), 114.05 (1 C, s), 120.47 (1 C, s), 131.74 (1 C, s), 147.78 (1 C, s), 149.83 (1 C, s)

HRMS (m/z, TOF FD+) ($C_{14}H_{18}O_5$) - Calculated: 266.1154 Da, Found: 266.1144 Da.

3.6 Synthesis of Diglycidyl Ether of Gastrodigenin (DGEDG)

A 500 mL three-neck round-bottom flask equipped with reflux condenser, overhead mechanical mixer, thermometer, and constant pressure dropping funnel was charged with 24.9 g gastrodigenin (0.20 mol), 149.0 g epichlorohydrin (1.61 mol), and 6.45 g tetrabutylammonium bromide (0.02 mol). The flask was heated to 50 °C with constant stirring. After 5 hours, the flask was removed from the heat, placed in an ice bath, and allowed to cool to approximately 5 °C before 72 ml of a 33 % w/w $NaOH_{(aq)}$ solution was added dropwise with constant stirring. The mixture was allowed to react overnight with the ice bath melting. The epoxy brine mixture was dissolved in methylene chloride and washed with deionized water. The organic phase was extracted three times, dried with anhydrous sodium sulfate, concentrated under reduced pressure, and placed in a vacuum oven overnight. The resulting pale yellow liquid is a mixture of 70 % di-epoxidized gastrodigenin and 30 % mono-epoxidized gastrodigenin with a total yield of 89 %. Further purification was carried out on a silica gel column using a hexanes/ethyl acetate gradient to obtain pure DGEGD. The epoxy equivalent weight was determined to be 119 g/eq. ($n \approx 0.01$) according to ASTM D-1652.[67] The chemical structure of diglycidyl ether of gastrodigenin is given in *Figure 27*.

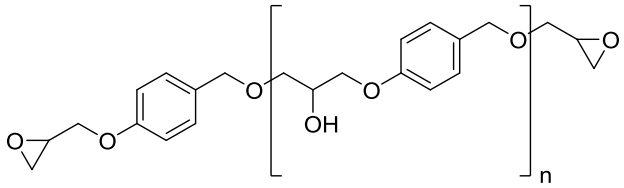

Figure 27. Chemical structure of diglycidyl ether of gastrodigenin.

Diglycidyl ether of gastrodigenin (DGEGD) was characterized by ^{1}H-NMR, ^{13}C-NMR and TOF HRMS. DGEGD is a colorless liquid at room temperature. The ^{1}H-NMR and ^{13}C-NMR multiplets and the calculated and measured TOF HRMS masses are given below. NMR spectra with peak assignments are available in Appendix A. Mass spectra are available in Appendix B.

^{1}H NMR ($CDCl_3$, 400 MHz) δ ppm 2.60 (1 H, dd, J=5.13, 2.79 Hz), 2.75 (1 H, dd, J=4.98, 2.64 Hz), 2.79 (1 H, dd, J=4.98, 4.10 Hz), 2.90 (1 H, dd, J=4.98, 4.10 Hz), 3.15-3.19 (1 H, m), 3.32 - 3.37 (1 H, m), 3.40 (1 H, dd, J=11.43, 5.86 Hz), 3.73 (1 H, dd, J=11.43, 2.93 Hz), 3.95 (1 H, dd, J=11.14, 5.57 Hz), 4.21 (1 H, dd, J=10.99, 3.08 Hz), 4.51 (2 H, q, J=11.63 Hz), 6.87 - 6.93 (2 H, m), 7.24 - 7.30 (2 H, m).

^{13}C NMR ($CDCl_3$, 101 MHz,) δ ppm 44.48 (1 C, s), 44.88 (1 C, s), 50.28 (1 C, s), 51.04 (1 C, s), 68.94 (1 C, s), 70.75 (1 C, s), 73.07 (1 C, s), 114.71 (2 C, s), 129.58 (2 C, s), 130.74 (1 C, s), 158.34 (1 C, s).

HRMS (m/z, TOF FD+) ($C_{13}H_{16}O_4$) - Calculated: 236.1049 Da, Found: 236.1062 Da.

3.7 Characterization of Monomers

Monomers synthesized in this work were characterized by NMR spectroscopy (^{1}H-NMR and ^{13}C-NMR), high resolution mass spectrometry (TOF HRMS), and gel permeation chromatography (GPC). Epoxy titration (ASTM D1652) was used to determine the epoxide equivalent weight.[67] Melting point ranges were measured on a Mel-Temp Electrothermal Melting Point Apparatus and densities at room temperature were measured using a density determination kit and Archimedes' principle according to Equation (17):

$$\frac{\text{solid density}}{\text{liquid density}} = \frac{\text{solid dry weight}}{\text{solid dry weight-solid immersed weight}} \quad (17)$$

where the solid density is the density of the polymer and the liquid density is the density of water at the temperature of the room.[68]

NMR spectra of monomers and pre-polymers synthesized in this work were collected using a Varian 400 MHz Fourier Transform Nuclear Magnetic Resonance Spectrometer. Samples were prepared in chloroform-*d* and the signals were referenced to the solvent peaks (7.26 and 77.3 ppm for ^{1}H and ^{13}C NMR, respectively). ^{1}H-NMR experiments were run for 32 scans at 298 K while ^{13}C-NMR experiments were run for 512 scans at 298 K.

Mass spectrometry measurements were recorded on a Waters GCT Premier High Resolution Time of Flight Mass Spectrometer (TOF MS) using liquid injection field desorption ionization (LIFDI). The analyte was applied to the filament in methylene chloride and the solvent was allowed to evaporate. The voltage field was ramped to 1.2 kV and the filament current was increased to 50 mA. Chloropentaflourobenzene was used as an internal standard (peak at 201.9605 Da).

GPC data were collected on a Waters 2695 Separation Module with three 7.8 × 300 mm columns in series (Waters Styragel HR4, HR2, and HR1) using Optima grade THF as an eluting solvent. The columns were conditioned for 30 min and then equilibrated for 30 min at a flow rate of 1 ml/min. A Waters 2414 Refractive Index Detector (RID) was used to monitor the eluate. GPC samples were prepared by dissolving ~ 3 mg/ml of sample in THF and then filtering with a 0.45 μm nylon membrane. Following column equilibration, each sample was run for 40 min at a flow rate of 1 ml/min. The presence of a single peak was used to qualitatively determine the purity of the epoxy resins.

Epoxy equivalent weights (EEWs) were determined according to ASTM D1652 and are summarized in Table 1.[67] The average repeat unit (n) was calculated based on the experimental EEW. Approximately, 400 mg of epoxy pre-polymer was dissolved in 10 ml of methylene chloride, 10 ml of a tetraethylammonium bromide in glacial acetic acid solution (250 mg/ml), and 6 drops of 0.1% crystal violet indicator in glacial acetic acid solution. The purple solution was titrated to a green color with 0.1 N perchloric acid in glacial acetic acid solution.

Table 1.

Epoxy equivalent weights (EEWs) of neat resins

Epoxy Resin	EEW (g/eq.) [a]	MW (g/mol)	n [b]
DGEVA	133	266 + 210n	0.00
DGEGD	119	236 + 180n	0.01
DGEBG	193	372 + 316n	0.04
Epon 862	172	312 + 256n	0.13
Epon 828	190	340 + 284n	0.14

[a] EEW determined according to ASTM D1652
[b] n = average repeat unit based on EEW and MW

3.8 Extent of Cure

Bimodal resin blends of synthesized epoxy resins and Epon 828 were prepared by mixing the two epoxy resins together at various weight ratios. In this work, W_{DGEVA} represents the weight fraction of DGEVA pre-polymer that is blended with Epon 828 pre-polymer prior to the addition of the di-amine. Likewise, W_{DGEGD} represents the weight fraction of DGEGD pre-polymer that is blended with Epon 828 pre-polymer. For example, a resin blend that is 25 wt. % DGEVA and 75 wt. % Epon 828 prior to the addition of the di-amine is defined as $W_{DGEVA} = 0.25$. Epoxy resin blends were heated to 45 - 50 °C and degassed under vacuum to melt any crystallized material and remove any volatile compounds. The EEWs of the resin blends calculated as given by Equation (18):

$$\mathrm{EEW_{Blend}} = \frac{W_{\mathrm{Total}}}{\frac{W_{\mathrm{E1}}}{\mathrm{EEW_{E1}}} + \frac{W_{\mathrm{E2}}}{\mathrm{EEW_{E2}}}} \tag{18}$$

where W_{Total} is the total weight of resin, and W_{E1}, W_{E2}, EEW_{E1}, and EEW_{E2} are the weight of epoxies 1 and 2 and the epoxy equivalent weight of epoxies 1 and 2, respectively.[69] The stoichiometric quantities of the di-amine (Amicure® PACM Curing Agent) were calculated according to Equation (19):

$$phr = \frac{\mathrm{AHEW} \times 100}{\mathrm{EEW_{Blend}}} \tag{19}$$

where *phr* is the parts by weight amine per hundred parts by weight epoxy resin and AHEW is the amine hydrogen equivalent weight ($AHEW_{PACM}$ = 52.59 g/eq.).[69] AHEW is the molecular weight of the amine (MW_{PACM} = 210.37 g/mol) divided by its number of active hydrogens. EEW and *phr* for the bimodal epoxy blends are presented in Table 2.

Table 2.

Epoxy equivalent weights (EEW) and parts per hundred resin (phr) of bimodal epoxy resin blends cured with Amicure® PACM

	DGEVA : Epon 828 : PACM		DGEGD : Epon 828 : PACM	
W_{ε} : $W_{\text{Epon 828}}$ [a]	EEW (g/eq.) [b]	*phr* [c]	EEW (g/eq.) [b]	*phr* [c]
1.00 : 0.00	133	39.50	119	44.19
0.75 : 0.25	144	36.54	131	40.06
0.50 : 0.50	157	33.58	146	35.93
0.25 : 0.75	172	30.62	165	31.80
0.00 : 1.00	190	27.66	190	27.66

[a] W_{ε} = weight fraction DGEVA or DGEGD prior to addition of diamine
[b] EEW = calculated from *EEW* of neat resins determined according to ASTM D1652 using (1)
[c] *phr* = parts diamine per hundred parts epoxy resin based on $AHEW_{PACM}$ = 52.59 g/eq.

The epoxy-amine resins were well mixed and degassed under vacuum for approximately 5 min to remove any trapped air. The resins were then poured into aluminum molds of uniforms dimensions of approximately 75 × 13 × 3.5 mm^3 and cured for 5 h at 90 °C, then post-cured at 160 °C for 2 hours. The cured samples were removed from the oven and allowed to cool to room temperature. All samples were transparent indicating the lack of macroscopic phase separation. Following the curing process, the samples were cut and sanded to uniform dimensions for DMA.

The extent of cure was measured using near-infrared (N-IR) spectroscopy. N-IR spectra (64 scans, 8 cm^{-1} resolution) of the epoxy pre-polymers and the epoxy-amine systems both before cure and after post-cure were obtained in the range of 4000-8000 cm^{-1} in absorbance mode at room temperature on a Thermo Scientific Nicolet iS50 FTIR spectrometer equipped with CaF_2 beamsplitter.

3.9 Polymer Properties

The viscoelastic properties of the cured epoxy-diamine thermosets were measured using a TA Instruments Q800 DMA. Each sample was prepared with uniform dimensions of 35 × 11 × 2.5 mm^3 and tested using a single cantilever geometry. The tests were performed at a frequency of 1.0 Hz, a deflection amplitude of oscillation of 7.5 μm, and a Poisson's ratio of 0.35. The heating ramp rate for each test was 2 °C min^{-1} from 0.0 to 200 °C. Each sample was run twice with the T_g of the each resin measured as the peak of the loss modulus curve (E''). This value is considered a conservative assignment of T_g as opposed to the peak of the tan δ curve and coincides more closely with the inflection of the storage modulus curve.

The theory of rubber elasticity was used to determine the molecular weight between crosslinks (M_c) according to Equation (20) and the cross-link density (v) according to Equation (21):

$$E'_{\text{rubbery}} = \frac{3\rho RT}{M_c} \tag{20}$$

$$E'_{\text{rubbery}} = 3\nu RT \tag{21}$$

where E'_{rubbery} is storage modulus in the rubbery region, R is the universal gas constant, T is the absolute temperature in K, and ρ is the density of the polymer. [31, 70-73] The value of the rubbery modulus was taken at approximately T_g + 50 °C based on the peak of the E'' curve. The density of the polymer sample was measured according to Archimedes' principle. It is important to note that the theory of rubber elasticity generally relates to polymers with low cross-link densities.[73] However, while the theory of rubber elasticity may not offer completely accurate measurements for M_c and v for highly cross-linked

epoxy-amine resins, these measurements still provide valuable insight into the polymer properties and relevant structure property relationship trends.

Chapter 4

Results and Discussion

4.1 Introduction

The overall goal of this thesis work was to develop renewable and viable alternatives to current commercially available petrochemical derived bisphenols and epoxy resins. In addition, an attempt was made to overcome obstacles in current bisphenol production that we considered problematic. For instance, excess phenol is typically reacted with a small bridging molecule such as acetone or formaldehyde in the presence of an acid to synthesize commercial bisphenols (BPA and BPF). In the present work, we report the electrophilic aromatic condensation of vanillyl alcohol with guaiacol to produce bisguaiacol isomers. The reaction is given in *Figure 28*, in which the major structural bisguaiacol isomer formed was determined to be *p,p'*- with respect to the location of the hydroxyls. The synthesis of bisguaiacol avoids the use of flammable and/or carcinogenic molecules like acetone and formaldehyde.[74] To produce a bio-based epoxy, bisguaiacol was then reacted with epichlorohydrin to produce a diglycidyl ether of bisguaiacol (DGEBG) as shown in *Figure 29*.

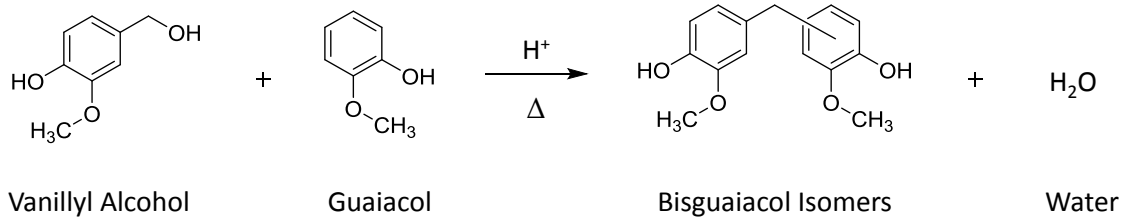

Figure 28. Electrophilic condensation of vanillyl alcohol and guaiacol to produce bisguaiacol isomers.

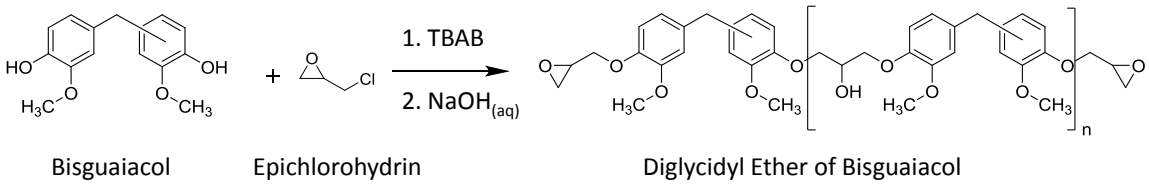

Figure 29. Synthesis of diglycidyl ether of bisguaiacol (DGEBG).

To study the influence of the methoxy group attached to the aromatic ring on cured polymer properties, diglycidyl ether of vanillyl alcohol (DGEVA) and diglycidyl ether of gastrodigenin (DGEGD) were also synthesized in the same manner as DGEBG. The molecules used in this study are shown in *Figure 30*. The epoxy pre-polymers were cured with stoichiometric equivalents of PACM (4,4'-methylenebiscyclohexanamine). The properties of the cured polymers were tested via dynamic mechanical analysis (DMA) to determine if these resins are thermomechanically suitable alternatives to current commercially available petroleum-based resins.

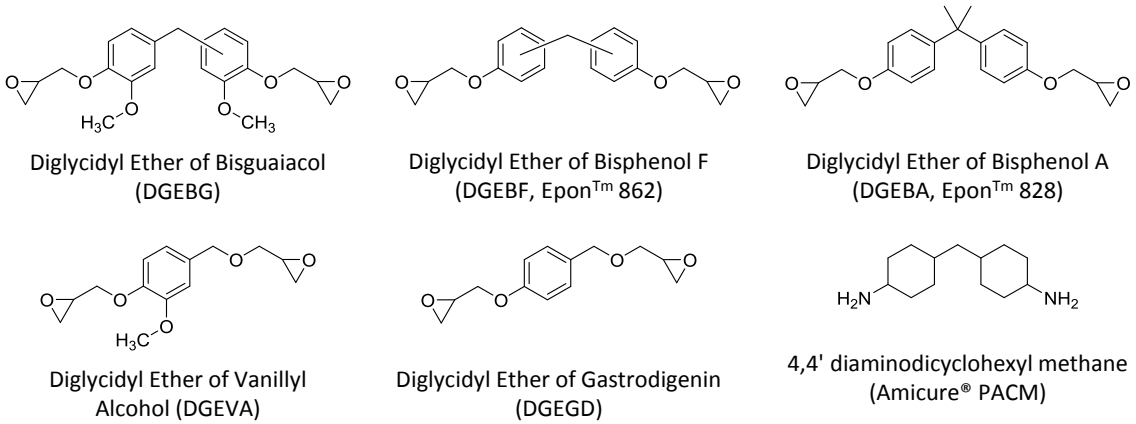

Figure 30. Simplified structures of molecules used in this study.
* Epoxy pre-polymers shown without repeat units, $n = 0$.

4.2 Synthesis of Bisguaiacol

Vanillyl alcohol and guaiacol were selected as starting materials in the production of a bio-based bisguaiacol. The route carried out for the production of bisguaiacol is a greener alternative to the commercial production of bisphenols. Vanillyl alcohol is a reduced form of vanillin, the main component of vanilla extract and a byproduct of lignin de-polymerization.[52, 54-56, 75-77] The choice to purchase vanillyl alcohol rather than to reduce vanillin for this study was based on the fact that the reduction of vanillin typically gives high yields and is so well understood, that this reaction is often performed in undergraduate chemistry labs.[78] To produce a symmetric monomer, guaiacol was chosen as the co-reactant; however, other phenolics such as phenol and creosol, could be condensed with vanillyl alcohol to give rise to asymmetric bisphenol monomers. In addition, guaiacol was also chosen because recent studies have shown that pyrolysis of lignins can return large quantities of guaiacols and other methoxy phenols.[48-50]

Bisguaiacol is similar in structure to conventional bisphenols, such as BPA and BPF; however, bisguaiacol bears methoxy substituents *ortho* to its hydroxyls. Commercially, production of petrochemical-based bisphenols has typically been achieved by bridging two molecules of phenol with a small aldehyde or ketone.[10, 11, 79, 80] BPA and BPF are identical in structure with one exception: BPA is produced from acetone giving rise to an isopropylene bridge, while BPF is produced from formaldehyde leading to a methylene bridge. Bisguaiacol bears a methylene bridge similar to BPF; however, it is important to note that formaldehyde was not used in the synthesis of bisguaiacol.

The condensation of bisphenols without the use of small bridging molecules like acetone and formaldehyde is an important step in the reduction of toxicity, especially since

formaldehyde is a known human carcinogen.[74] Meylemans et al. previously synthesized renewable bisphenols from vanillin that display similar structures to the bisguaiacol isomers produced in this work.[79] We attempted to overcome two areas of concern in their synthetic pathway. First, rather than reduce vanillin to a vanillyl alcohol, the authors converted vanillin to creosol (4-methylguaiacol) through hydrogenation, then use formaldehyde, acetaldehyde, and propionaldehyde to bridge the creosol molecules. In addition, the methyl substituent on creosol is *para* to the hydroxyl, effectively blocking the electrophilic condensation of the creosols at the *para* position. Thus, the main isomers synthesized are the *o,p'* and *m,p'* isomers. These isomers are typically undesired commercially and removed during recrystallization processes because they do not give rise to linear polymers.[9, 10, 13, 14] In our efforts, the use of formaldehyde was avoided in the production of bisguaiacol though reduction of vanillin to vanillyl alcohol, which already bears the methylene bridge *para* to the aryl hydroxyl. The proposed mechanism for the synthesis of bisguaiacol is shown in *Figure 31*.

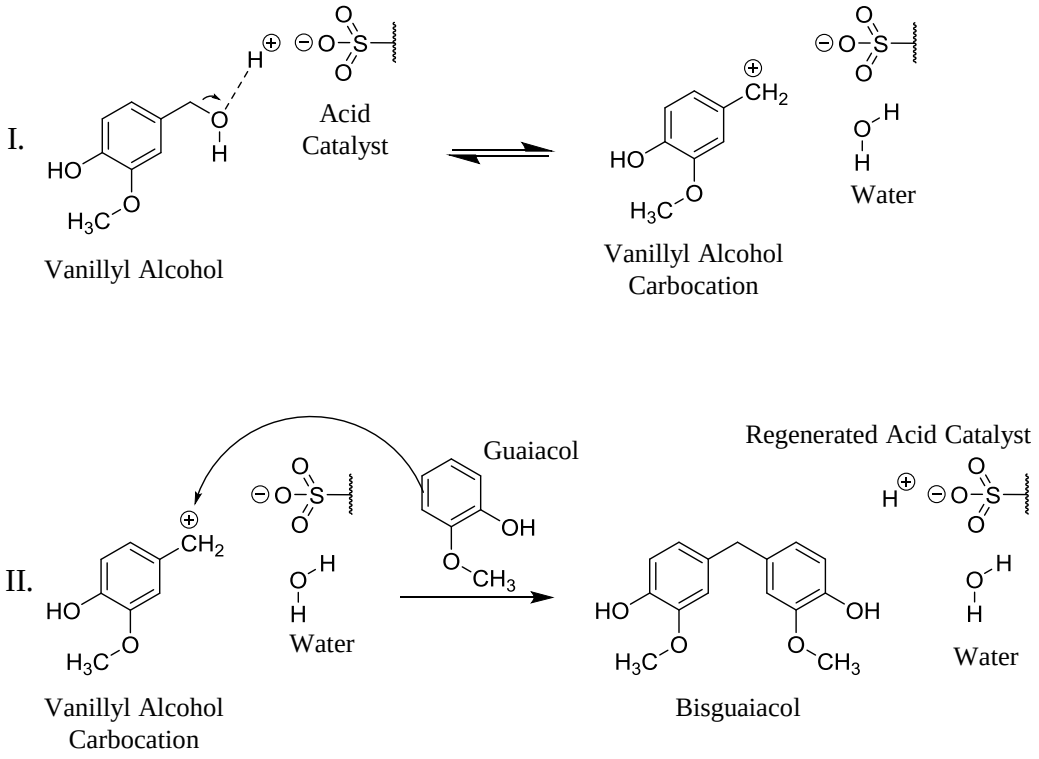

Figure 31. Detailed mechanism for the electrophilic aromatic condensation of vanillyl alcohol and guaiacol.

The electrophilic condensation of vanillyl alcohol with guaiacol in the presence of an ion exchange acid catalyst resin produces three structural isomers as shown in *Figure 33a*. Some higher molecular weight oligomers were formed in this reaction and removed via silica gel chromatography. Industrially, the bisguaiacol isomers could be recrystallized through a process similar to BPA and BPF recrystallization.[10, 79, 81] All three of the structural bisguaiacol isomers have at least one *para* linkage since the aliphatic hydroxyl of vanillyl alcohol is located *para* to its aryl hydroxyl. Furthermore, the hydroxyl of guaiacol is *para* directing; thus, the major structural isomer produced by the reaction is the symmetric *p,p'*-bisguaiacol. Likewise, the methoxy of guaiacol is also *para* directing,

consequently the second major isomer formed is *m,p'*-bisguaiacol. Hydroxyls are generally stronger *para* directors than methoxy groups.[7]

To determine the relative concentration of isomers produced, the *p,p'*-isomer was purified via silica gel chromatography and its ^{1}H-NMR spectrum was compared to the ^{1}H-NMR spectrum of the mixture of isomers produced by the reaction. Through purification, *p,p'*-bisguaiacol, *m,p'*-bisguaiacol, and a third isomer, which is believed to be the *o,p*'-isomer, were confirmed (the NMR spectra of the mixture of bisguaiacol isomers, the *p,p'*-bisguaiacol, and the *o,p'*-bisguaiacol can be found in Appendix A). *Figure 32* presents an overlay of the ^{1}H-NMR spectrum of the mixture of bisguaiacol structural isomers and the ^{1}H-NMR spectrum of the purified *p,p'*-bisguaiacol in the region of 6.6 to 6.9 ppm with the aromatic protons assigned. The *p,p'*-bisguaiacol is symmetric; therefore, it possesses only three chemically different aromatic protons. These three protons are can be viewed in the NMR spectra in *Figure 32* as a doublet at 6.84-6.86 ppm, a doublet with 2nd order splitting at 6.68-6.70 ppm, and a singlet at 6.67 ppm. In contrast to the *p,p'*-bisguaiacol, the *m,p'*-bisguaiacol is asymmetric and therefore has six chemically different protons. Two of these protons are represented as doublets at 6.77-6.78 ppm and 6.83-6.85 ppm. Another proton is displayed as a singlet at 6.76 ppm. The other protons cannot be identified by this spectrum because the *p,p*-bisguaiacol aromatic proton peaks overlap them. In addition, accurate measurements via integration cannot be made because of the significant overlapping of peaks in this region.

Overlapping in the region of 3.8-4.0 ppm where the methoxy and methylene bridge protons of the isomers appear is minimal. Therefore, accurate measurements could be made via integration of the peaks in this region to determine relative isomer concentrations.

Figure 33 shows the ^{1}H-NMR spectra in the region of ~ 3.8-4.0 ppm of the mixture of structural isomers produced by the reaction and the purifired *p,p'*-bisguaiacol. On the left of *Figure 33*, the NMR spectrum of the purified *p,p'*-bisguaiacol shows two distinct peaks: a singlet at 3.83 ppm with an integration of 6.0 and a singlet at 3.85 ppm with an integration of 2.0. The singlet at 3.83 ppm corresponds to the six methoxy protons, which are all chemically equivalent, while the singlet at 3.85 corresponds to the two methylene bridge protons. In the spectrum on the right of *Figure 33*, the peak at 3.81 ppm representing the two methylene bridge protons of the *m,p'*-bisguaiacol and two peaks at 3.83 and 3.86 ppm representing the six methoxy protons. The *o,p'*-bisguaiacol shows a peak at 3.93 ppm representing the 2 methylene bridge protons and peaks at 3.88 and 3.84 ppm representing the six methoxy protons. These peaks corresponding to the *o,p'*-bisguaiacol are almost indistinguishable from noise; however, they were confirmed after isolation of the isomer via chromatography. The ^{1}H-NMR of purified *o,p'*-bisguaiacol can be found in Appendix A. The *m,p'*-bisguaiacol was not isolated from the *p,p'*-bisguaiacol via chromatography over the course of this study. The integration of the peaks in the region of 3.8-4.0 ppm indicates approximately 82 ± 4 % p,p' isomer, 15 ± 3 % m,p'-isomer, and 3 ± 1 % o,p'-isomer present.

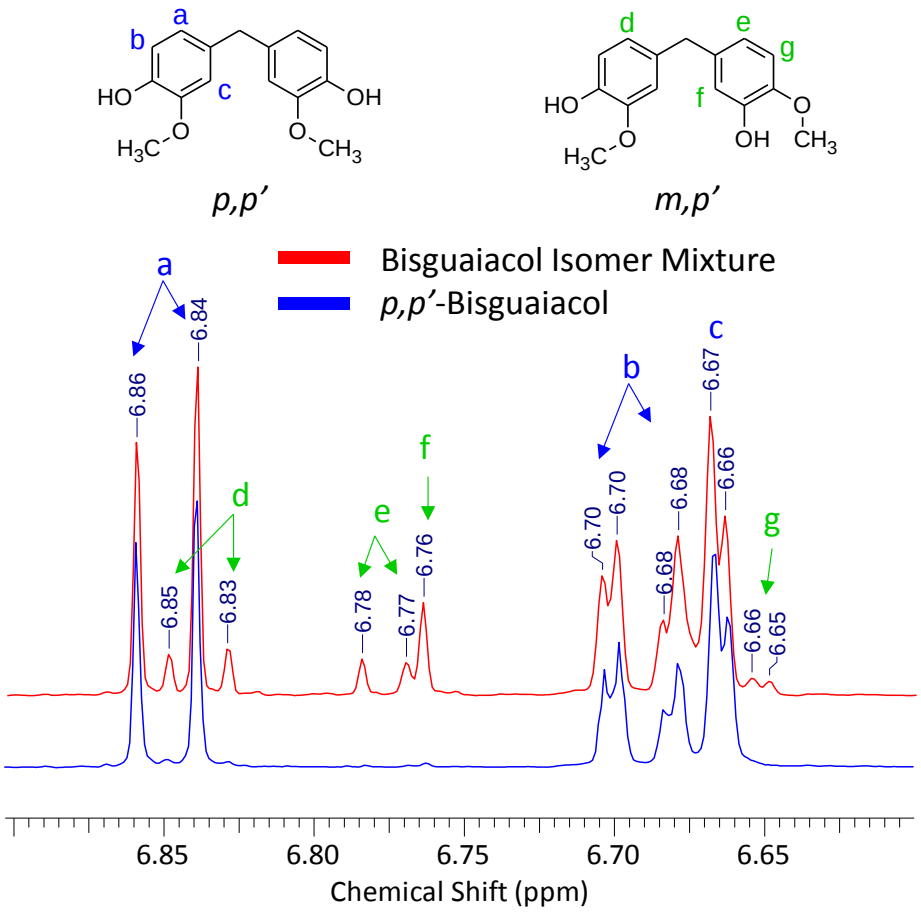

Figure 32. ^{1}H-NMR of bisguaiacol structural isomers at 6.6-6.9 ppm with aromatic proton assignments.
Top: Structures of bisguaiacol regioisomers. *Bottom:* Overlay of NMR spectra of bisguaiacol isomers and of purified *p,p'*-bisguaiacol.
*****Samples dissolved in $CDCl_3$.

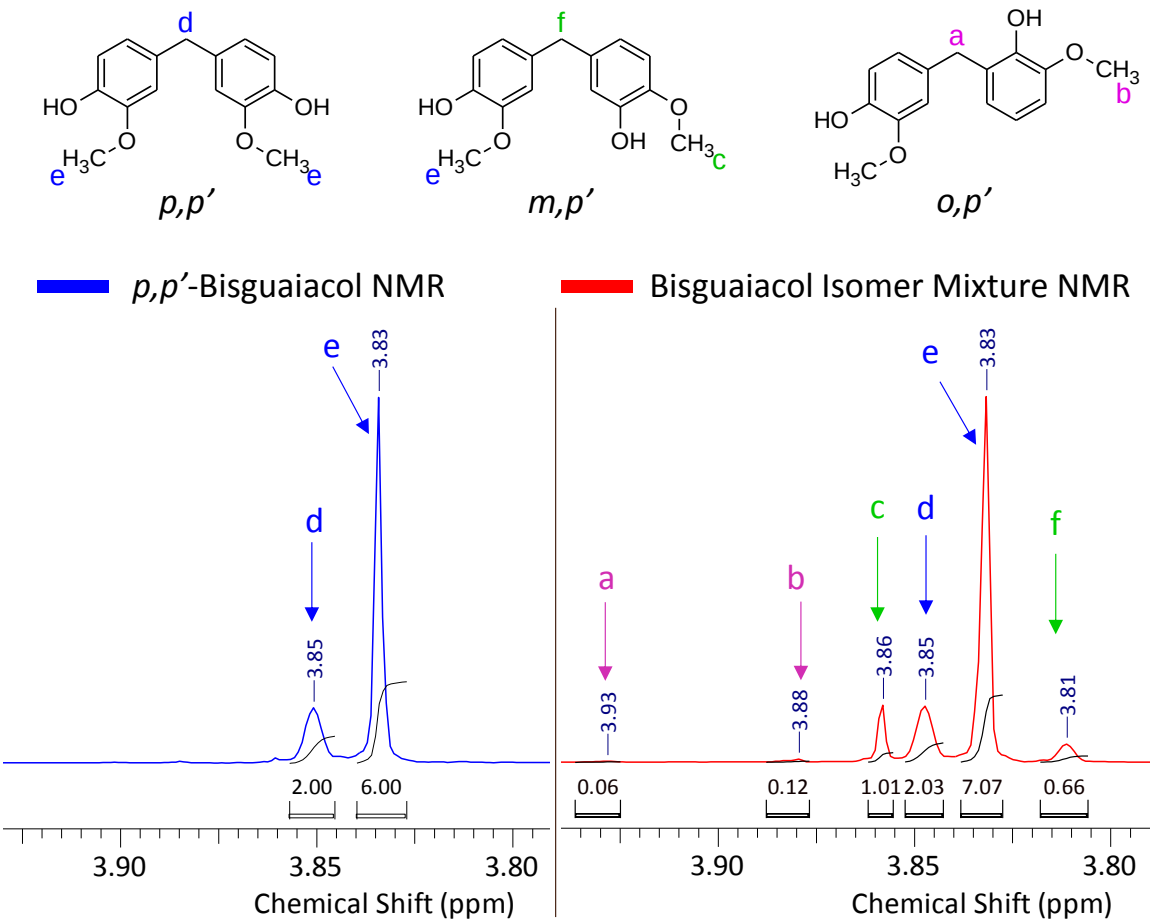

Figure 33. ^{1}H-NMR of bisguaiacol structural isomers at 3.8-4.0 ppm with the methoxy and methylene bridge proton assignments. *Top:* Structures of bisguaiacol regioisomers. *Left:* NMR spectrum of purified *p,p'*-bisguaiacol isomer. *Right:* NMR spectrum of *p,p'*-, *m,p'*-, *o,p*'- isomers produced in the reaction. *Samples dissolved in $CDCl_3$.

4.3 Synthesis and Characterization of Epoxy Pre-polymers

All epoxy pre-polymers in this work were produced through a similar reaction pathway. Production of glycidyl ethers is a well-known industrial process which involves reacting the bisphenol monomer with epichlorohydrin and a base to produce an epoxy brine.[2, 3, 6, 7] Tetrabutylammonium bromide is employed as a phase transfer catalyst to move the

phenolate ion into the organic phase.[7] The reaction is typically carried out in excess epichlorohydrin to minimize formation of higher molecular weight epoxy oligomers. Increasing the quantity of epichlorohydrin typically gives lower *n* values. In addition, epichlorohydrin acts as a reactive solvent eliminating the need for additional solvents in the synthesis. Following the reaction, epichlorohydrin can be recovered via distillation and the epoxy brine can be washed with water to remove salts formed. DGEBG was synthesized using this process, producing a low molecular weight resin with some high molecular weight oligomers. The EEW of the solid DGEBG prior to silica gel chromatography was determined to be 210 g/eq. (n = 0.15).

DGEBG is similar in structure to BPA and BPF based epoxy resins (Epon 828 and 862, respectively). The major difference between these resins is that bisguaiacol epoxy resins bear a single methoxy group *ortho* to the glycidyl ethers while Epon resins do not. Bisguaiacol epoxy resins more closely resemble BPF epoxy resins in that both epoxies have methylene bridges while BPA based resins have a more rigid isopropylene bridge. However, there exists significant variability in the position of the methylene bridge on the aromatic rings of the bisguaiacol epoxy resins and BPF based epoxy resins. For instance, bisguaiacol epoxy resins will always have at least one *para* linkage while BPF resins may exhibit any combination of regioisomers. Purification of these isomers is not generally practical. Thus, a proper structure-property study was not feasible through comparison of cured DGEBG and Epon 862 resins. In order to understand the effect of the methoxy group *ortho* to the glycidyl ether on the properties of cured polymer networks, two single aromatic epoxies were synthesized. Diglycidyl ether of vanillyl alcohol (DGEVA) was synthesized and used as a model compound for the methoxy group. Diglycidyl ether of gastrodigenin

(DGEGD) was produced similarly to DGEVA. Gastrodigenin (4-(hydroxymethyl)phenol) has an identical structure to vanillyl alcohol with the exception that it does not contain a methoxy substituent on the aromatic ring. Thus, these two molecules allowed us to look directly at the influence of a single methoxy. Interestingly, gastrodigenin and its oxidized form, 4-hydroxybenzaldehyde, can be found in an orchid known as *Gastrodia elata,* making these molecules another potential bio-based source for the production of epoxy resins.[82]

Vanillyl alcohol and gastrodigenin each have one aryl hydroxyl and one aliphatic hydroxyl. The aromatic hydroxyl is much more acidic than the aliphatic hydroxyl, thus more reactive with epichlorohydrin. The production of DGEVA and DGEGD generally yields 70-85 % of diepoxidized product and 15-30 % of mono-epoxidized product in which the aliphatic hydroxyl is unreacted. The concentration of mono-glycidyl ether in the product mixture was determined by ^{1}H-NMR (NMR overlays can be found in Appendix A). The protons on the oxirane ring generally appear as characteristic doublet of doublets between 2.5 and 2.9 ppm in $CDCl_3$. The ratio of the areas under these doublets is a rough indicator of the quantity of mono-glycidyl ether present. In addition, the mono-glycidyl ether will exhibit a doublet at approximately 4.6 ppm in $CDCL_3$ corresponding to the aliphatic CH_2. The purification of the diglycidyl ether was crucial for an accurate structure-property study as mono-glycidyl ethers act as chain terminators in the cured epoxy polymer network, effectively decreasing crosslinking and lowering T_gs (see Appendix E). However, the decreased reactivity of the aliphatic hydroxyl toward epoxidation is not necessarily a negative characteristic. In fact, mono-glycidyl ethers with hydroxyls present could be favorable in other applications.

Multiple methods were used to characterize the epoxy resins both synthesized and purchased for this study including: ^{1}H-NMR, ^{13}C-NMR, EEW titration, GPC, and MS. An experimental EEW close to or equal to the theoretical EEW along with a single sharp peak in its GPC trace suggest only a single compound exists. Care was taken to ensure that DGEVA and DGEGD were at least 99 % pure with n values close to zero, so that accurate conclusions could be drawn on the effect of the methoxy substituent on polymer properties. Epon 828 and Epon 862 were not purified. GPC and EEW titration of the Epon resins indicate approximately 13-14 % by mole of high molecular weight oligomers. GPC traces on epoxy resins along with their respective monomers are shown in *Figure 34*. Analysis of the GPC traces indicate that BPA, bisguaiacol, vanillyl alcohol, and gastrodigenin all elute from the column approximately 0.2-0.3 minutes faster than their respective epoxy counterparts. For example, DGEBG elutes at approximately 27.98 minutes while bisguaiacol elutes at 27.75 minutes. One explanation for this observation may be that at very low molecular weights the columns were not able to separate by size alone and polarity may have influenced elution time.

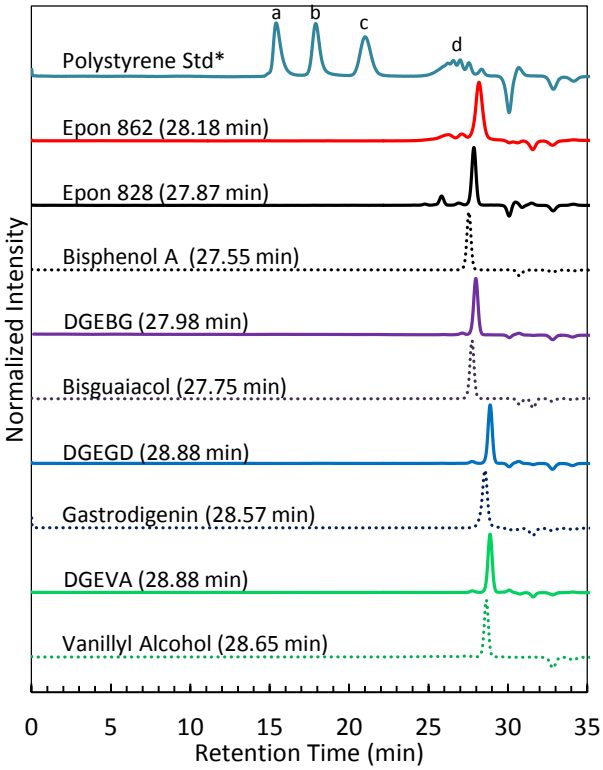

Figure 34. Overlay of GPC traces of epoxy pre-polymers and their respective precursors with elution times shown in parentheses. The polystyrene standards have the following number average molecular weights:
a) 532,000 Da, b) 59,300 Da, c) 8,650 Da, d) 492 Da.

4.4 Synthesis of Epoxy-Amine Systems and Extent of Cure

All epoxy pre-polymers were cured with stoichiometric quantities of PACM that were determined by EEW titrations according to ASTM D1652. Each epoxy pre-polymer has two oxirane rings leading to a functionality of two, whereas each diamine monomer has four active protons resulting in a functionality of four. Thus, the theoretical stoichiometric ratio of epoxy to amine is 2:1. The epoxy-amine reaction begins with the ring opening attack of the primary amine on the terminal CH_2 of the oxirane ring.[30] Subsequently, a secondary amine and hydroxyl are formed. The reaction proceeds as the secondary amine

attacks another oxirane ring forming a cured polymer network. However, secondary amines are less reactive than primary amines and as the polymer network grows, sterics and decreased molecular mobility hinder the reaction of the secondary amine with another oxirane ring as vitrification occurs.[30, 32] To overcome this obstacle and achieve full curing, the epoxy-amine systems are usually subjected to post-curing processes in which they are heated well above their anticipated T_gs.[30] With post-curing, full conversions are usually attained. Palmese and McCullough studied the effect of epoxy-amine stoichiometry on cured polymer properties and determined that the small deviations from the theoretical 2:1 ratio significantly decreased the E' and T_g.[31] To achieve the highest possible T_gs and E', the theoretical 2:1 ratio was used in this work.

The extent of reaction is typically measured by differential scanning calorimetry (DSC); however, infrared spectroscopy is a more powerful tool allowing for accurate determination of both epoxy and amine conversions.[30] While DSC can provide the overall extent of reaction, it cannot be used to determine the extent of cure of the epoxy and amine groups individually. An overlay of N-IR spectra of DGEVA cured with PACM at 90 °C for 4 hours followed by post-cure at 160 °C for 2 hours is shown in *Figure 35***.** The dotted blue line represents the epoxy-amine system less than 5 minutes after mixing and prior to exposure to elevated temperatures. The solid red line represents the cured polymer network after post-cure. The spectra in *Figure 35* is representative of all epoxy-amine systems in this study. Additional FTIR spectra are available in Appendix C. The oxirane ring of the epoxy pre-polymer absorbs at approximately 4530 and 6060 cm^{-1}. An absorbance at 4925 cm^{-1} is characteristic of primary amines, while 6535 cm^{-1} is characteristic of both primary and secondary amines. During curing, the oxirane ring

overtones at 4530 and 6060 cm^{-1}, the primary amine stretching at approximately 4925 cm^{-1}, and the primary and secondary amine at 6535 cm^{-1} will decrease while an absorption around 6060-7000 cm^{-1} corresponding to hydroxyl formation will increase. The bands at 4925, 6060, and 6535 cm^{-1} can only be used to qualitatively measure the extent of cure due to band overlapping. Since the peak at 4500 cm^{-1} does not overlap other peaks it can be used to quantitatively determine the extent of cure according to Equation (22) in which peaks at 5790 cm^{-1} were used as internal references.

$$\text{Extent of cure} = \frac{\frac{ABS_{\text{Precure at 4530cm-1}}}{ABS_{\text{Precure-ref}}} - \frac{ABS_{\text{Postcure at 4530cm-1}}}{ABS_{\text{Postcure-ref}}}}{\frac{ABS_{\text{Precure at 4530cm-1}}}{ABS_{\text{Precure-ref}}}} \qquad (22)$$

Within the limits of N-IR spectroscopy, all resins were determined to be 99 + % cured following post-cure.

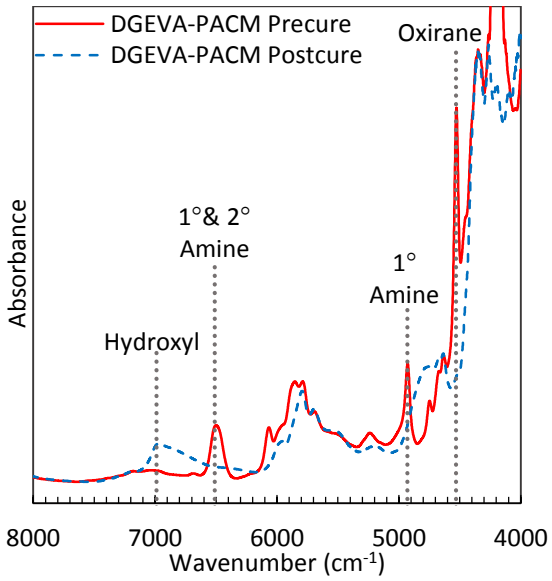

Figure 35. Overlay of Near-IR spectra of pre-cured and post-cured DGEVA and PACM.

4.5 Effect of Methoxy Group on Epoxy-Amine Polymer Properties

To investigate the effect of the methoxy group on the cured polymer properties, DGEVA and DGEGD were both cured with stoichiometric equivalents of PACM. In addition, to determine whether these epoxy pre-polymers would have good miscibility with other resins and produce predictable properties, both DGEVA and DGEGD were blended with Epon 828 at varying weight ratios from 0 to 100 % and cured with stoichiometric equivalents of PACM. Homogeneity in the mixtures was determined qualitatively through visual assessment. All polymers appeared transparent and of uniform color. In addition, extent of cure was determined by N-IR as previously discussed.

The properties of the cured polymer samples were measured by DMA using a heating rate of 2 °C/min. A slow heating rate was chosen to obtain accurate measurements since the T_g is a function of heating rate, whereby a faster heating rate will give a higher T_g.[1, 83] The DMA thermograms of the DGEVA-Epon 828-PACM and DGEGD-Epon 828-PACM systems are shown in *Figure 36*. E' and E'' for the DGEVA-Epon 828-PACM systems are overlaid in *Figure 36a* and *Figure 36b*, respectively. Likewise, the E' and E'' of the DGEGD-Epon 828-PACM systems are shown in *Figure 36c* and *Figure 36d*. The tan δ curves for the two systems can be found in the Appendix D, Figures D1-D3. The T_g was recognized as the peak of the E'' curve. Analysis of the DMA thermograms provides insight into the effect of the methoxy group. A single additional methoxy *ortho* to the glycidyl ether significantly affects both the T_g and the E' at 25 °C. The DGEVA-PACM system possesses a T_g of 100 °C, while the DGEGD-PACM system possesses a higher T_g of 123 °C. Although the presence of a methoxy effectively lowers the T_g, the opposite is true for E' at 25 °C. The E' at 25 °C for DGEVA-PACM was measured as 3.02 GPa whereas

this measurement for DGEGD-PACM was only 2.29 GPa. On blending with Epon 828, similar trends were observed. DGEVA-based resins were found to consistently possess higher E' at 25 °C and lower T_gs than DGEGD-based resins. The E'' curves of the DGEVA-Epon 828-PACM systems show a small peak at 40 - 50 °C corresponding to β relaxations. β relaxations represent small chain motions while α relaxations indicate long range molecular motions.[2] All polymer blends display a single sharp E″ corresponding to α relaxations indicating good miscibility of the systems.

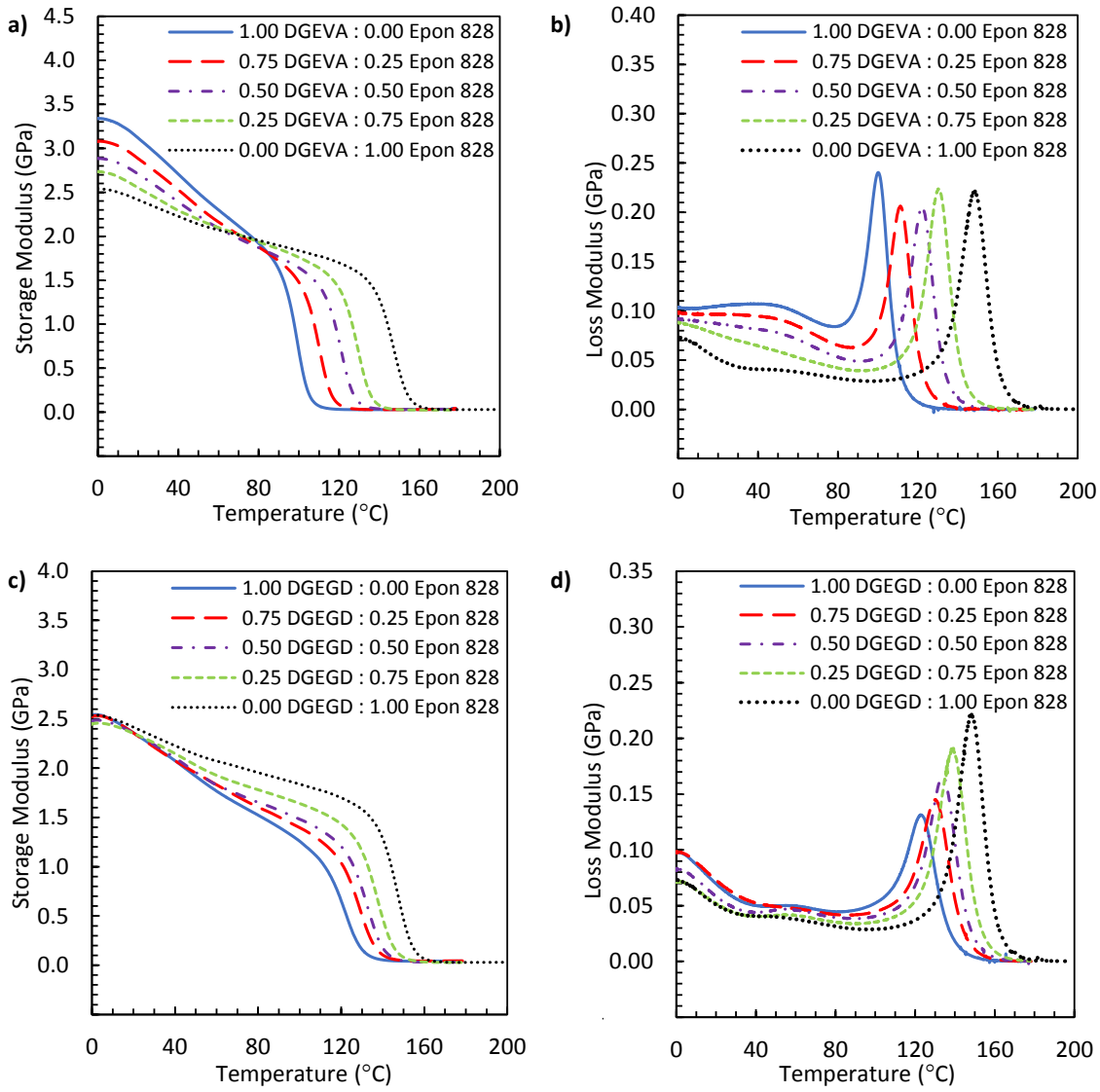

Figure 36. DMA thermograms of cured DGEVA-Epon 828 blends and cured DGEGD-Epon 828 blends at various weight ratios. All samples were cured with Amicure ® PACM.

The T_gs of the neat DGEVA and DGEGD resins cured with PACM were significantly lower than that of Epon 828 and Epon 862 cured with PACM. This occurrence is attributed to the methylene bridge between the aromatic ring and the glycidyl ether group of the DGEVA and DGEGD resins that allows for increased mobility and rotational freedom in

the polymer networks. Hu et al. reported similar findings when studying a symmetric aromatic epoxy system similar to DGEGD used in this work, except their resin exhibited a methylene bridge between the aromatic ring and both glycidyl ether groups.[42] They obtained a T_g more than 100 °C lower than Epon 828 when cured with PACM. In addition, the researchers cured a diglycidyl ether of hydroquinone (a single aromatic epoxy with no methylene bridges) with diethyl toluene diamine and obtained a T_g approximately 20 °C higher than cured Epon 828. Thus, adding methylene bridges between the aromatic ring and the glycidyl ether groups significantly lowers T_gs.

The T_gs and E's at 25 °C for the bimodal blends are summarized in Table 3. The DGEGD-Epon 828-PACM blends all possess a similar E′ at 25 °C, approximately 2.3 GPa with a range of less than 100 MPa. These values are within experimental error and it is concluded that blending DGEGD with Epon 828 does not change E' at 25 °C. However, the DGEVA-Epon 828-PACM blends show a direct relationship between E' at 25 °C and the weight fraction of DGEVA, wherein increasing W_{DGEVA} in the blend increases E'. These results suggest E' is directly affected by the chemical structure. It has been suggested that the oxygen of the methoxy group can act as a proton acceptor in hydrogen bonding.[7, 84] The presence of the methoxy group in the cured polymer network may indicate increased hydrogen bonding at lower temperatures, explaining the observed increase in E' at 25 °C. The DGEGD and Epon 828 resins are similar in structure such that they do not have substituents attached to their aromatic rings attributing to their similar E' whereas the additional methoxy group may potentially increase stiffness in the bulk polymer network. A structural representation of the proposed hydrogen bonding is shown in *Figure 37*.

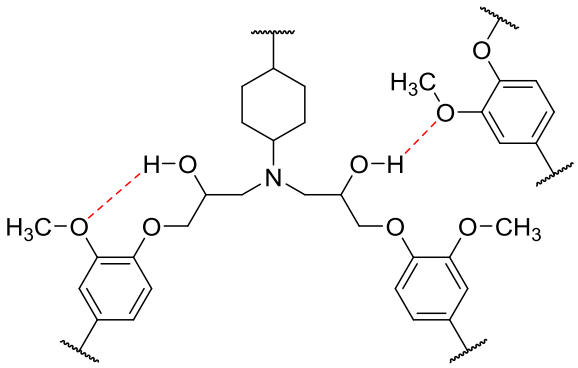

Figure 37. Possible hydrogen bonding between methoxy and hydroxyl groups in cured vanillyl alcohol based epoxy-amine resins.

The experimental T_gs of the bimodal blends were compared to empirical T_gs by means of the Fox equation (23):

$$\frac{1}{T_g} = \frac{W_1}{T_{g,1}} + \frac{W_2}{T_{g,2}} \qquad (23)$$

where T_g is the glass transition of the blended polymer cured with PACM and T_1, T_2, W_1, and W_2 are the T_gs of the cured polymers and weight fractions of the two epoxy resins, respectively. [2, 42]The reciprocal of the glass transitions of the blends $1/T_g$ were plotted against their weight fractions. The plot of $1/T_g$ against $1\text{-}W_{\text{Epon 828}}$ is shown in *Figure 38a*. The data fits the linear trend set by the Fox equation with $R^2 > 0.97$. This suggests the epoxy resins have good miscibility with each other and that the Fox equation can be used to predict T_gs for these bimodal epoxy blends cured with PACM. In addition, the bulk polymer densities of the resin blends at room temperature were measured and plotted against their respective weight fractions. This plot is shown in *Figure 38b***.** The polymer densities also show a linear relationship in which ρ (taken at 25 °C) increases with the decrease in the weight fraction of Epon 828. The data fit the linear trend with $R_2 > 0.99$.

Decrease in network density with increasing Epon 828 may be attributed to the longer chain backbone of Epon 828 in comparison to that of DGEVA and DGEGD. In addition, DGEVA blends consistently display higher ρ values then DGEGD blends. McAninch et al. suggests that higher E' at lower temperatures may be related to higher ρ values at lower temperatures.[73]

Table 3.

Glass transition temperature (T_g) and storage moduli (E') of epoxy resin blends cured with PACM

W_{ε} : $W_{\text{Epon 828}}$ [a]	DGEVA : Epon 828 : PACM			DGEGD : Epon 828 : PACM		
	T_g [a] (°C)	T_g [b] (°C)	E' [c] (GPa)	T_g [a] (°C)	T_g [b] (°C)	E' [c] (GPa)
1.00 : 0.00	100	107	3.02	123	132	2.29
0.75 : 0.25	111	119	2.80	130	139	2.28
0.50 : 0.50	122	130	2.63	134	143	2.30
0.25 : 0.75	130	139	2.49	139	148	2.31
0.00 : 1.00	149	158	2.37	149	158	2.37

[a] T_g measured as the temperature at the peak maximum of the loss modulus (E'') curve.
[b] T_g measured as the temperature at the peak maximum of the tan δ curve.
[c] E' measured at 25 °C.

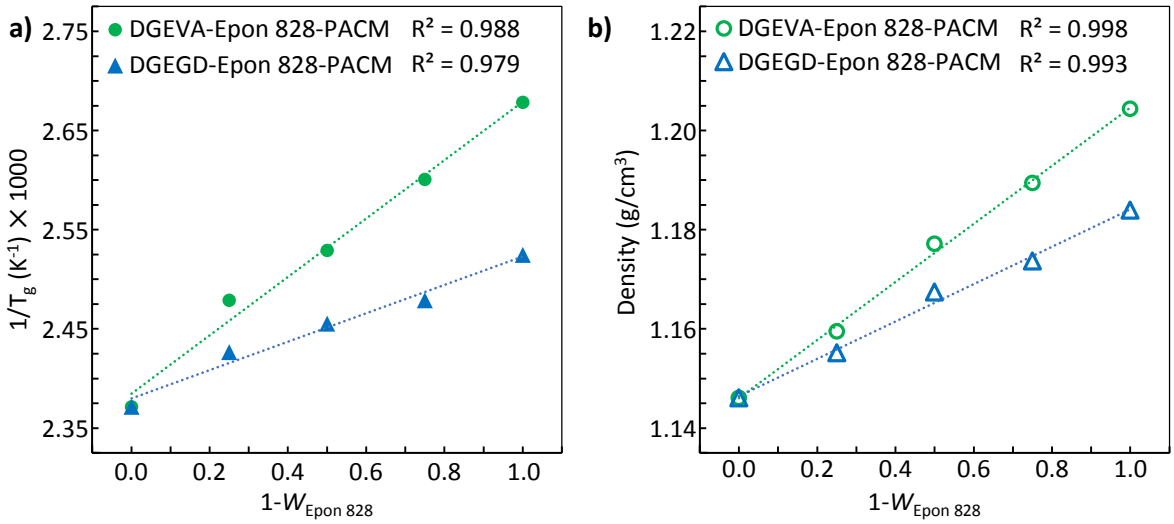

Figure 38. Properties of DGEVA – Epon 828 - PACM and DGEGD - Epon 828 - PACM blends.
a. $1/T_g$ of bimodal blends cured with PACM fit to Fox equation.
b. Bulk polymer density of bimodal blends cured with PACM.

4.6 Properties of DGEBG Polymer Blend

Due to the high melting point of DGEBG at low molecular weight ($n \leq 0.15$), this resin was not cured with PACM by itself. Attempts to prepare a DGEBG-PACM polymer were unsuccessful, as the reaction took off violently upon addition of PACM to a molten DGEBG. Since Epon 828 displays good miscibility with both the DGEVA and DGEGD resins, a DGEBG blend was also prepared. A 1:1 by weight blend of DGEBG and Epon 828 was prepared to lower the melting point and a stoichiometric quantity of PACM was added. The blend was cured and the extent of cure was measured to be 99 % via N-IR.

Figure 39 shows the overlays of DMA thermograms (E' and E'') of various epoxy resins cured with stoichiometric equivalents of PACM (tan δ curves can be found in the Appendix D, *Figures* D1-D3). Interestingly, 1:1 DGEBG-Epon 828 blend cured with PACM has a T_g of 134 °C and an E' at 25 °C of 3.08 GPa. The increased E' at 25 °C of the DGEBG system

is consistent with the results of the DGEVA-based polymers. A T_g of 120 °C is predicted for a pure DGEBG-PACM system based on the Fox Equation. In addition, following the observed trend this resin would have an E' at 25 °C greater than 3 GPa. Epon 862 (DGEBF) cured with PACM possesses a T_g close to the 1:1 DGEBG - Epon 828 system, but a lower E' at 25 °C. Likewise, the T_g of Epon 862-PACM (131 °C) is slightly higher than the predicted T_g of DGEBG-based system because Epon 862 lacks methoxy groups on the aromatic ring. However, the T_g of Epon 862 is lower than that of Epon 828 (149 °C) because the BPF bears a methylene bridge while BPA bears an isopropylene bridge. The isopropylene bridge decreases the rotational freedom of the backbone.

As previously mentioned, Epon 862 is a BPF-based resin with a methylene bridge. The methylene linkage of Epon 862 exists between the two phenols, while the methylene linkage of DGEGD is located between the aromatic ring and glycidyl ether. Increased rotational freedom caused by the position of the methylene bridge in DGEGD may explain the lower T_g observed in the DGEGD system. Table 4 summarizes the measured polymer properties. No trends were observed regarding the molecular weight between crosslinks. These *M*c values are obtained from the *E's* in the rubbery regions well above the T_gs of the samples. Since the modulus in this region is relatively low, thicker samples (~ 5 mm) may need to be tested to obtain accurate rubbery modulus results.[73]

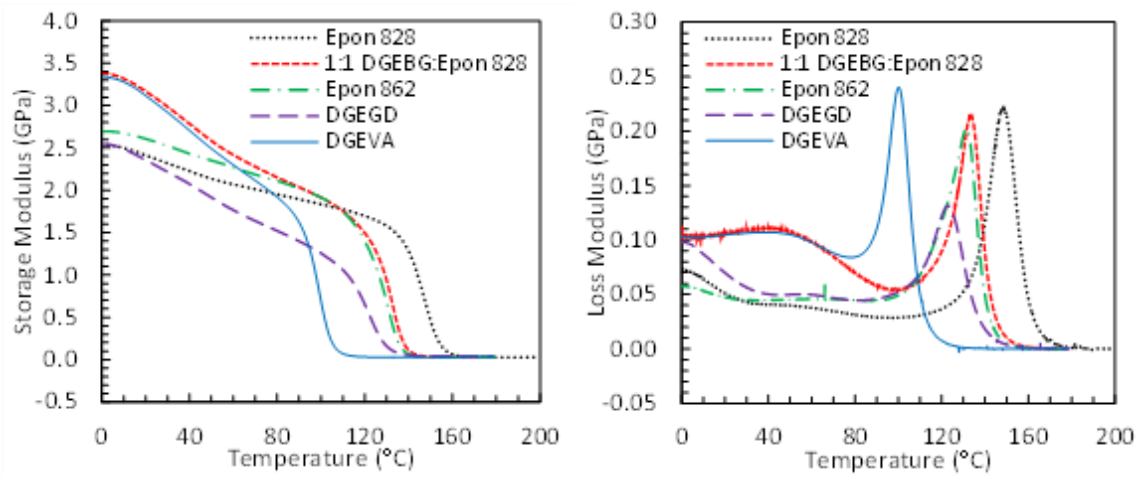

Figure 39. DMA thermograms of epoxy resins cured with PACM.

Table 4.

Properties of epoxy resins cured with Amicure® PACM

Epoxy Resins [a]	T_g [b] (°C)	T_g [c] (°C)	E' [d] (GPa)	ρ [e] (g/cm^3)	M_c [f] (g/mol)	ν [g] (mmol/cm^3)
DGEVA	100	107	3.02	1.18	422	2.85
DGEGD	123	132	2.29	1.20	303	3.91
1:1 DGEBG : Epon 828	134	140	3.08	1.18	416	2.83
Epon 862	131	138	2.57	1.18	484	2.43
Epon 828	149	158	2.37	1.15	465	2.46

[a] Cured with stoichiometric quantity of PACM.
[b] T_g measured as the temperature at the peak maximum of the loss modulus (E'') curve.
[c] T_g measured as the temperature at the peak maximum of the tan δ curve.
[d] E' measured at 25 °C.
[e] ρ measured according to Archimedes' principle.
[f] M_c measured at T_g + 50 °C from $E' = 3\rho RT/M_c$.
[g] $\nu = \rho/M_c$.

Chapter 5

Conclusions and Recommendations for Future Work

5.1 Conclusions

This thesis focused on the potential to use lignin derived compounds, specifically vanillin and its reduced form, vanillyl alcohol, as potential non-toxic starting materials for the production of new bio-based epoxy polymers and composites. Lignin and its derivatives were chosen due to their aromatic character and natural abundance. Innovatively engineered bio-based epoxy resins should incorporate the aromaticity that inherently provides the rigid structural and thermal integrity found in conventional BPA-based epoxy resins. Bisguaiacol, a new bio-based bisphenolic compound, was successfully condensed from vanillyl alcohol and guaiacol without the need of small bridging compounds such as acetone and formaldehyde. Diglycidyl ether of bisguaiacol (DGEBG), a new bio-based epoxy pre-polymer, was synthesized from bisguaiacol and epichlorohydrin according to known glycidylation procedures. DGEBG possessed a high melting point (> 100 ºC); therefore, thermal processing of this resin prior to curing was difficult. However, this resin showed good miscibility with other commercially available resins and blends could be tailored to obtain desired properties. DGEBG blended with Epon 828 (diglycidyl ether of bisphenol A, DGEBA) and cured with a standard cycloaliphatic diamine (PACM) displayed promising thermomechanical properties (T_g > 130 ºC and E' > 3 GPa at 25 ºC). In addition, a diglycidyl ether of vanillyl alcohol (DGEVA) and diglycidyl ether of gastrodigenin (DGEDG) were successfully synthesized to investigate the effect of a methoxy substituent *ortho* to the glycidyl ether on the viscoelastic properties of the cured epoxy-amine polymers. DMA results indicated that the addition of a methoxy group to the

aromatic ring decreased the T_g and increased E' at 25 °C. The DGEGD resin showed a similar E' at 25°C to that of Epon 828. One possible explanation for the decrease in T_g is that the methoxy group may hinder tighter packing of the molecules during curing. Meanwhile, a higher E' at 25 °C may possibly be attributed to increased hydrogen bonding due to the presence of the methoxy. The T_gs of the bimodal blends of the vanillyl alcohol and gastrodigenin-based epoxies and Epon 828 cured with PACM showed excellent fit to the Fox equation. In addition, a direct relationship between weight fraction of DGEVA to Epon 828 and E′ was observed such that increasing the amount of DGEVA in the resin increased E′ in the glassy region. These results suggest that cured epoxy thermosets with predictable thermomechanical properties can be obtained through various blending of the aforementioned resins.

5.2 Recommendations for Future Work

One of the inherent difficulties over the course of this thesis work was obtaining purified monomers, particularly bisguaiacol. The reaction to synthesize bisguaiacol yields an amber to brownish oil from which pure bisguaiacol was obtained via silica gel flash chromatography; however, industrially, silica gel chromatography is neither a cost effective nor a viable option. Recrystallization of conventionally synthesized *p,p'*-bisphenol A is so well studied that there exists a plethora of patents dealing solely with this unit operation.[9, 12-14] Therefore, it is recommended that future experiments be carried out as to determine both economical and environmentally friendly methods for the recrystallization and purification of bisguaiacol.

The extremely high melting point observed in the bisguaiacol epoxy resin was yet another difficulty encountered over the course of this study. DGEBA resins are liquid at

room temperature and they can be easily processed and/or well mixed with amine curing agents without solvents. However, DGEBG resins must first be melted at high temperatures prior to mixing. However, epoxy-amine systems will begin to polymerize instantly at elevated temperatures allowing little, if any time, to transfer the well mixed resin to a mold before gelation begins. Such was the case with DGEBG resins mixed with PACM; therefore, it is recommended that the curing of DGEBG with additional amine curing agents via different protocols then that used in this work be investigated in the future. Despite this, it is worthy to note that solid epoxy resins with high melting points are not necessarily a drawback in all applications. In fact, DGEBG resins may lend themselves to applications that require a malleable resin which can be physically molded in place prior to curing.

Epoxy-amine resins systems are well studied and understood; however, most studies are based on DGEBA resins. Very few studies have looked into the effect of small substituent groups on the aromatic ring and the effect of aliphatic bridges in the epoxy-amine polymer network. It is recommended that the kinetics of the curing of vanillyl alcohol and gastrodigenin epoxy resins with diamines be studied via N-IR. Such a study would indicate whether or not the methoxy moiety has an effect on the rate of polymerization. In addition, it would be beneficial to understand how the rate of curing is influenced by phenolic and aliphatic glycidyl ethers. It would also be beneficial to investigate the thermogravimetic properties of these resins to determine the effect of the methoxy group on polymer degradation. No mechanical tests were performed over the course of this research; however, mechanical testing of the aforementioned resins may give insight into the toughness and strength of these resins. Finally, epoxy resins are quite often

used as adhesives; therefore, it is recommended that a comparative adhesive study be carried out using a single lap joint shear strength test.

In this study, it was determined that the presence of the methoxy group in vanillin-based epoxy resins resulted in a tradeoff between T_g and the glassy E'. Future efforts should be directed toward the design a new epoxy resins that incorporate the increased E' at room temperature and also displays higher T_gs. We hypothesize that a trifunctional epoxy monomer would lead to a higher crosslinking density resulting in a higher T_g as well. Therefore, in effort to test this hypothesis a trifunctional phenolic analogue was prepared from vanillyl alcohol and 4-methylcatechol via electrophilic aromatic condensation in the presence of a heterogeneous styrene-divinylbenzene sulfonic acid catalyst. This vanillyl alcohol/4-methylcatechol trifunctional monomer was recrystallized from methylene chloride. Work is currently ongoing to epoxidize this monomer. The overall reaction pathway is given in *Figure 40*. The ^{1}H-NMR of the trifunctional phenolic analogue with multiplets and proton assignments is given in *Figure 41*.

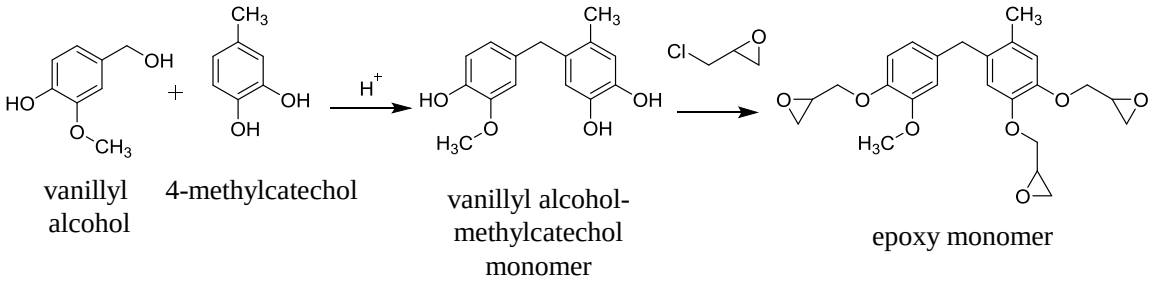

Figure 40. Synthesis of trifunctional epoxy monomer from vanillyl alcohol and 4-methylcatechol.

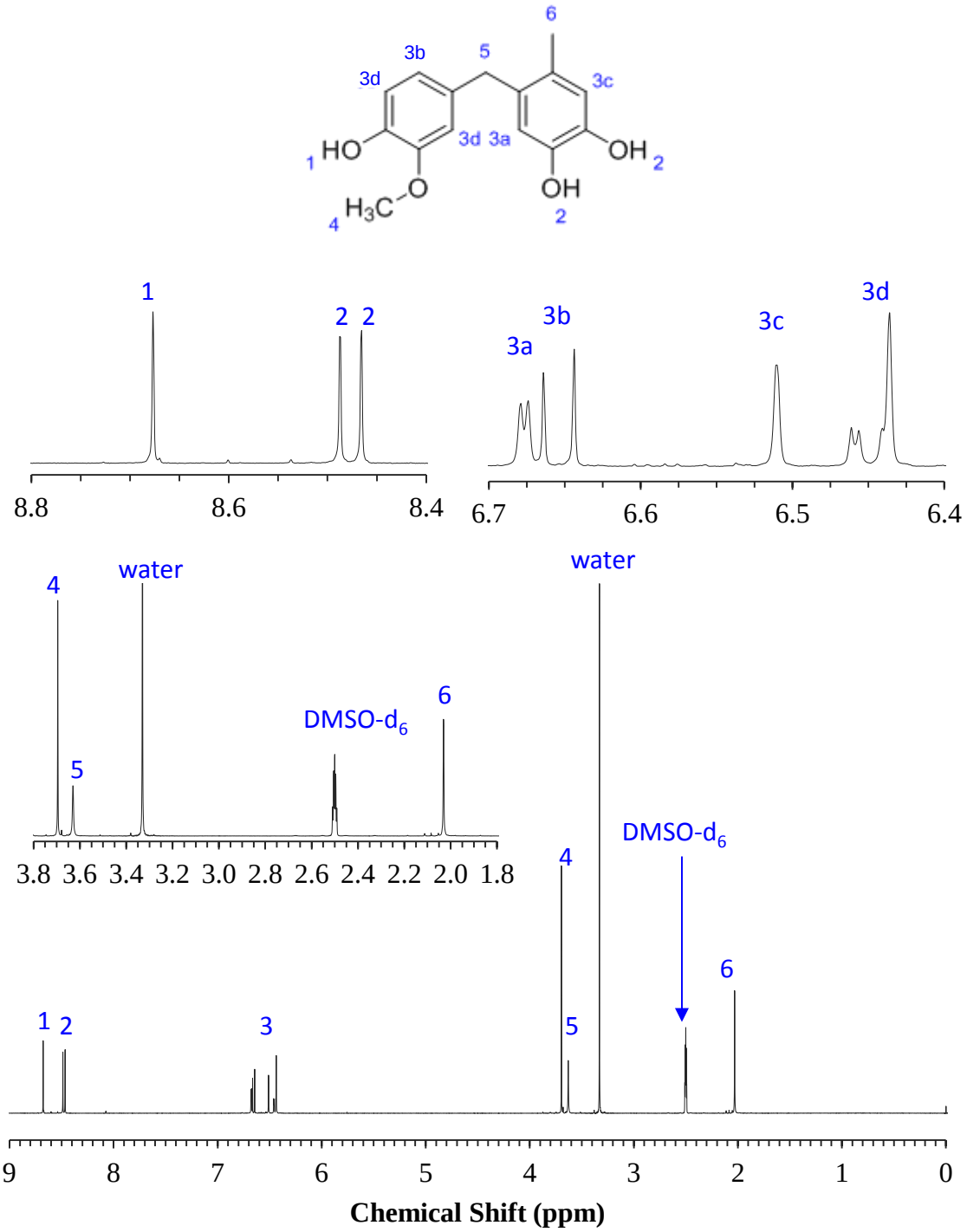

^{1}H NMR (400 MHz, DMSO-d6) d ppm 2.03 (s, 3 H), 3.63 (s, 2 H), 3.70 (s, 3 H), 6.44 - 6.46 (m, 2 H), 6.51 (s, 1 H), 6.65 (d, J=8.19 Hz, 1 H), 6.68 (d, J=1.95 Hz, 1 H), 8.47 (s, 1 H), 8.49 (s, 1 H), 8.68 (s, 1 H)

Figure 41. ^{1}H-NMR of vanillyl alcohol – methyl catechol monomer with proton assignments.

References

[1] L. H. Sperling, *Introduction to Physical Polymer Science*, 4th ed. Hoboken, NJ: Wiley, 2006.

[2] J. R. Fried, *Polymer Science and Technology*, 2nd ed. Upper Saddle River, NJ: Prentice Hall Professional Technical Reference, 2003.

[3] G. G. Odian, *Principles of Polymerization*, 3rd ed. New York: Wiley, 1991.

[4] R. Auvergne, S. Caillol, G. David, B. Boutevin, and J.-P. Pascault, "Biobased Thermosetting Epoxy: Present and Future," *Chem. Rev.* , vol. 114, pp. 1082-1115, 2014.

[5] D. Feldman and A. Barbalata, *Synthetic Polymers: Technology, Properties, Applications*, 1st ed. London: Chapman Hill, 1996.

[6] I. Skeist, *Epoxy Resins*. New York: Reinhold Pub. Corp., 1958.

[7] L. G. Wade, *Organic Chemistry*, 6th ed. Upper Saddle River, N.J.: Pearson Prentice Hall, 2006.

[8] *Epoxy Resins: Chemistry and Technology*, 2nd ed. New York: Marcel Dekker, Inc., 1988.

[9] G. F. Dugan and J. A. H. Widiger, "Process for purifying 4, 4'-isopropylidenediphenol," US3326986, 1967.

[10] L. Neagu, "Synthesis of Bisphenol A with Heterogeneous Catalysts, Masters Thesis," Master of Science, Chemical Engineering, Queens University, Canada, 1998.

[11] W. Zhang, Y. Li, M. He, and Q. Chen, "Synthesis of bisphenol F by using modified cation exchange resin," *Huagong Jinzhan*, vol. 26, pp. 1032-1035, 2007.

[12] B. Jackson, "Method of Producing Bisphenol A," Canada Patent, 2003.

[13] D. J. Little, "Recrystallization of bisphenol A by azeotropically drying the solvent," US4638102, 1987.

[14] A. K. Mendiratta and W. F. Morgan, "Purification of bisphenol-A," EP0109033A2, 1984.

[15] "NTP-CERHR Expert Panel Report on the Reproductive and Developmental Toxcity of Bisphenol A," National Toxicology Program, Research Triangle Park, NC2007.

[16] (2013). *Biomonitoring Summary Bisphenol A*. CDC. Available: http://www.cdc.gov/biomonitoring/BisphenolA_BiomonitoringSummary.html

[17] J. A. Rogers, L. Metz, and V. W. Yong, "Review: Endocrine disrupting chemicals and immune responses: A focus on bisphenol-A and its potential mechanisms," *Molecular Immunology,* vol. 53, pp. 421-430, 2013.

[18] L. N. Vandenberg, R. Hauser, M. Marcus, N. Olea, and W. V. Welshons, "Human exposure to bisphenol A (BPA)," *Reprod. Toxicol.,* vol. 24, pp. 139-177, 2007.

[19] "European Union Summary Risk Assessment Report - 4,4'-isopropylidenediphenol (Bisphenol A)," European Chemicals Bureau, United Kingdom2003.

[20] A. A. Gardziella, A. Pilato, and A. Knop, *Phenolic Resins: Chemistry, Applications, Standardization, Safety and Ecology* 2nd ed. New York: Springer-Verlag Berlin Heidelberg, 2000.

[21] J. D. Durig, "Comparisons of Epoxy Technology for Protective Coatings and Linings in Wastewater Facilities," presented at the The Industrial Protective Coatings Conference and Exhibit, Houston, TX, 1999.

[22] S. Eladak, T. Grisin, D. Moison, M.-J. Guerquin, T. N'Tumba-Byn, S. Pozzi-Gaudin, *et al.*, "A new chapter in the bisphenol A story: bisphenol S and bisphenol F are not safe alternatives to this compound," *Fertility and Sterility,* vol. 103, pp. 11-21.

[23] B. M. Bell, J. R. Briggs, R. M. Campbell, S. M. Chambers, P. D. Gaarenstroom, J. G. Hippler, *et al.*, "Glycerin as a renewable feedstock for epichlorohydrin production. The GTE process," *Clean: Soil, Air, Water,* vol. 36, pp. 657-661, 2008.

[24] E. Santacesaria, R. Tesser, M. Di Serio, L. Casale, and D. Verde, "New process for producing epichlorohydrin via glycerol chlorination," *Ind. Eng. Chem. Res.,* vol. 49, pp. 964-970, 2010.

[25] G. D. Sergeevich and L. Z. Nikolaevich, "Hydrochlorination of glycerol--the role of the water on the process," *J. Chem. Chem. Eng.,* vol. 5, pp. 1179-1182, 2011.

[26] F. Yang, M. A. Hanna, and R. Sun, "Value-added uses for crude glycerol - a byproduct of biodiesel production," *Biotechnol. Biofuels,* vol. 5, p. 13, 2012.

[27] Z. W. Wicks, F. N. Jones, S. P. Pappas, and D. A. Wicks, *Organic Coatings: Science and Technology,* 3rd ed. Hoboken, NJ: John Whiley & Sons, Inc, 2007.

[28] J. J. LaScala, "The effects of triglyceride structure on the propeties of plant oil-based resins," Doctor of Philosophy Dissertation, Chemcal Engineering, University of Delaware, Delaware, 2002.

[29] (2013). *D.E.R. Solid Epoxy Resins. Product Safety Assessment*. Available: http://msdssearch.dow.com/PublishedLiteratureDOWCOM/dh_08ec/0901b803808ecde7.pdf

[30] M. G. Gonzalez, J. C. Cabanelas, and J. Baselga, "Applications of FTIR on epoxy resins - identification, monitoring the curing process, phase separation and water uptake. ," presented at the Infrared Spectroscopy: Materials Science, Engineering and Technology, 2012.

[31] G. R. Palmese and R. L. McCullough, "Effect of epoxy-amine stoichiometry on cured resin material properties," *J. Appl. Polym. Sci.,* vol. 46, pp. 1863-73, 1992.

[32] S. Paz-Abuin, A. Lopez-Quintela, M. Varela, M. Pazos-Pellin, and P. Prendes, "Method for determination of the ratio of rate constants, secondary to primary amine, in epoxy-amine systems," *Polymer,* vol. 38, pp. 3117-3120, 1997.

[33] *Monomers, Polymers and Composites from Renewable Resources,* 1st ed. Amsterdam: Elsevier 2008.

[34] X. Pan, P. Sengupta, and D. C. Webster, "High Biobased Content Epoxy-Anhydride Thermosets from Epoxidized Sucrose Esters of Fatty Acids," *Biomacromolecules,* vol. 12, pp. 2416-2428, 2011.

[35] X. Pan, P. Sengupta, and D. C. Webster, "Novel biobased epoxy compounds: epoxidized sucrose esters of fatty acids," *Green Chem.,* vol. 13, pp. 965-975, 2011.

[36] M. Stemmelen, F. Pessel, V. Lapinte, S. Caillol, J. P. Habas, and J. J. Robin, "A fully biobased epoxy resin from vegetable oils: From the synthesis of the precursors by thiol-ene reaction to the study of the final material," *J. Polym. Sci., Part A: Polym. Chem.,* vol. 49, pp. 2434-2444, 2011.

[37] Z. Wang, X. Zhang, R. Wang, H. Kang, B. Qiao, J. Ma, *et al.,* "Synthesis and Characterization of Novel Soybean-Oil-Based Elastomers with Favorable Processability and Tunable Properties," *Macromolecules* vol. 45, pp. 9010-9019, 2012.

[38] M. A. R. Meier, J. O. Metzger, and U. S. Schubert, "Plant oil renewable resources as green alternatives in polymer science," *Chem. Soc. Rev.,* vol. 36, pp. 1788-1802, 2007.

[39] M. Chrysanthos, J. Galy, and J.-P. Pascault, "Preparation and properties of bio-based epoxy networks derived from isosorbide diglycidyl ether," *Polymer,* vol. 52, pp. 3611-3620, 2011.

[40] J. Lukaszczyk, B. Janicki, and A. Frick, "Investigation on synthesis and properties of isosorbide based bis-GMA analogue," *J. Mater. Sci.: Mater. Med.,* vol. 23, pp. 1149-1155, 2012.

[41] J. Lukaszczyk, B. Janicki, and M. Kaczmarek, "Synthesis and properties of isosorbide based epoxy resin," *Eur. Polym. J.,* vol. 47, pp. 1601-1606, 2011.

[42] F. Hu, J. J. La Scala, J. M. Sadler, and G. R. Palmese, "Synthesis and Characterization of Thermosetting Furan-Based Epoxy Systems," *Macromolecules* vol. 47, pp. 3332-3342, 2014.

[43] F. Hu, S. K. Yadav, J. J. La Scala, J. M. Sadler, and G. R. Palmese, "Preparation and Characterization of Fully Furan-Based Renewable Thermosetting Epoxy-Amine Systems," *Macromol. Chem. Phys.*, p. Ahead of Print, 2015.

[44] J. Holladay, J. White, J. Bozell, and D. Johnson, "Top Value-Added Chemicals from Biomass - Volume II—Results of Screening for Potential Candidates from Biorefinery Lignin," Pacific Northwest National Laboratory, Richland, WA2007.

[45] W. Thielemans, "Lignin and carbon nanotube utilization in bio-based composites, Ph.D Dissertation," Ph.D., University of Delaware, 2004.

[46] T. Saito, R. H. Brown, M. A. Hunt, D. L. Pickel, J. M. Pickel, J. M. Messman, *et al.*, "Turning renewable resources into value-added polymer: development of lignin-based thermoplastic," *Green Chem.*, vol. 14, pp. 3295-3303, 2012.

[47] F. G. Calvo-Flores and J. A. Dobado, "Lignin as Renewable Raw Material," *ChemSusChem*, vol. 3, pp. 1227-1235, 2010.

[48] D. K. Shen, S. Gu, K. H. Luo, S. R. Wang, and M. X. Fang, "The pyrolytic degradation of wood-derived lignin from pulping process," *Bioresour. Technol.*, vol. 101, pp. 6136-6146, 2010.

[49] H. S. Choi and D. Meier, "Fast pyrolysis of Kraft lignin-Vapor cracking over various fixed-bed catalysts," *J. Anal. Appl. Pyrolysis*, vol. 100, pp. 207-212, 2013.

[50] H. E. Jegers and M. T. Klein, "Primary and secondary lignin pyrolysis reaction pathways," *Ind. Eng. Chem. Process Des. Dev.*, vol. 24, pp. 173-83, 1985.

[51] J. D. Araujo, "Production of vaillin from lignin present in the Kraft black liquor of the pulp and paper industry," Doctor of Philosophy, Chemical Engineering, University of Porto, 2008.

[52] M. B. Hocking, "Vanillin: synthetic flavoring from spent sulfite liquor," *J. Chem. Educ.*, vol. 74, pp. 1055-1059, 1997.

[53] "Part 3 - Aroma chemicals from petrochemical feedstocks, in: Study into the establishment of an aroma and fragrance fine chemicals value chain in South Africa," Triumph Venture Capital, Ltd, South Africa2004.

[54] E. A. Borges da Silva, M. Zabkova, J. D. Araujo, C. A. Cateto, M. F. Barreiro, M. N. Belgacem, *et al.*, "An integrated process to produce vanillin and lignin-based polyurethanes from Kraft lignin," *Chem. Eng. Res. Des.*, vol. 87, pp. 1276-1292, 2009.

[55] C. Fargues, A. Mathias, and A. Rodrigues, "Kinetics of Vanillin Production from Kraft Lignin Oxidation," *Ind. Eng. Chem. Res.*, vol. 35, pp. 28-36, 1996.

[56] J. D. P. Araujo, C. A. Grande, and A. E. Rodrigues, "Vanillin production from lignin oxidation in a batch reactor," *Chem. Eng. Res. Des.*, vol. 88, pp. 1024-1032, 2010.

[57] C. Aouf, J. Lecomte, P. Villeneuve, E. Dubreucq, and H. Fulcrand, "Chemo-enzymatic functionalization of gallic and vanillic acids: synthesis of bio-based epoxy resins prepolymers," *Green Chem.,* vol. 14, pp. 2328-2336, 2012.

[58] T. Koike, "Progress in Development of Epoxy Resin Systems Based on Wood Biomass in Japan," *Polymer Engineering and Science,* vol. 52, pp. 701-717, 2012.

[59] "Process for the Production of Hardenable Synthetic Epoxy Resins," Great Britian Patent GB923772, 1963.

[60] M. Fache, R. Auvergne, B. Boutevin, and S. Caillol, "New vanillin-derived diepoxy monomers for the synthesis of biobased thermosets," *Eur. Polym. J.,* vol. 67, pp. 527-538, 2015.

[61] M. Fache, E. Darroman, V. Besse, R. Auvergne, S. Caillol, and B. Boutevin, "Vanillin, a promising biobased building-block for monomer synthesis," *Green Chem.,* vol. 16, pp. 1987-1998, 2014.

[62] L. G. Wade, *Organic Chemistry*, Sixth edition. ed.

[63] D. A. Skoog, F. J. Holler, and S. R. Crouch, *Principles of Instrumental Analysis*, 6th ed. Belmont, CA: Thomson Brooks/Cole, 2007.

[64] J. H. Nelson, *Nuclear Magnetic Resonance Spectroscopy*. Upper Saddle River, NJ: Prentice Hall, 2003.

[65] P. W. Atkins and J. De Paula, *Atkins' Physical Chemistry,* 8th ed. Oxford ; New York: Oxford University Press, 2006.

[66] K. P. Menard, *Dynamic Mechanical Analysis: A Practical Approach*. Boca Raton, FL: CRC Press, 1999.

[67] "ASTM D1652-11, Standard Test Method for Epoxy Content of Epoxy Resins," ed. West Conshohocken, PA: ASTM International, 2011.

[68] D. Halliday, R. Resnick, and J. Walker, *Fundamentals of Physics*. Hoboken, NJ: Wiley, 2014.

[69] (1999). *Dow Liquid Epoxy Resins, Dow Chemical Company, 1999*. Available: http://epoxy.dow.com/resources/literature.htm

[70] V. Bellenger, J. Verdu, and E. Morel, "Effect of structure on glass transition temperature of amine crosslinked epoxies," *J. Polym. Sci., Part B: Polym. Phys.,* vol. 25, pp. 1219-34, 1987.

[71] G. Levita, S. De Petris, A. Marchetti, and A. Lazzeri, "Crosslink density and fracture toughness of epoxy resins," *J. Mater. Sci.,* vol. 26, pp. 2348-52, 1991.

[72] F. Meyer, G. Sanz, A. Eceiza, I. Mondragon, and J. Mijovic, "The effect of stoichiometry and thermal history during cure on structure and properties of epoxy networks," *Polymer,* vol. 36, pp. 1407-14, 1995.

[73] I. M. McAninch, G. R. Palmese, J. L. Lenhart, and J. J. La Scala, "Characterization of epoxies cured with bimodal blends of polyetheramines," *J. Appl. Polym. Sci.,* vol. 130, pp. 1621-1631, 2013.

[74] "Report on Carcinogens, Thirteenth Edition.," National Toxicology Program. Department of Health and Human Services, Public Health Service NC, USA2014.

[75] H.-R. Bjorsvik and F. Minisci, "Fine Chemicals from Lignosulfonates. 1. Synthesis of Vanillin by Oxidation of Lignosulfonates," *Org. Process Res. Dev.,* vol. 3, pp. 330-340, 1999.

[76] I. A. Pearl, "Reactions of vanillin and its derived compounds. I. The reaction of vanillin with silver oxide," *J. Am. Chem. Soc.,* vol. 68, pp. 429-32, 1946.

[77] I. A. Pearl and D. L. Beyer, "Reaction of vanillin with silver oxide in the presence of technical caustic," *Ind. Eng. Chem.,* vol. 44, pp. 2893-4, 1952.

[78] C. S. Lecher. (2007). *Sodium Borohydride Reduction of Vanillin: A Low Solvent Synthesis of Vanillyl Alcohol*. Available: http://greenchem.uoregon.edu/PDFs/GEMsID90.pdf

[79] H. A. Meylemans, T. J. Groshens, and B. G. Harvey, "Synthesis of Renewable Bisphenols from Creosol," *ChemSusChem,* vol. 5, pp. 206-210, 2012.

[80] C. F. Lim and J. M. Tanski, "Structural Analysis of Bisphenol-A and its Methylene, Sulfur, and Oxygen Bridged Bisphenol Analogs," *J. Chem. Crystallogr.,* vol. 37, pp. 587-595, 2007.

[81] Q. Chen, W. Huang, P. Chen, C. Peng, H. Xie, Z. K. Zhao, *et al.,* "Synthesis of Lignin-Derived Bisphenols Catalyzed by Lignosulfonic Acid in Water for Polycarbonate Synthesis," *ChemCatChem,* vol. 7, pp. 1083-1089, 2015.

[82] X. Yang, J. Zhu, Y. R, L. JP, L. Li, and H. Zhang, "Phenolic constituents from the rhizomes of Gastrodia elata.," *Nat Prod Res,* vol. 21, pp. 180-186, 2007.

[83] E. L. Rodriguez, "STP1249-EB, The Glass Transition Temperature of Glassy Polymers using Dynamic Mechanical Analysis," ed. Philadelphia, Pa: ASTM International, 1994, pp. 225-268.

[84] M. Palusiak and S. J. Grabowski, "Methoxy group as an acceptor of proton in hydrogen bonds," *Journal of Molecular Structure,* vol. 642, pp. 97-104, 2002.

Appendix A

^{1}H and ^{13}C NMR Spectra

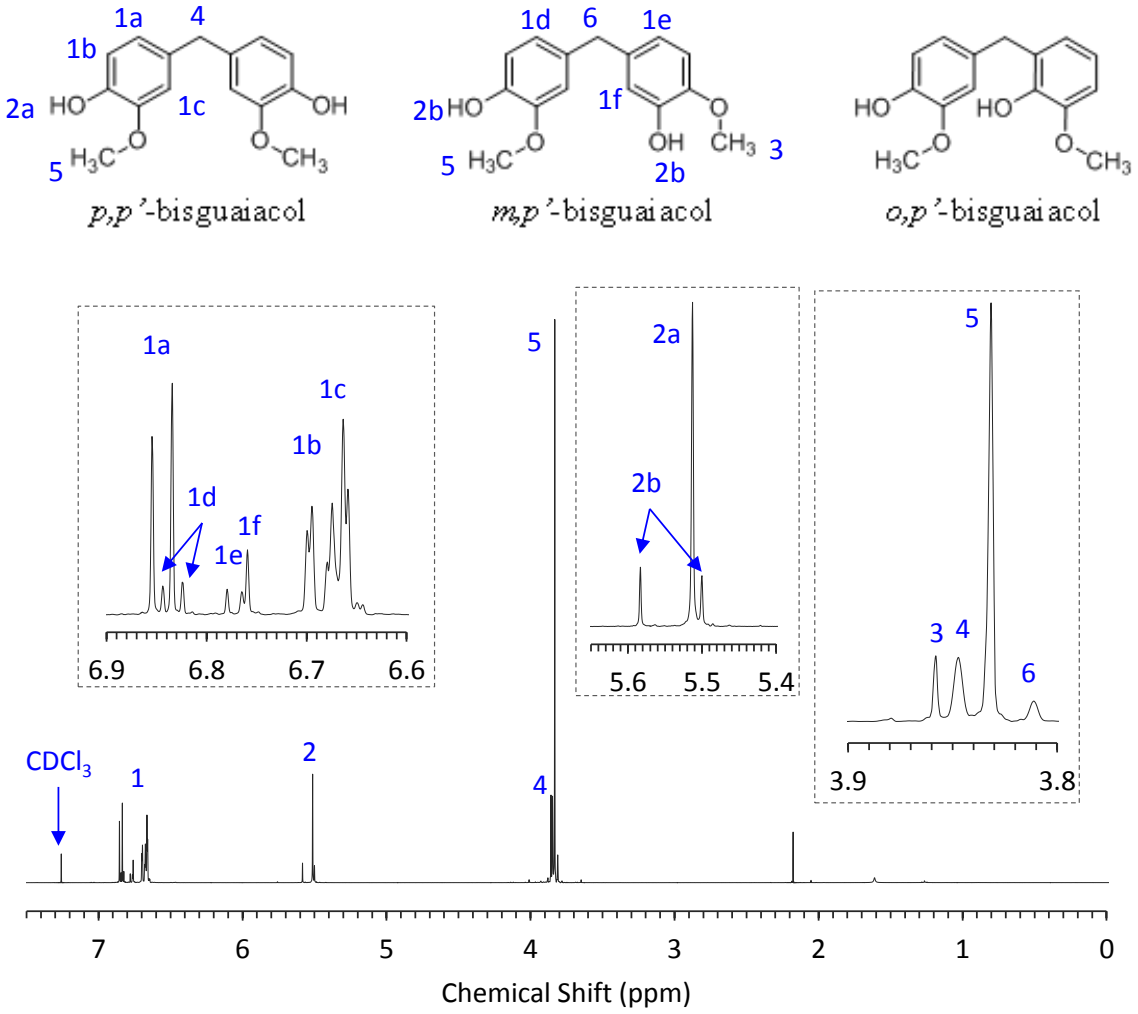

Figure A1. ^{1}H-NMR of bisguaiacol isomers with proton assignments.

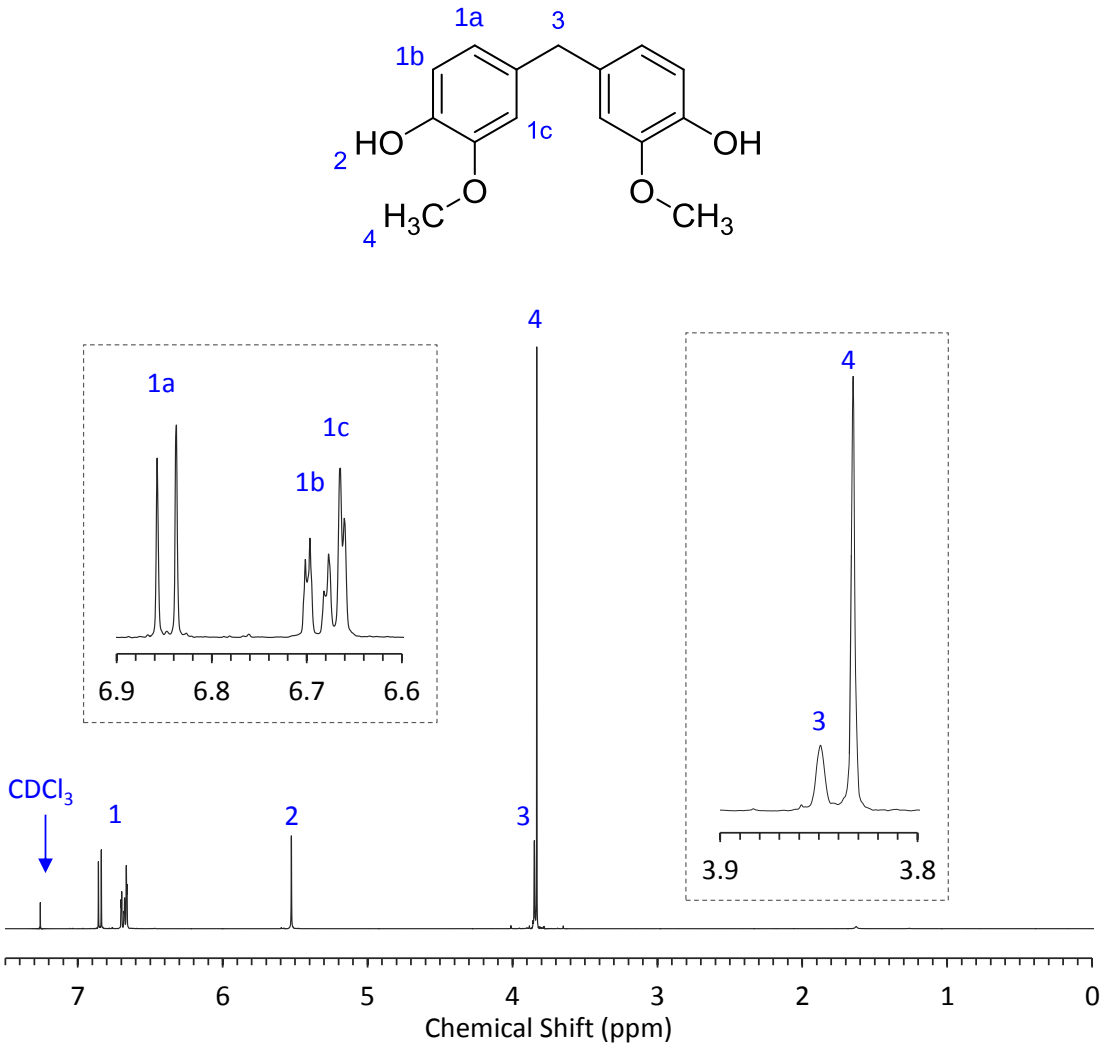

Figure A2. ^{1}H-NMR of *p,p'*-bisguaiacol with proton assignments.

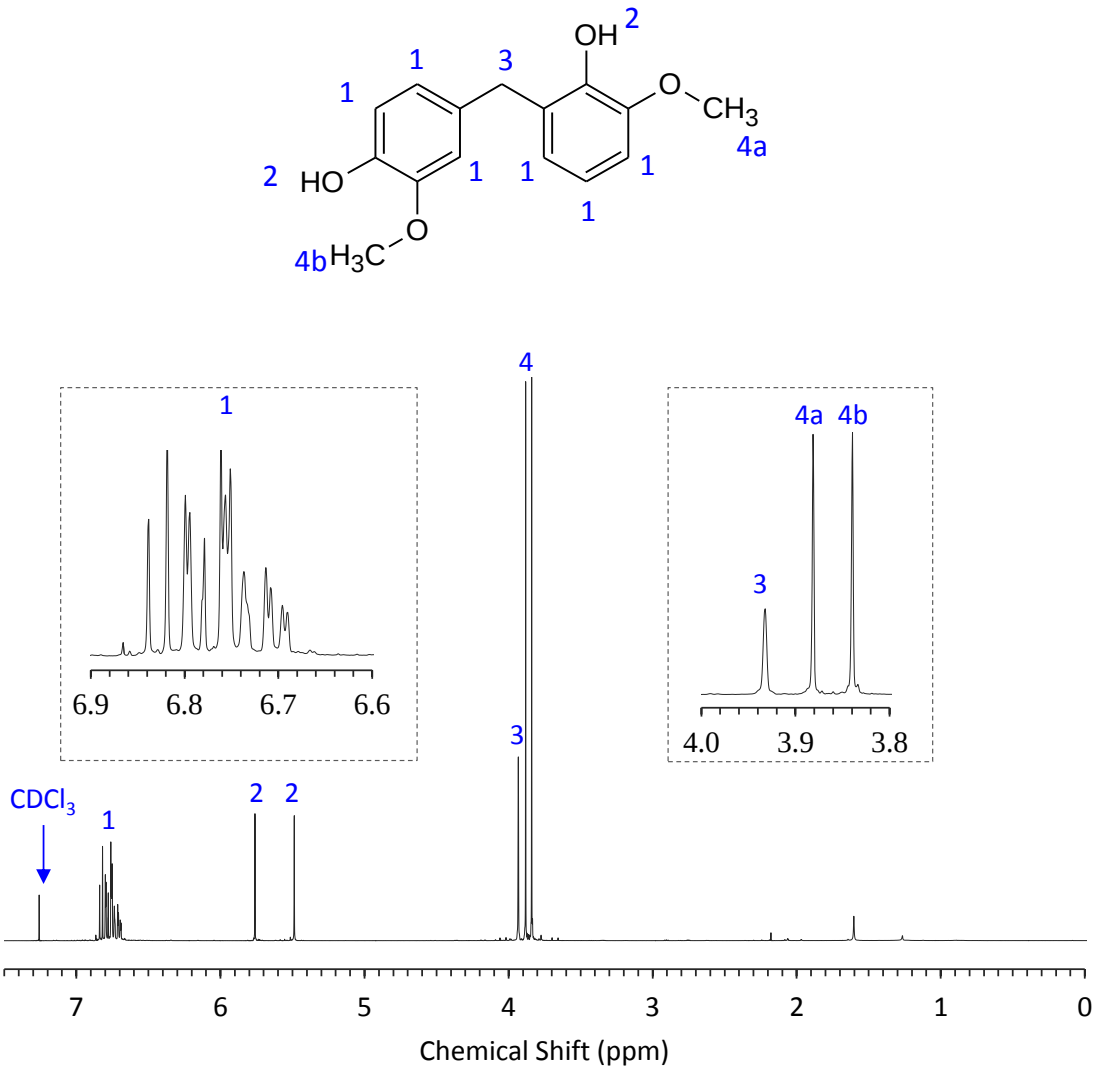

Figure A3. ^{1}H-NMR *o,p'*-bisguaiacol with proton assignments.

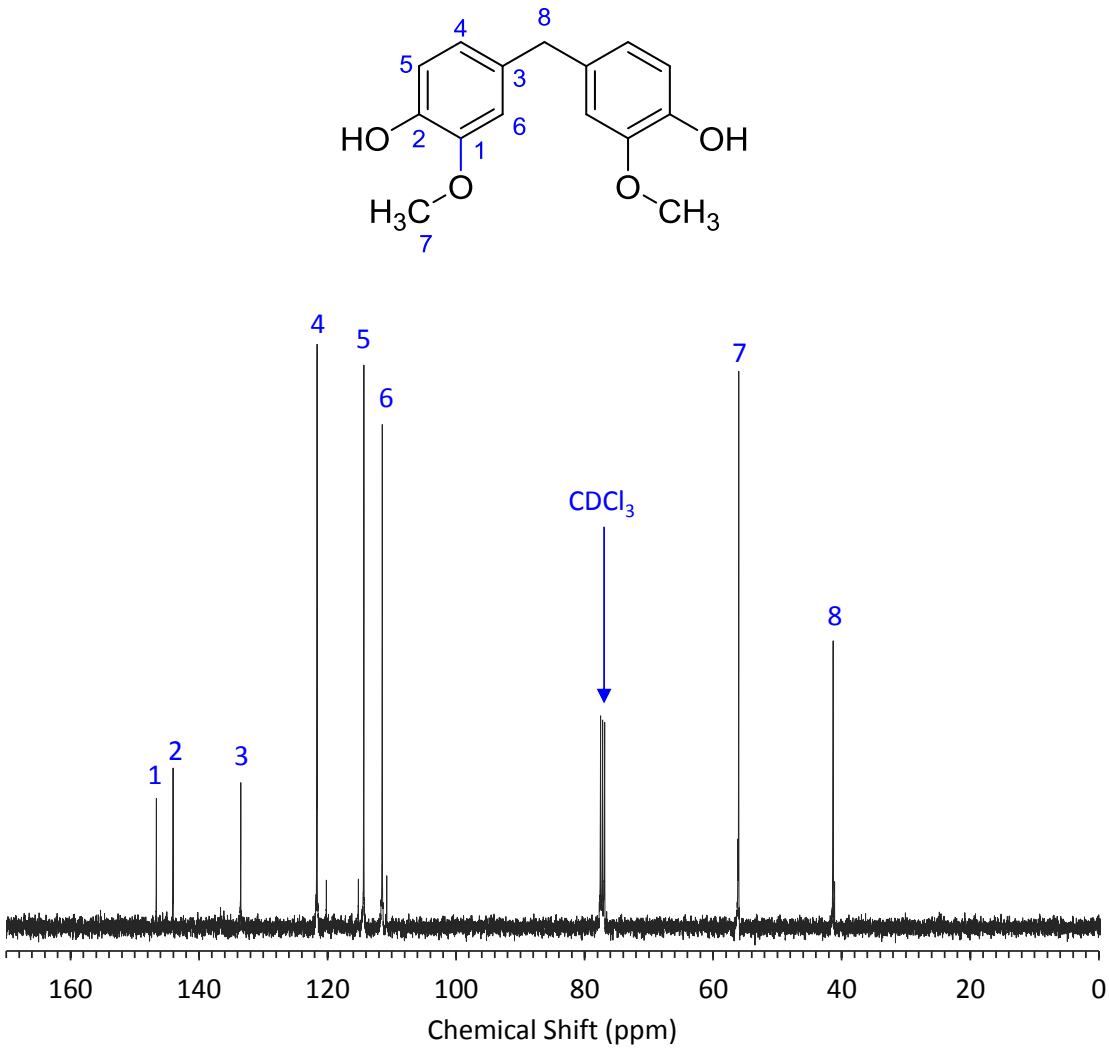

Figure A4. ^{13}C-NMR of bisguaiacol with carbon assignments.

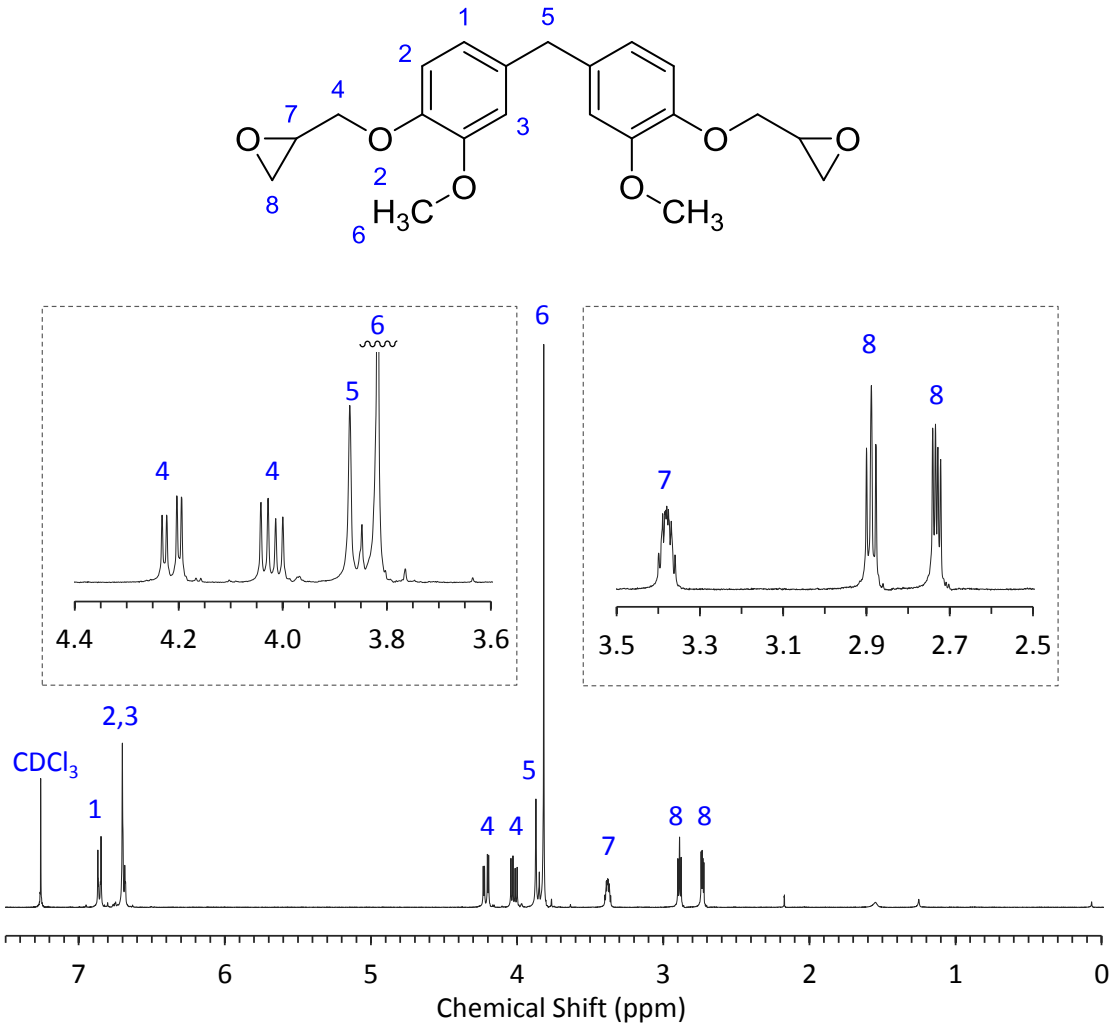

Figure A5. ^{1}H-NMR of diglycidyl ether of bisguaiacol (DGEBG) with proton assignments.

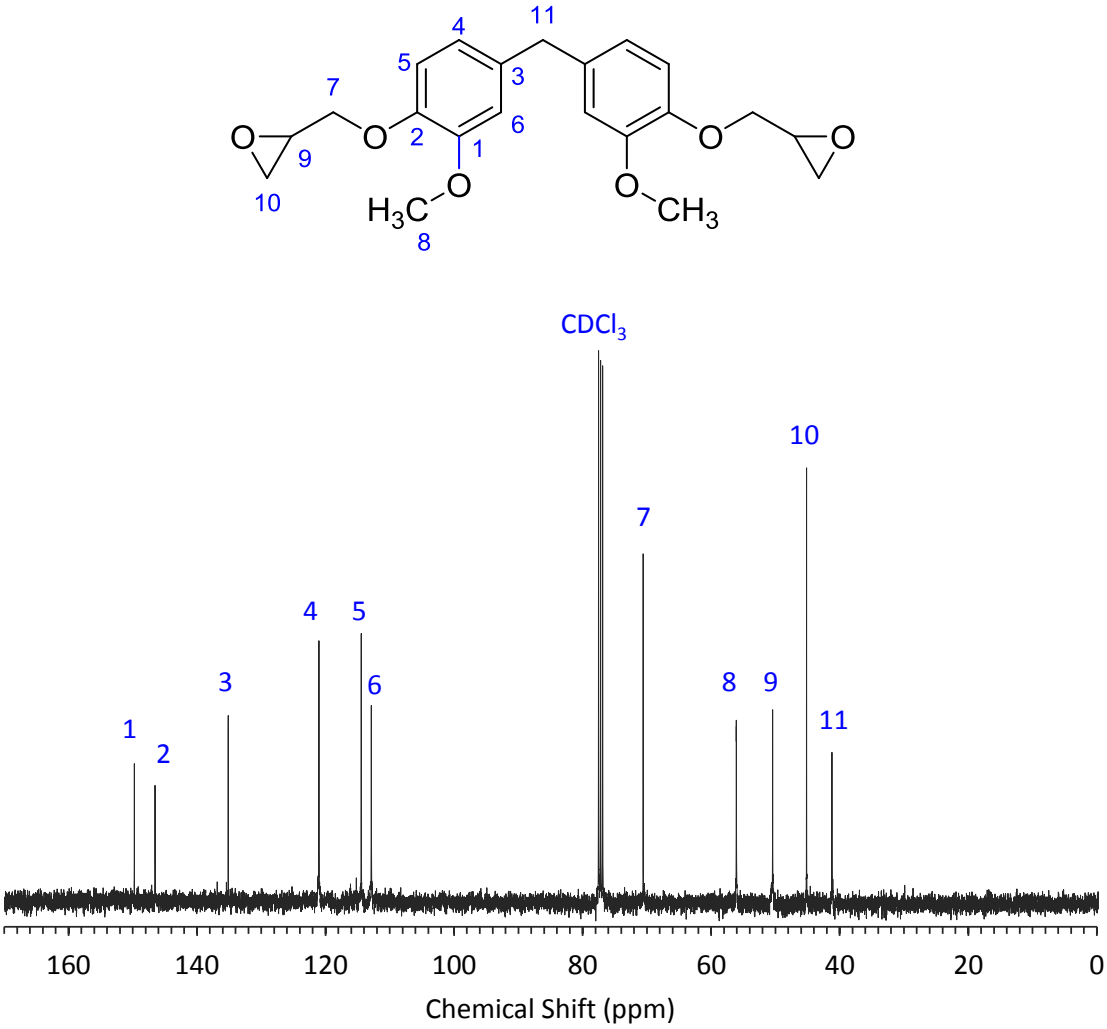

Figure A6. ^{13}C-NMR of diglycidyl ether of bisguaiacol (DGEBG) with carbon assignments.

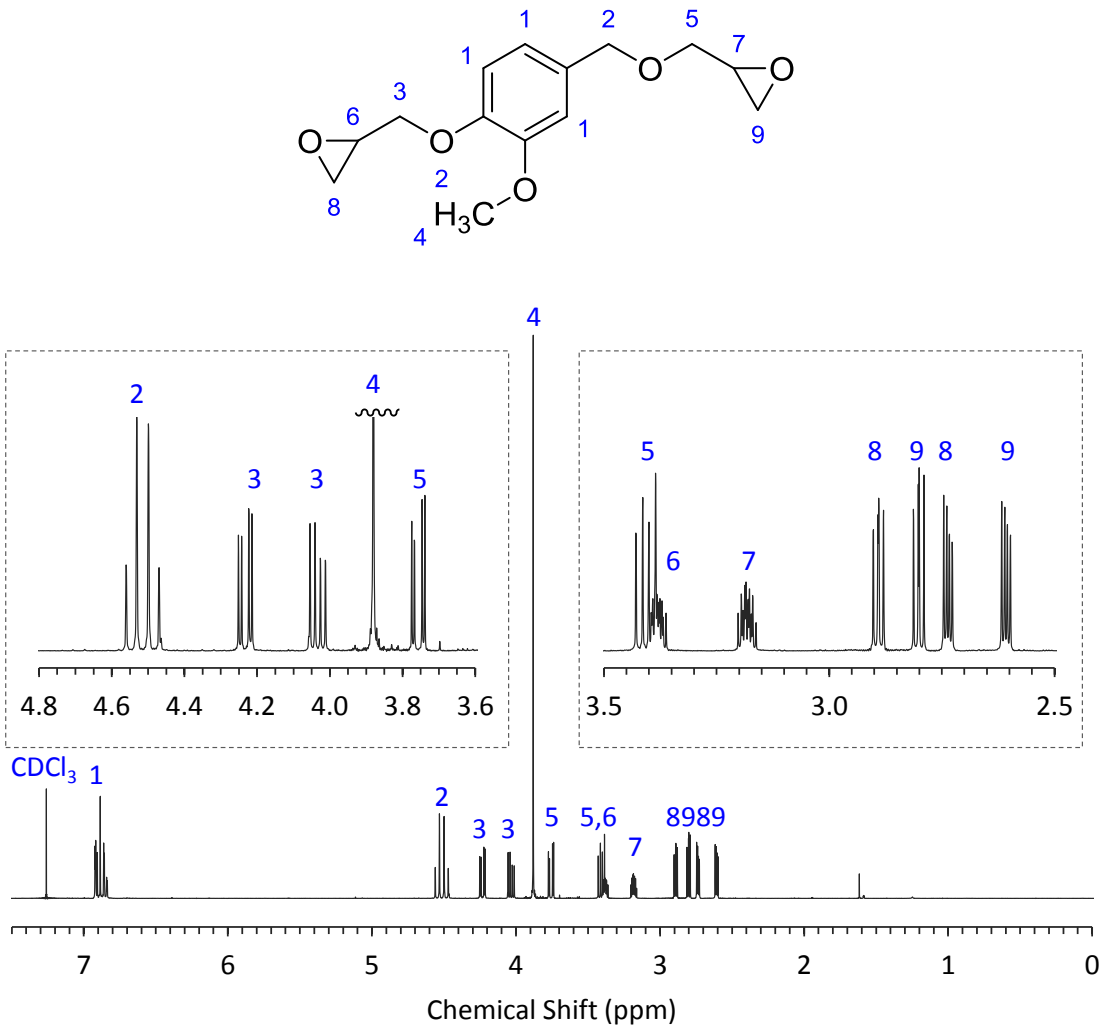

Figure A7. ^{1}H-NMR of diglycidyl ether of vanillyl alcohol (DGEVA) with proton assignments.

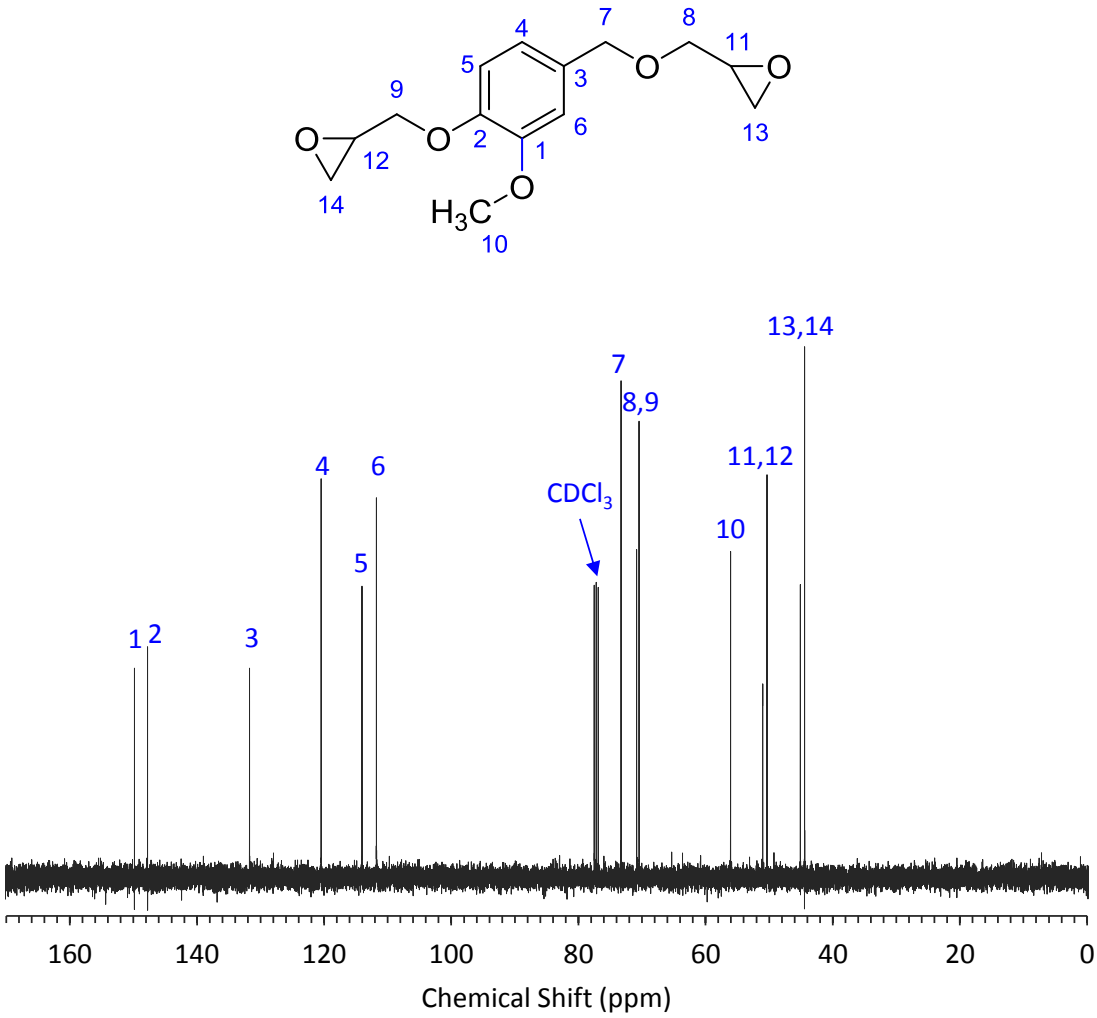

Figure A8. ^{13}C-NMR of diglycidyl ether of vanillyl alcohol (DGEVA) with carbon assignments.

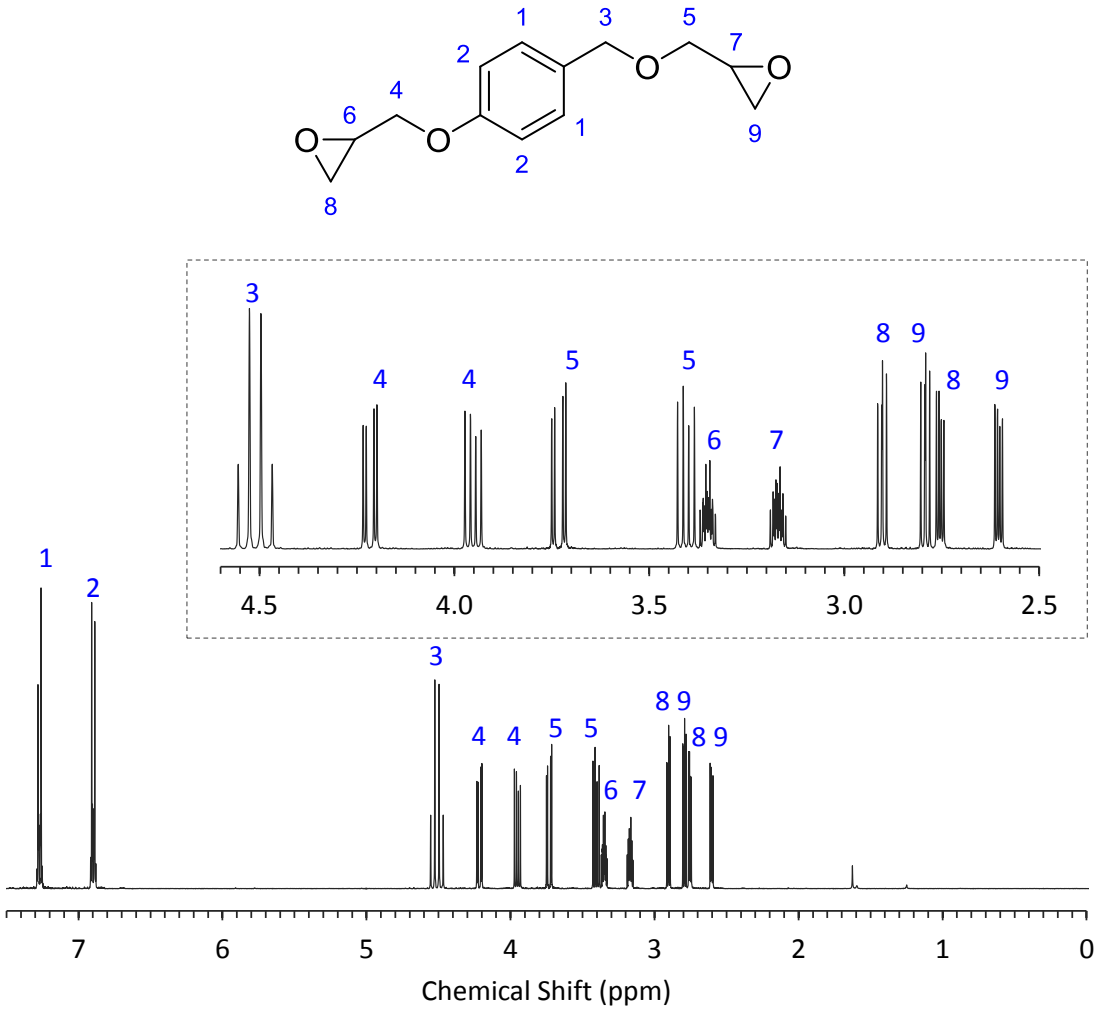

Figure A9. ^{1}H-NMR of diglycidyl ether of gastrodigenin (DGEGD) with proton assignments.

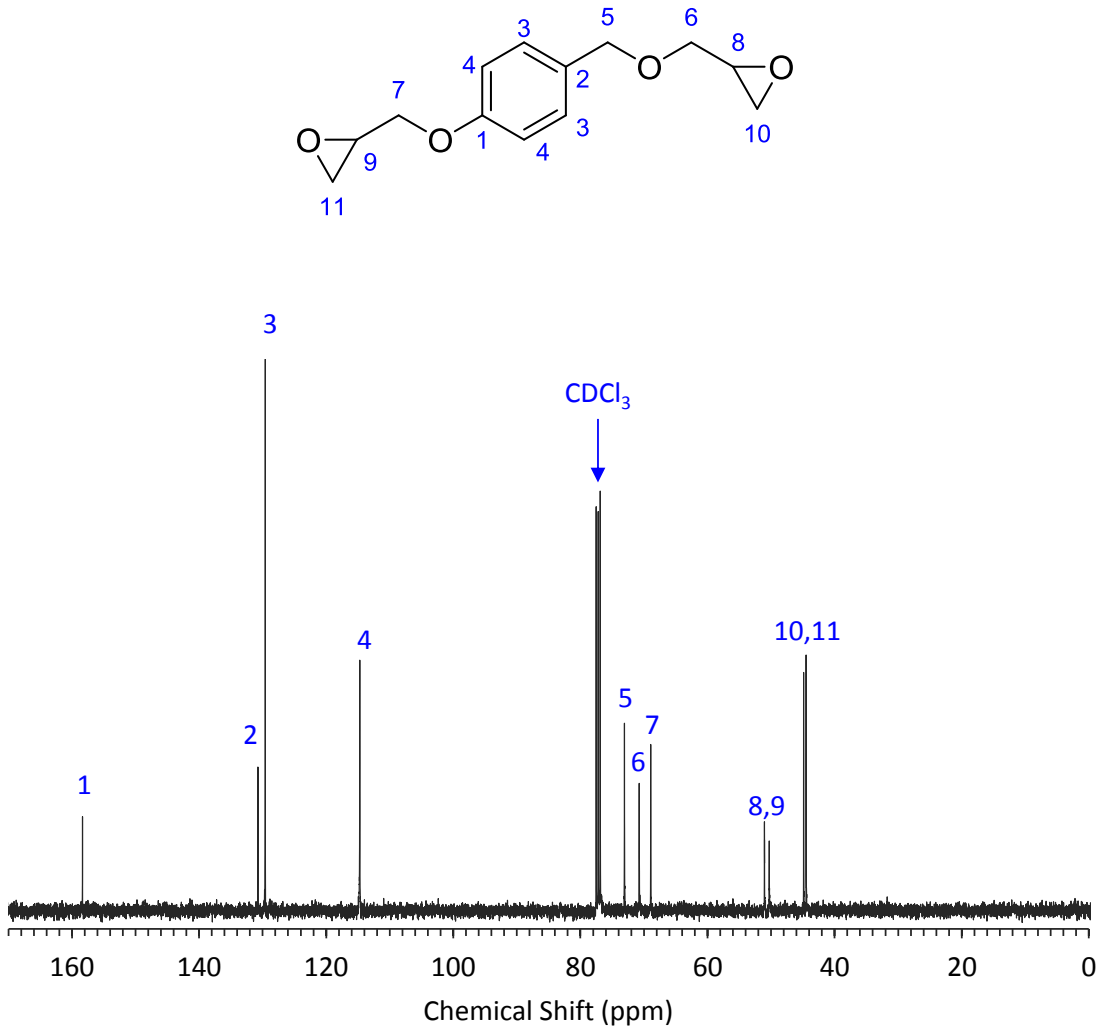

Figure A10. ^{13}C-NMR of diglycidyl ether of gastrodignenin (DGEGD) with carbon assignments.

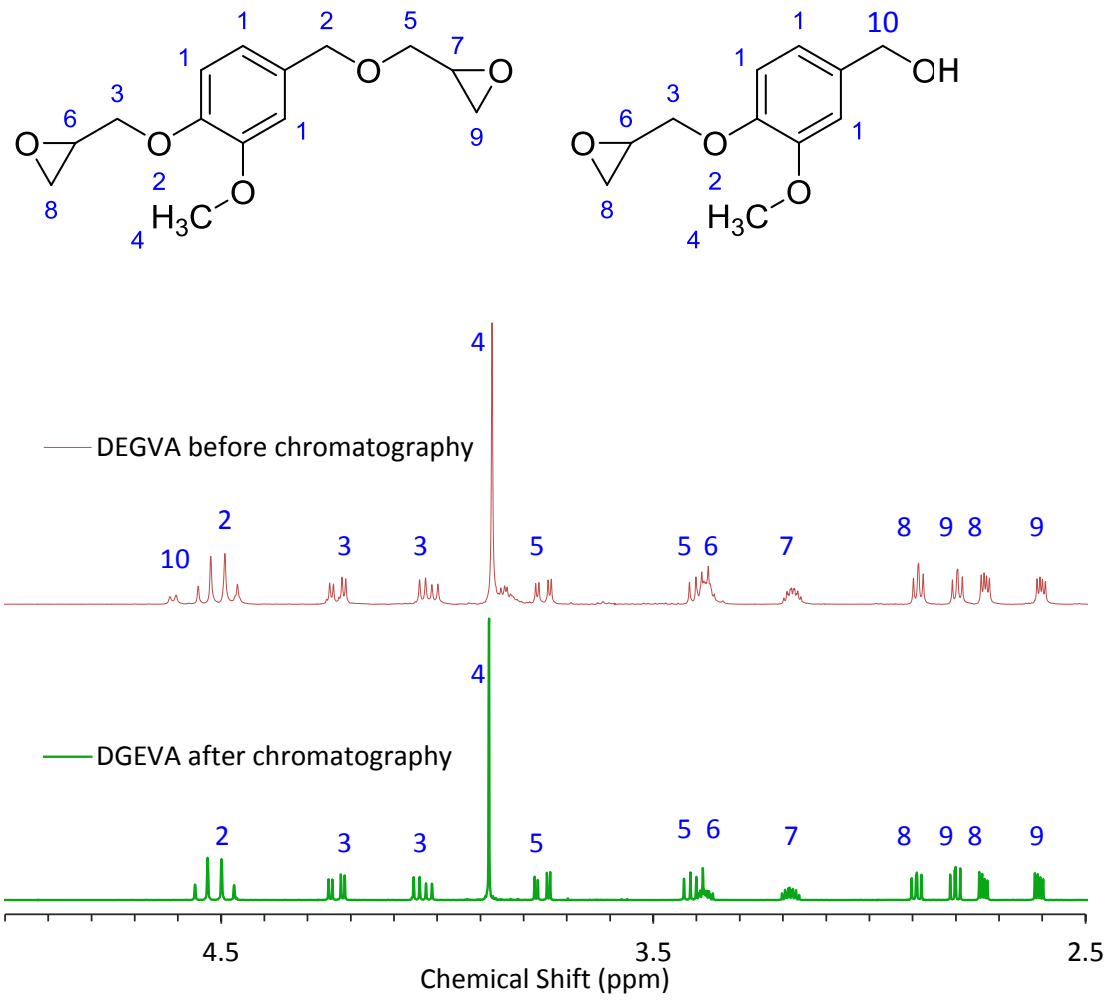

Figure A11. ^{1}H-NMR of diglycidyl ether of vanillyl alcohol (DGEVA) with proton assignments before and after purification via silica gel chromatography. Before chromatography, a peak at 4.6 ppm represents the presence of monoglycidyl ether of vanillyl alcohol (~15 % based on integration).

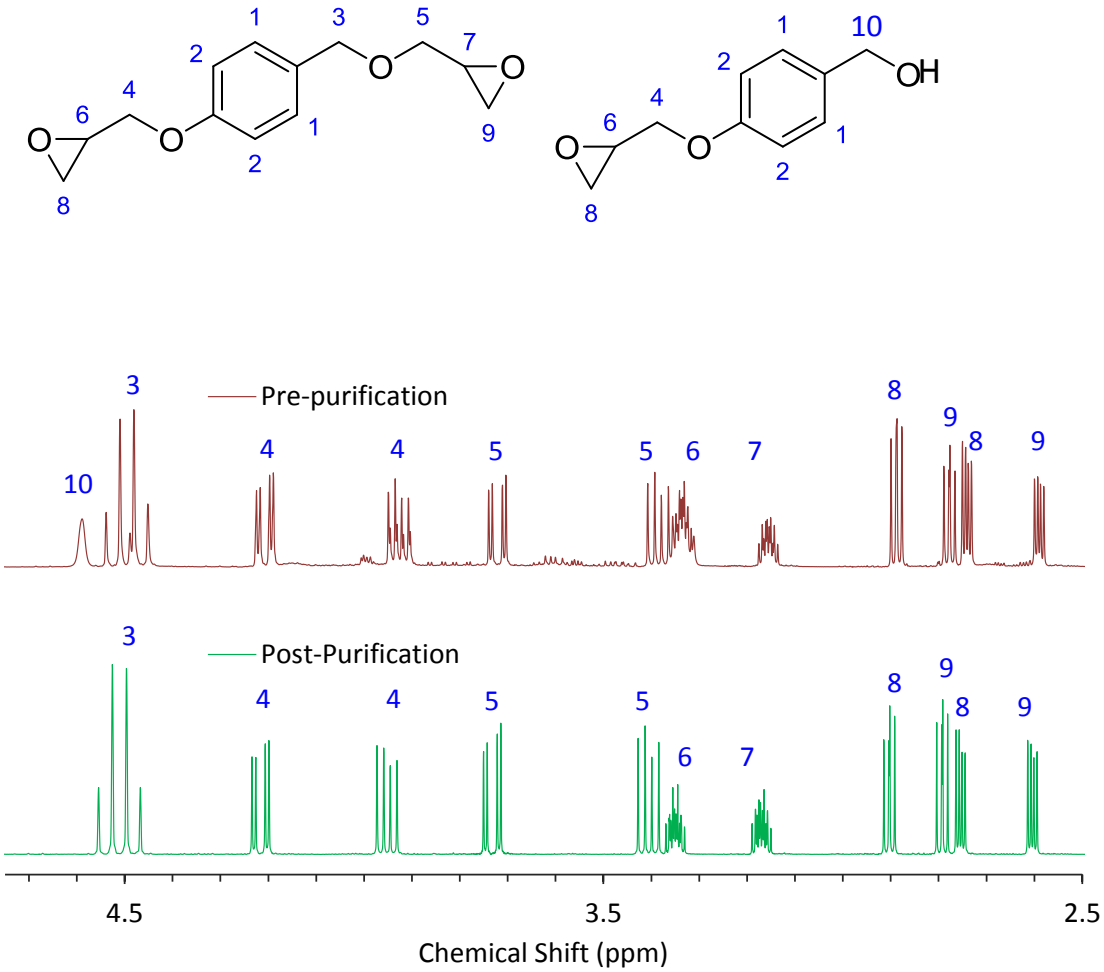

Figure A12. [1]H-NMR of diglycidyl ether of gastrodigenin (DGEGD) with proton assignments before and after purification via silica gel chromatography. Before chromatography, a peak at ~ 4.6 ppm represents the presence of monoglycidyl ether of gastrodigenin (~30 % based on integration).

Appendix B

Mass Spectrometry Spectra

Single Mass Analysis
Tolerance = 20.0 mDa / DBE: min = -1.5, max = 50.0
Element prediction: Off

Monoisotopic Mass, Odd and Even Electron Ions
11 formula(e) evaluated with 3 results within limits (up to 20 closest results for each mass)
Elements Used:
C: 0-15 H: 0-24 O: 0-7

C14H17O5
EDH_1 844 (19.693)

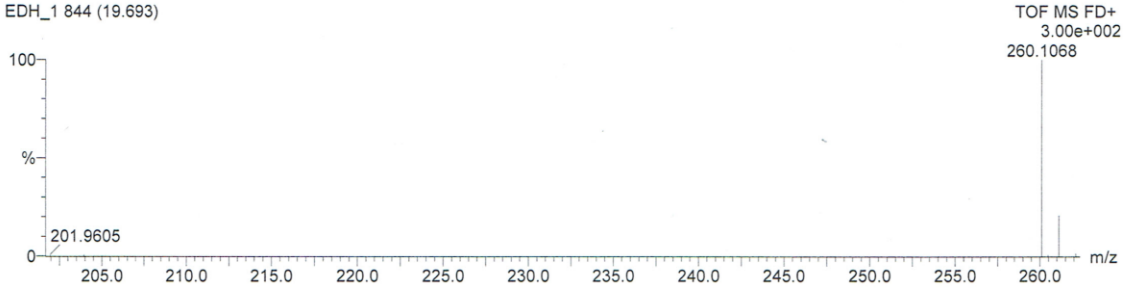

Minimum:				-1.5		
Maximum:		20.0	50.0	50.0		
Mass	Calc. Mass	mDa	PPM	DBE	i-FIT	Formula
260.1068	260.1049	1.9	7.3	8.0	1.7	C15 H16 O4
	260.0896	17.2	66.1	4.0	9.6	C11 H16 O7
	260.1260	-19.2	-73.8	3.0	9.1	C12 H20 O6

Figure B1. Time of flight mass spectrum of Bisguaiacol.

Single Mass Analysis
Tolerance = 20.0 mDa / DBE: min = -1.5, max = 50.0
Element prediction: Off

Monoisotopic Mass, Odd and Even Electron Ions
8 formula(e) evaluated with 1 results within limits (up to 20 closest results for each mass)
Elements Used:
C: 0-21 H: 0-24 O: 0-7
C14H18O5
EDH_4 74 (1.727)

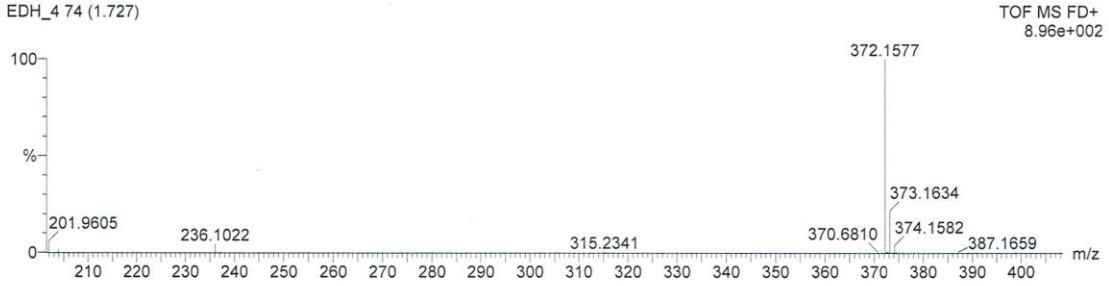

Minimum:				-1.5		
Maximum:		20.0	50.0	50.0		
Mass	Calc. Mass	mDa	PPM	DBE	i-FIT	Formula
372.1577	372.1573	0.4	1.1	10.0	0.9	C21 H24 O6

Figure B2. Time of flight mass spectrum of DGEBG.

Single Mass Analysis
Tolerance = 20.0 mDa / DBE: min = -1.5, max = 50.0
Element prediction: Off

Monoisotopic Mass, Odd and Even Electron Ions
9 formula(e) evaluated with 1 results within limits (up to 20 closest results for each mass)
Elements Used:
C: 0-14 H: 0-24 O: 0-7
C14H17O5
EDH_1 32 (0.747) Cm (32:39)

TOF MS FD+
3.04e+004

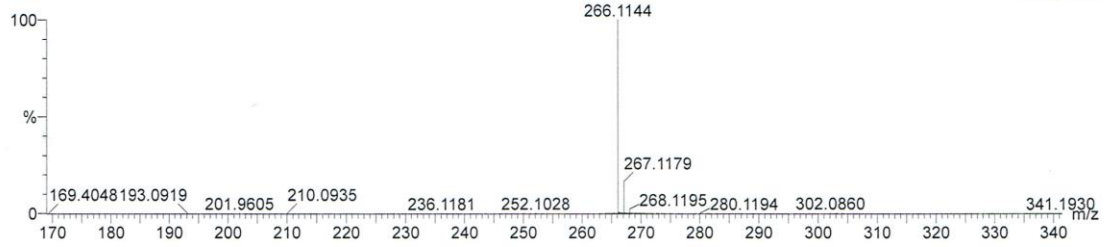

Minimum:				-1.5		
Maximum:		20.0	50.0	50.0		
Mass	Calc. Mass	mDa	PPM	DBE	i-FIT	Formula
266.1144	266.1154	-1.0	-3.8	6.0	2.4	C14 H18 O5

Figure B3. Time of flight mass spectrum of DGEVA.

Single Mass Analysis
Tolerance = 20.0 mDa / DBE: min = -1.5, max = 50.0
Element prediction: Off

Monoisotopic Mass, Odd and Even Electron Ions
4 formula(e) evaluated with 1 results within limits (up to 20 closest results for each mass)
Elements Used:
C: 0-16 H: 0-16 O: 0-4
C21H24O6+C18H20O5
EDH_2 219 (5.110)

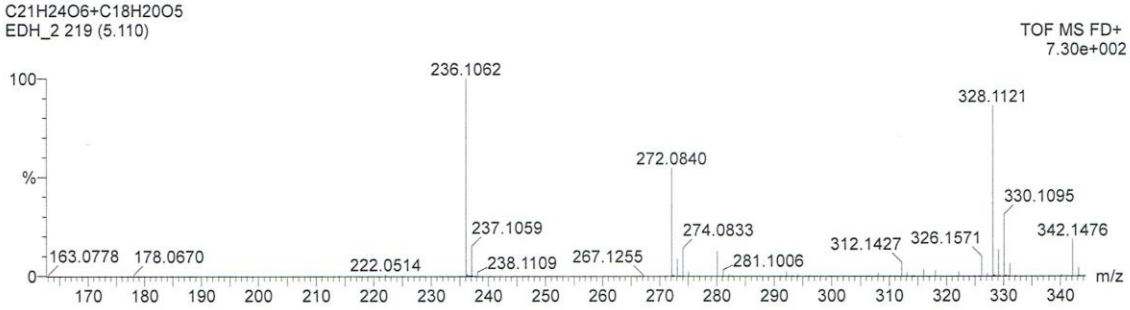

Minimum:				-1.5		
Maximum:		20.0	50.0	50.0		
Mass	Calc. Mass	mDa	PPM	DBE	i-FIT	Formula
236.1062	236.1049	1.3	5.5	6.0	0.1	C13 H16 O4

Figure B4. Time of flight mass spectrum of DGEGD.

Appendix C

Near-IR Spectra

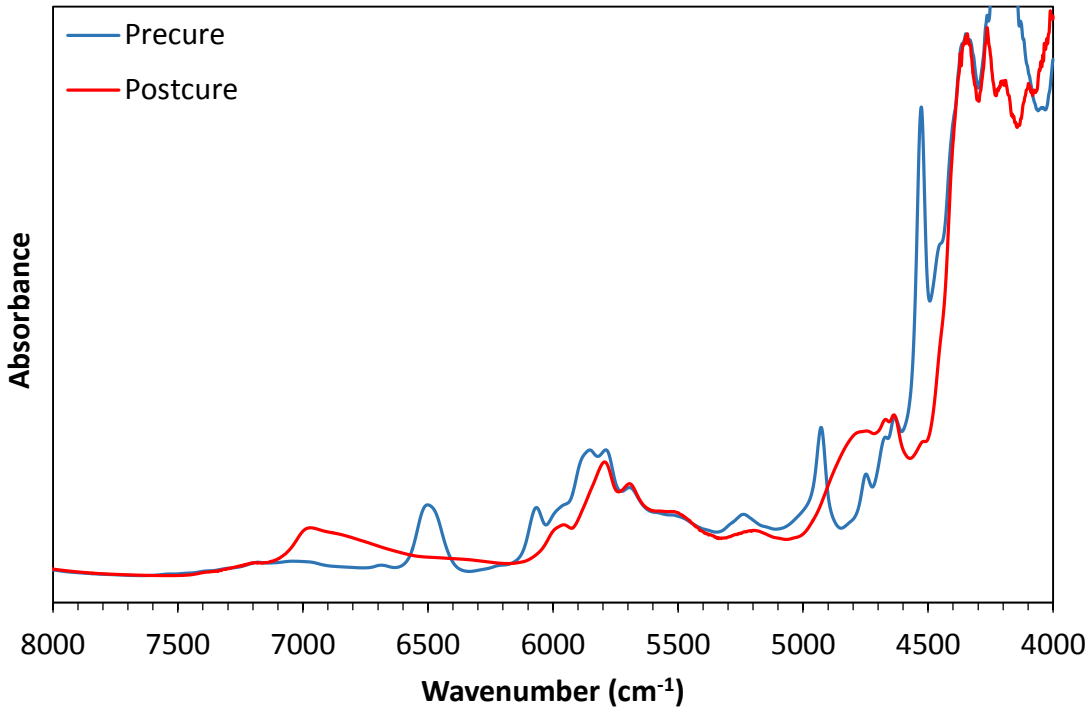

Figure C1. Near-IR spectra of DGEVA cured with PACM both before and after cure.

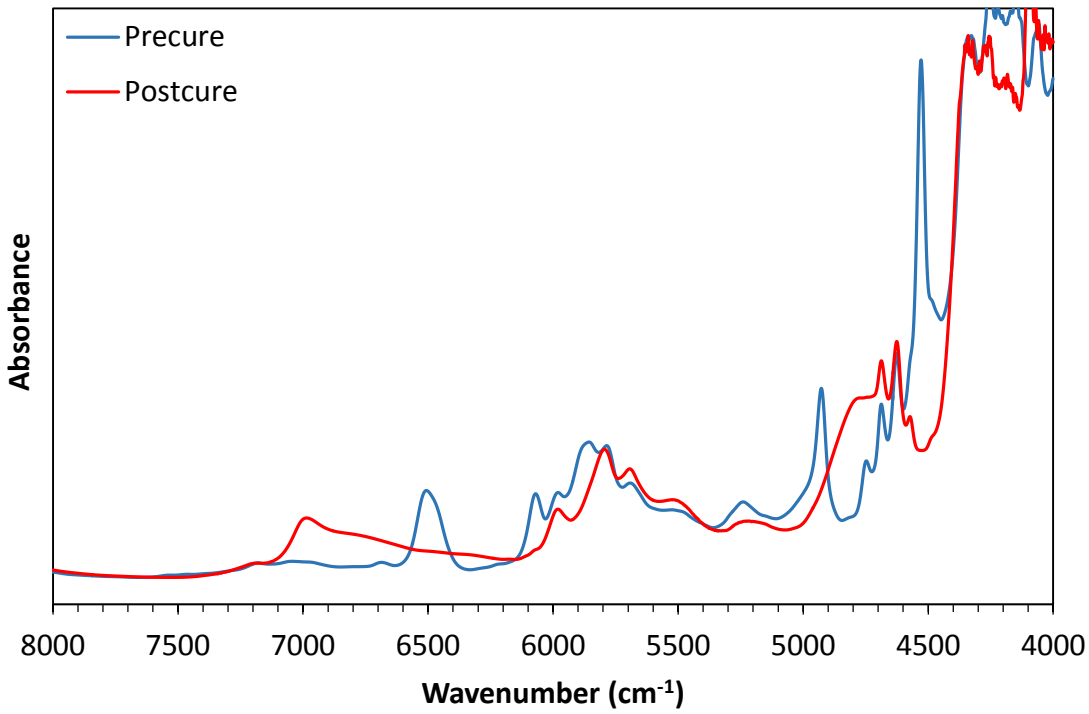

Figure C2. Near-IR spectra of DGEGD cured with PACM both before and after cure.

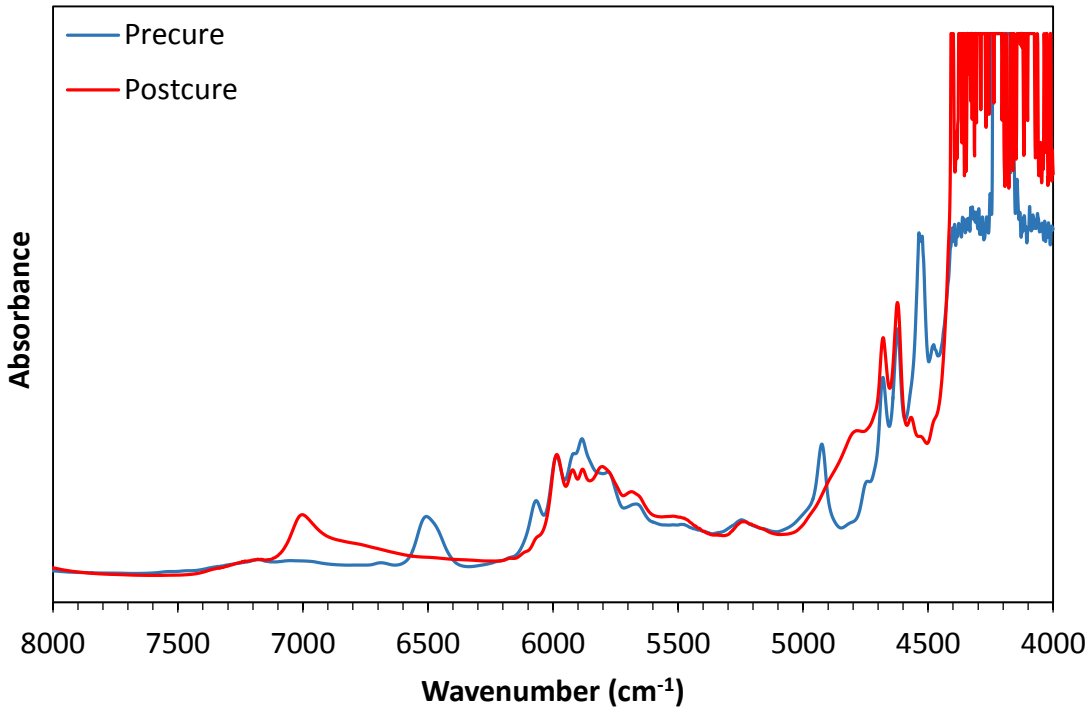

Figure C3. Near-IR spectra of Epon 828 cured with PACM both before and after cure.

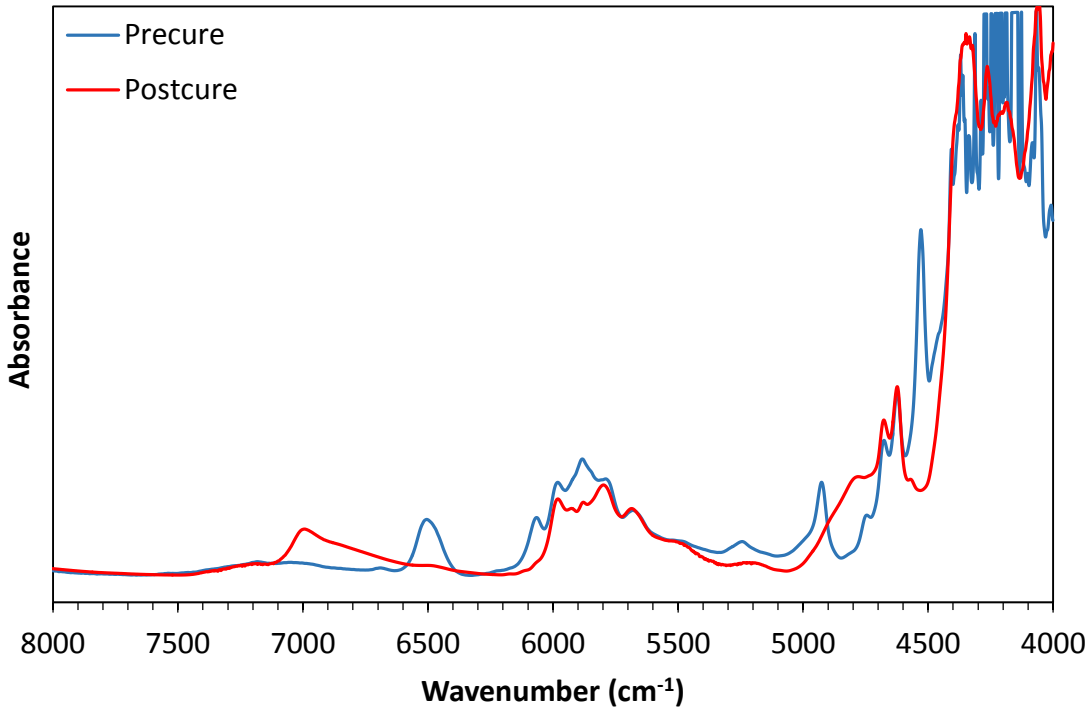

Figure C4. Near-IR spectra of 50:50 DGEBG - Epon 828 cured with PACM both before and after cure.

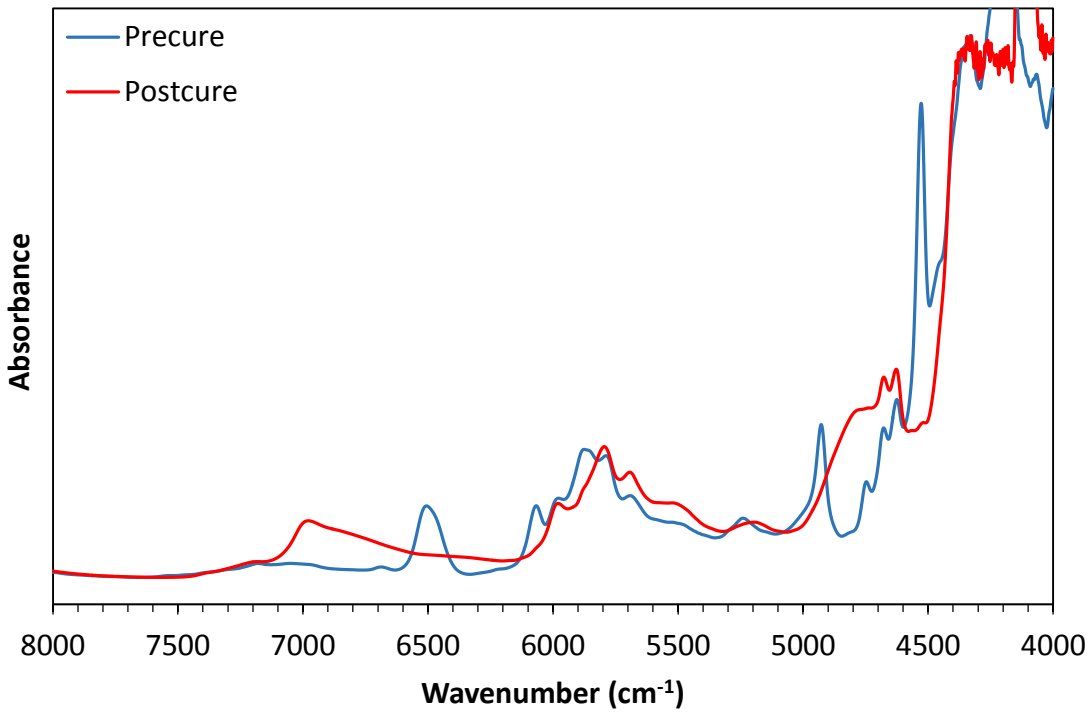

Figure C5. Near-IR spectra of 75:25 DGEVA - Epon 828 cured with PACM both before and after cure.

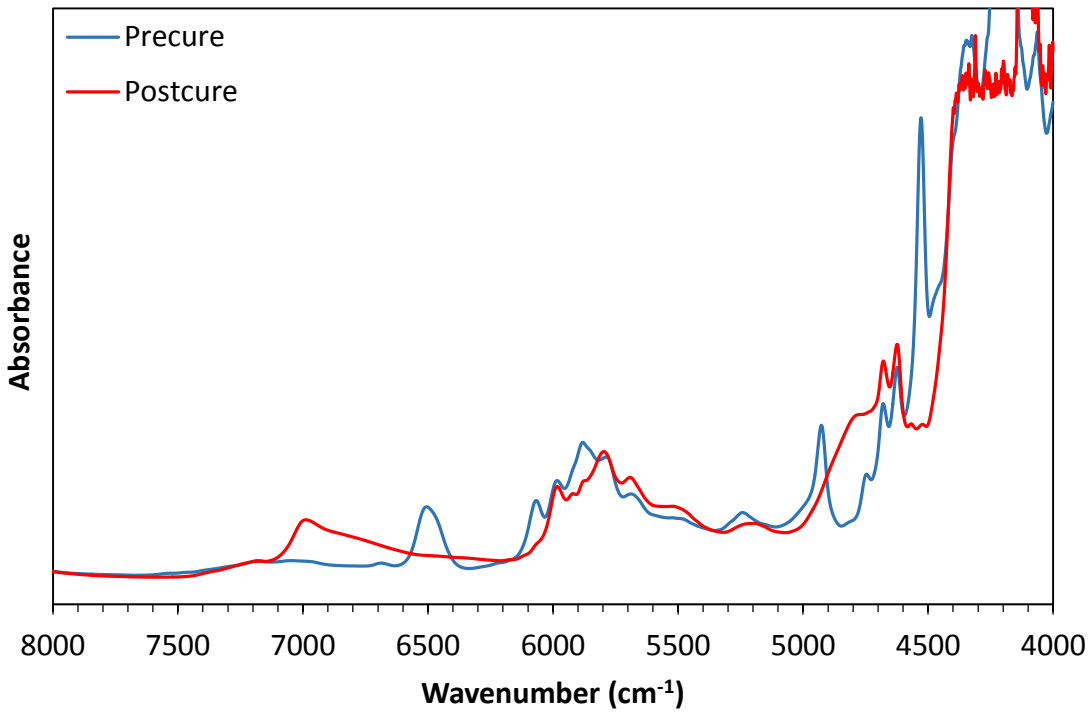

Figure C6. Near-IR spectra of 50:50 DGEVA - Epon 828 cured with PACM both before and after cure..

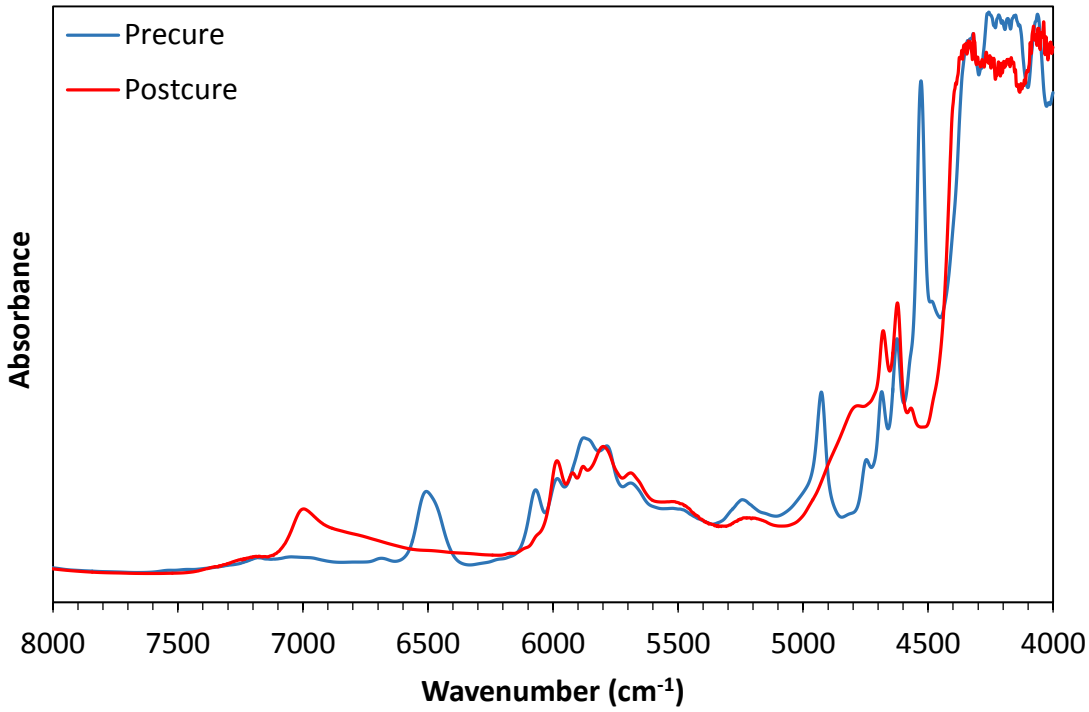

Figure C7. Near-IR spectra of 25:75 DGEVA - Epon 828 cured with PACM both before and after cure..

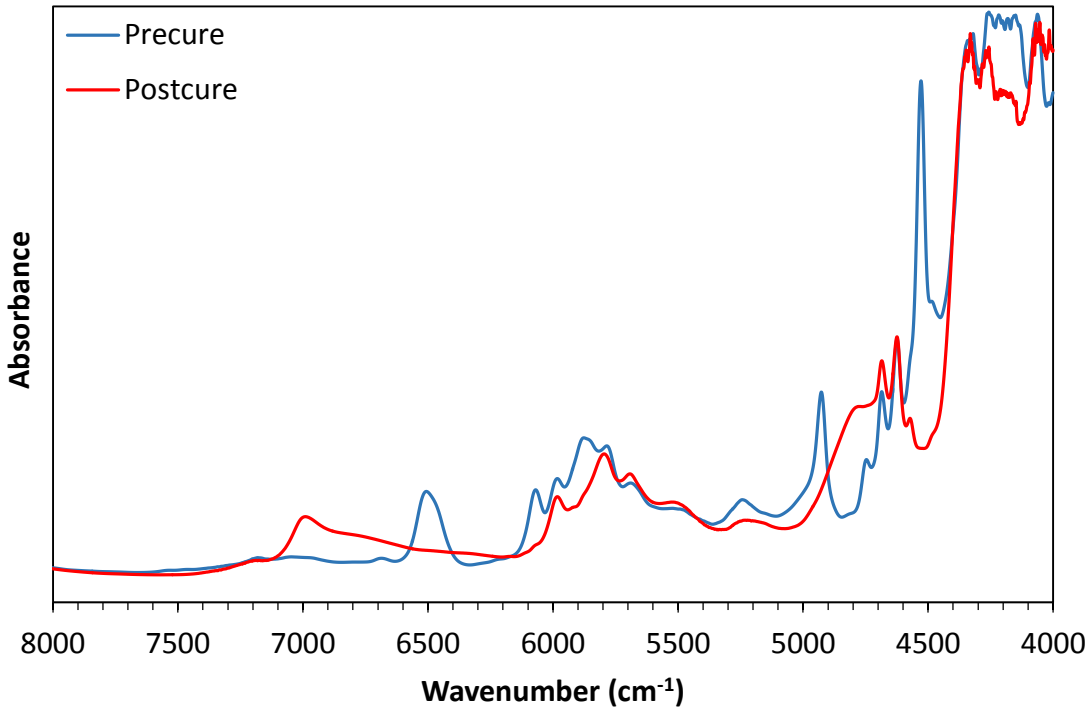

Figure C8. Near-IR spectra of 75:25 DGEGD - Epon 828 cured with PACM both before and after cure.

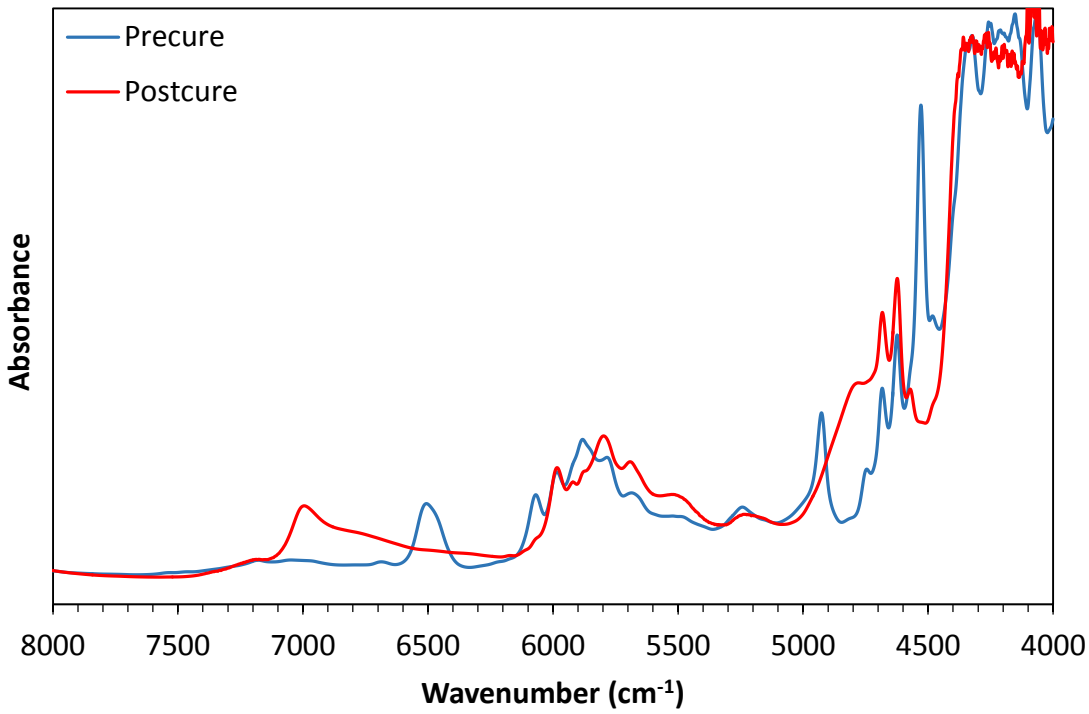

Figure C9. Near-IR spectra of 50:50 DGEGD - Epon 828 cured with PACM both before and after cure.

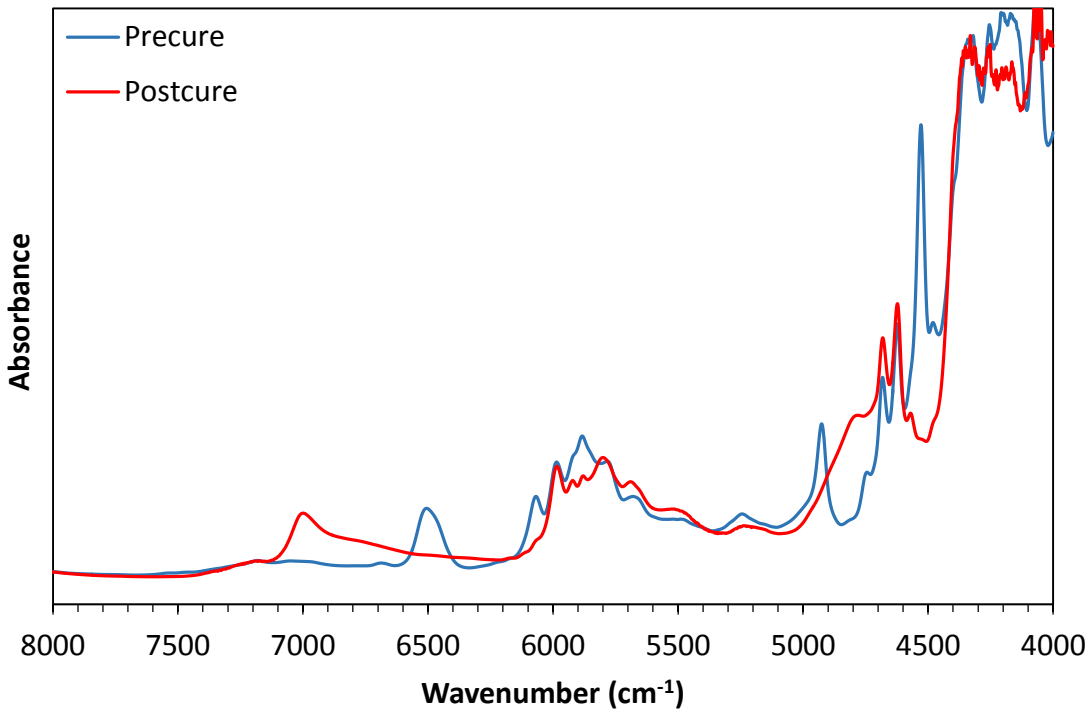

Figure C10. Near-IR spectra of 25:75 DGEGD - Epon 828 cured with PACM both before and after cure.

Appendix D

Tan Delta Curves of Cured Epoxy-Amine Resins

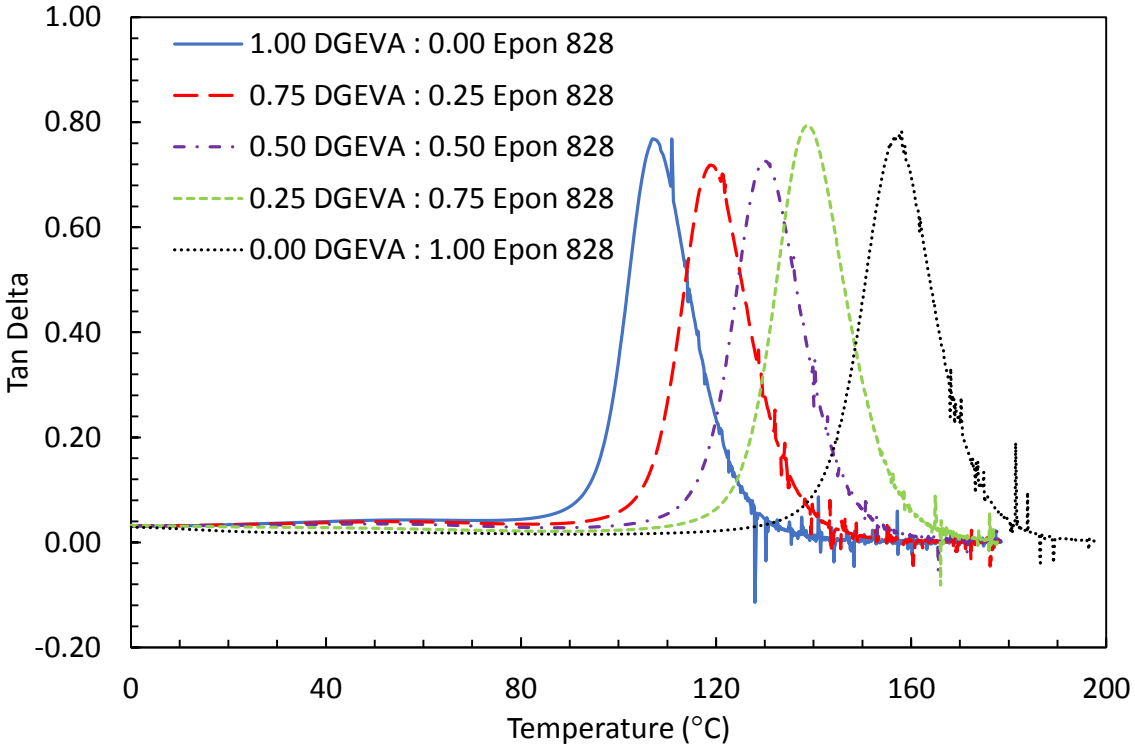

Figure D1. Tan δ curves of cured DGEVA-Epon 828 blends at various weight ratios. All samples were cured with Amicure ® PACM. Measured on TA Instruments Q800 DMA in single cantilever mode.

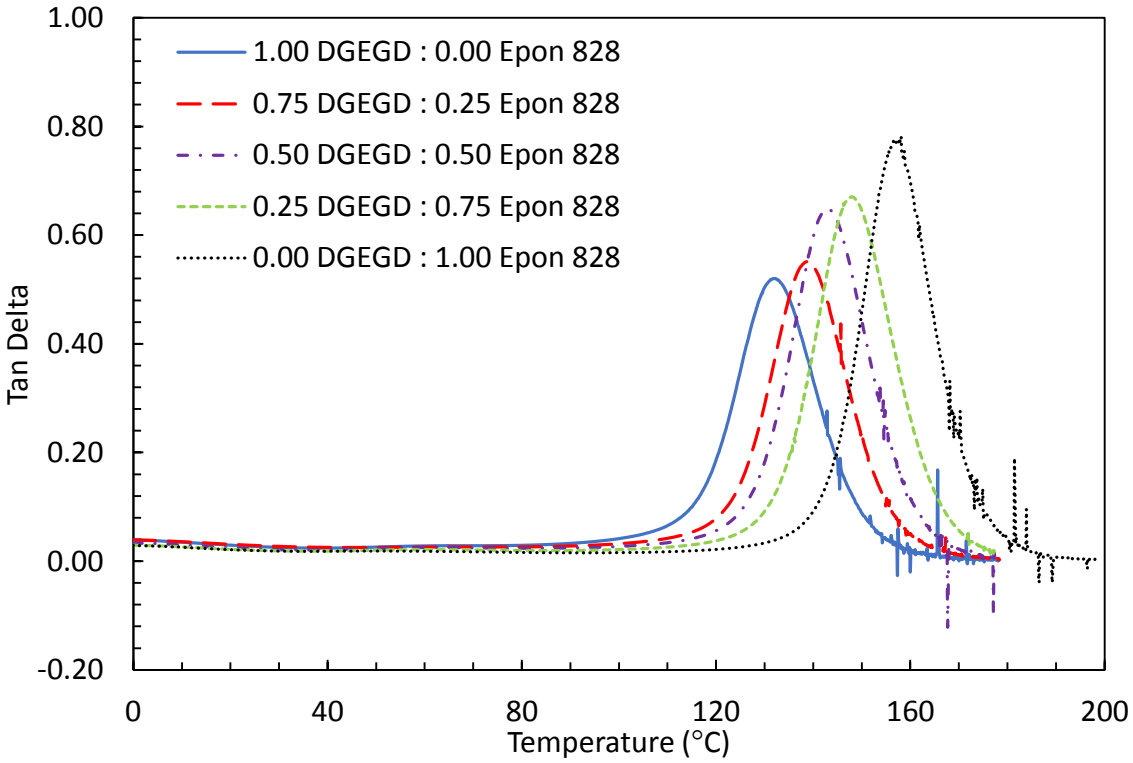

Figure D2. Tan δ curves of cured DGEGD-Epon 828 blends at various weight ratios. All samples were cured with Amicure ® PACM. Measured on TA Instruments Q800 DMA in single cantilever mode.

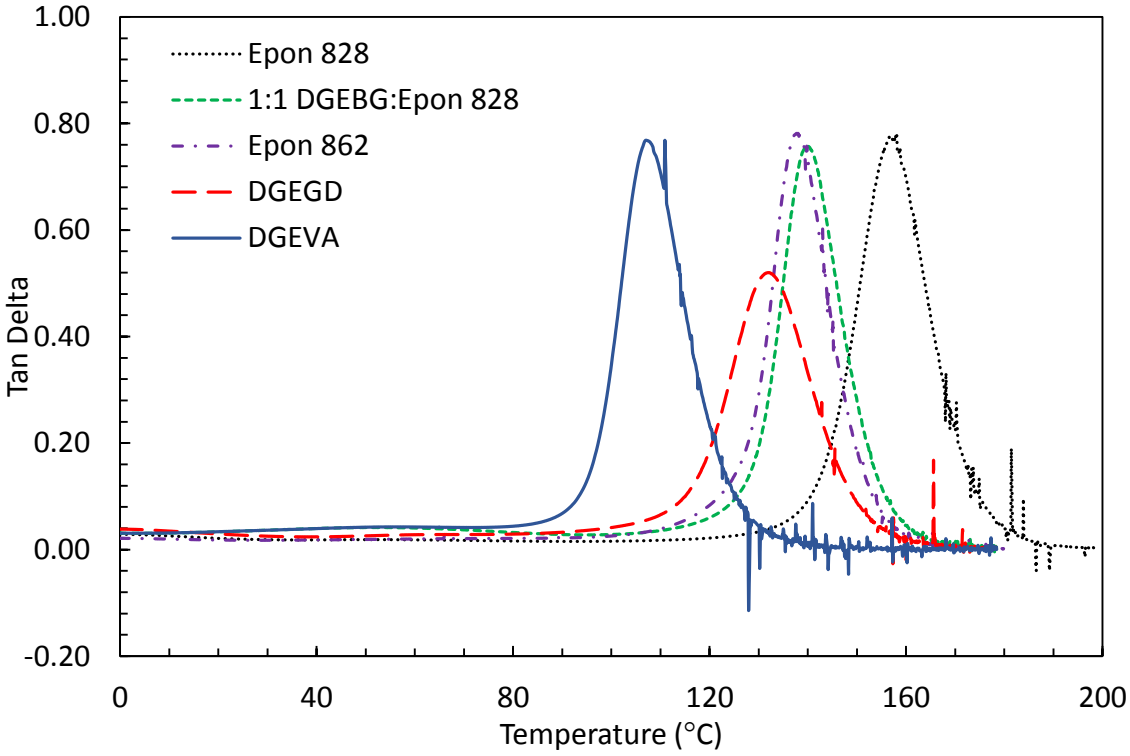

Figure D3. Tan δ curves of epoxy resins cured with Amicure ® PACM. Measured on TA Instruments Q800 DMA in single cantilever mode.

Appendix E

DMA Data of Polymers Containing Mono-Epoxidized Impurities

The hydroxyls directly bonded to the aromatic ring of both vanillyl alcohol and gastrodigenin are more reactive toward epichlorohydrin then the aliphatic hydroxyls. Therefore, synthesis of epoxy resins via reaction with epichlorohydrin yields a mixture of diglycidyl ethers and monoglycidyl ethers. In this thesis, the reaction of vanillyl alcohol with epichlorohydrin yields approximately 85 % di-epoxy and 15 % mono-epoxy (where the aliphatic hydroxyl remains unreacted). The EEW of this mixture was determined via epoxy titration. This mono- and di-epoxidized vanillyl alcohol mixture was blended with Epon 828 at various weight ratios and the resins were cured with stoichiometric quantities of Amicure PACM. Similarly, the reaction of gastrodigenin with epichlorohydrin produces a mixture of mono- and di-epoxidized product. The ratio of monoglycidyl ether to diglycidyl ether for the epoxidized gastrodigenin mixture was determined to be 30:70. The EEW of the epoxidized gastrodigenin mixture was determined via epoxy titration and the resin was blended with various weight ratios of Epon 828. Again, these resin blends were cured with stoichiometric quantities of PACM. All samples were cured and prepared as previously described in the Chapter 3 and tested on a TA Q800 DMA using a single cantilever geometry. Tests were performed at a frequency of 1 Hz, a deflection amplitude of oscillation of 7.5 μm, a Poison's ratio of 0.35, and a heating rate of 2 °C min^{-1}. *Figure E1* and *E2* display DMA thermograms of the DGEVA/MGEVA – Epon 828 resin blends and the DGEGD/MGEGD – Epon 828 resin blends cured with PACM. Comparison of the following data with the purified di-epoxy data reported in Chapter 4 suggests the presence of mono-epoxy product decreases the T_gs of the cured epoxy-amine polymer systems.

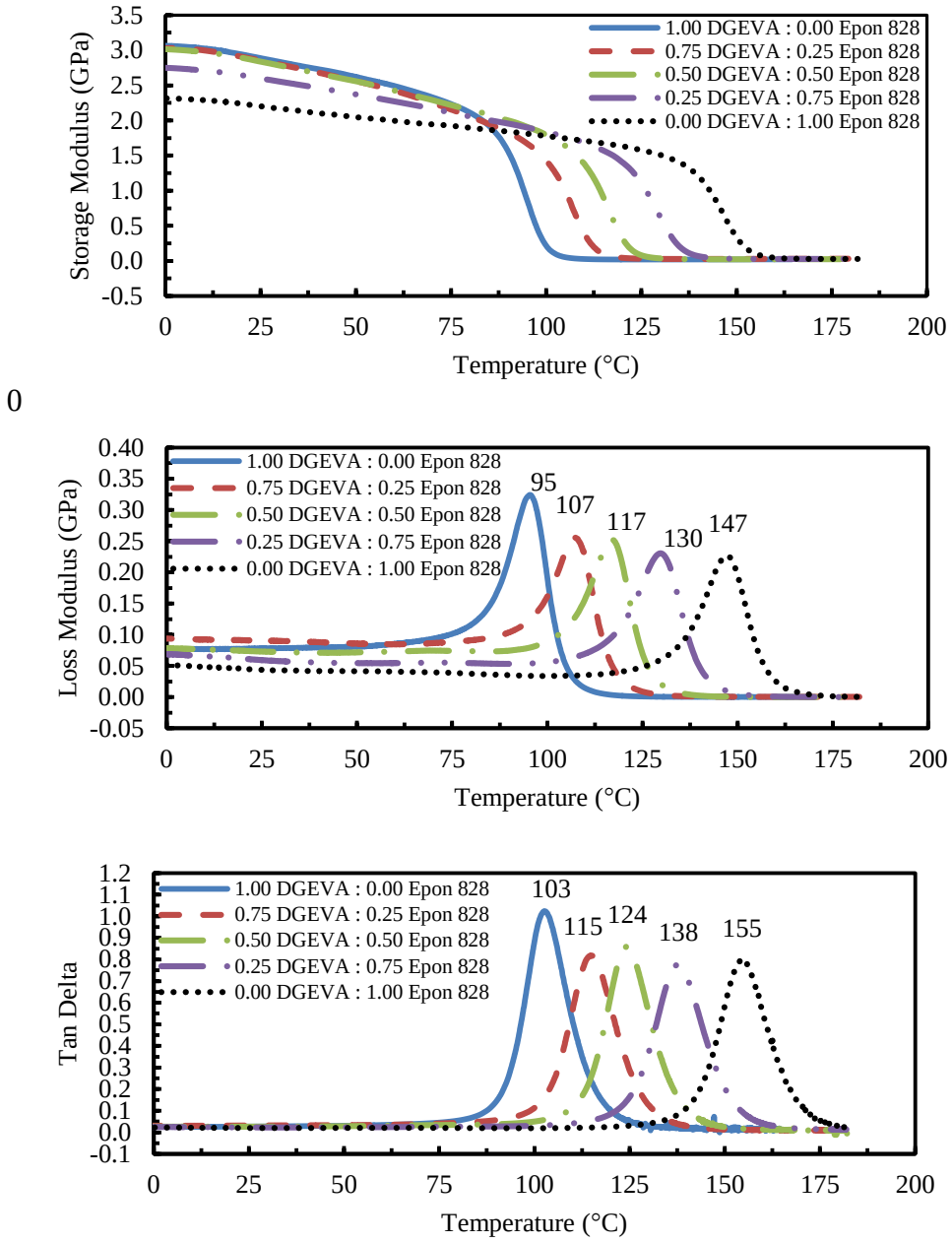

0

Figure E1. DMA Thermograms of DGEVA/MGEVA-Epon 828 blends cured with PACM.
DGEVA in these samples contains approximately 85 % di-epoxy and 15 % mono-epoxy.

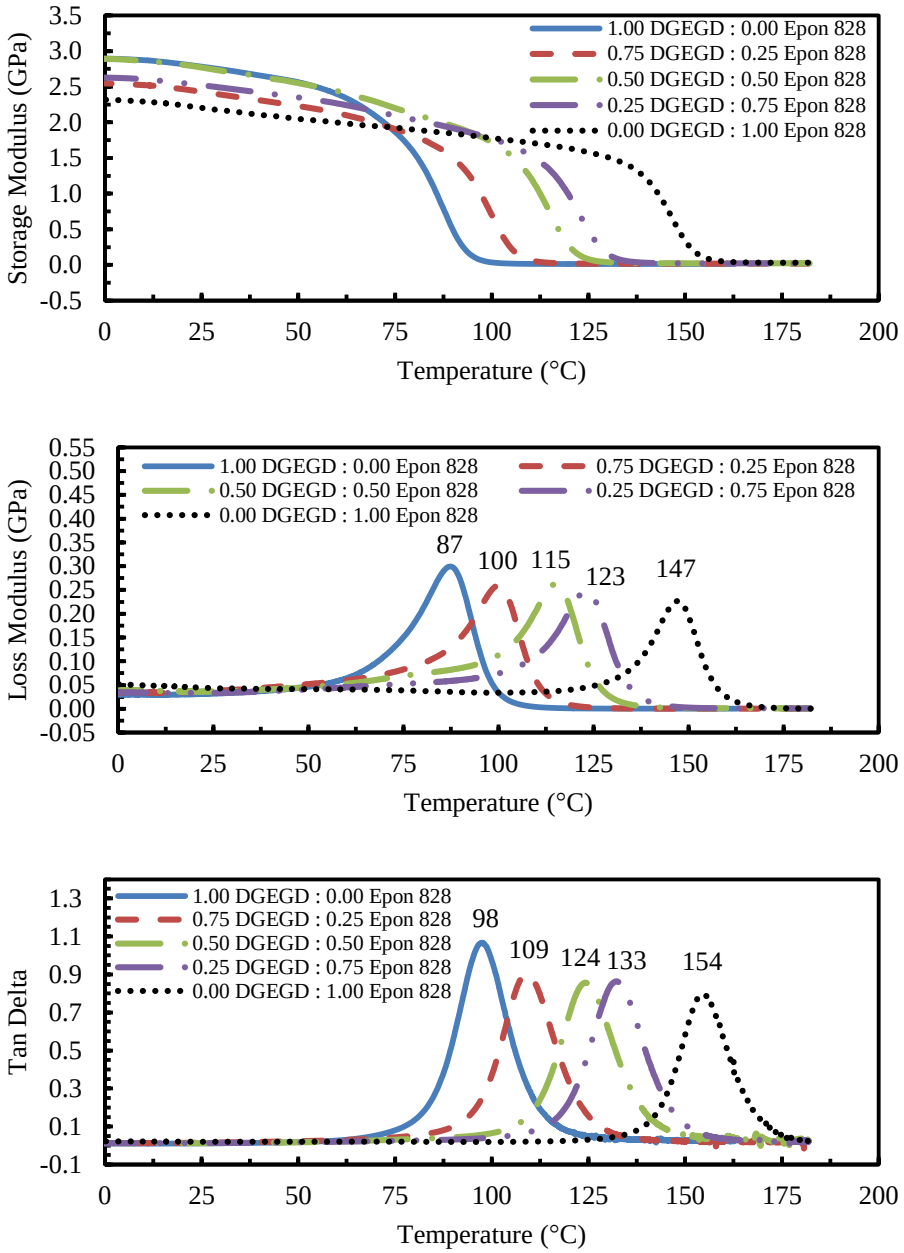

Figure E2. DMA Thermograms of DGEGD/MGEGD-Epon 828 blends cured with PACM.
DGEGD in these samples contains approximately 70 % di-epoxy and 30 % mono-epoxy.